Dear Editor:

Thank you for allowing us to revise and improve our manuscript. We are grateful to all the three reviewers for their expert advice and constructive feedback on our manuscript. We have done our best to incorporate all the comments into our manuscript in this revised version. We believe the reviewer's input greatly improved the quality of our manuscript. The revised manuscript has also gone through an English proofreading service. Below is our detailed responses. Reviewers' comments are in black and our responses are in blue. Texts and quotes from the manuscript are given within quotation marks (" ").

Response to reviewer #1

Review of "Interaction of Dust Aerosols with Land/Sea Breezes over the Eastern Coast of the Red Sea from LIDAR Data and High-resolution WRF-Chem Simulations" by Sagar P. Parajuli et al. submitted to Atmospheric Chemistry and Physics. This paper is focused on the effect of aerosols onto breeze circulation over the Eastern Coast of the Red Sea employing direct observations and WRF-Chem model. The paper is well structured and written and the results are sound and novel. Specifically, I am very much impressed with WRF-based estimates of the contribution of dust (along with the other components) the aerosol optical depth, the reported consistency of the vertical distribution of the aerosols across different observational diagnostic and model results and the role of breezes in dust deposition in the coastal environment with complicated orography. I would suggest to single out these conclusions somehow. I suggest acceptance of the paper with few minor caveats and suggestions.

Thank you very much for pointing out the strengths of the paper. We have revised the conclusions as you have kindly suggested.

(1) 'Study cite' section (2.1) is rather related to the concept and strategy (BTW given

nice fig. 1). It would be useful to rename it accordingly.

Thank you for the suggestion. Section 2.1 provides a brief description of the study site and introduces the breeze circulation, which is typical to the Arabian Red Sea coastal Plain. Breeze circulation is a key feature investigated in this study, along with its interactions with dust. Therefore, we would like to retain the title. However, considering your comment, we have moved Figure 1 to the discussion section and revised the text with pertaining information about the study site.

(2) Lines 186+ The use of MERRA2 should be better justified. MERRA is not spectral reanalysis and does have some minor to moderate problems over the coastlines and orography. This needs to be commented, better with references evaluating MERRA against alternative products in such conditions. Also in the Conclusions it might be useful to mention as a potential avenue the use of this case study for validating alternative HR products, like ERA5.

We are aware that MERRA-2 might have problems over the coastlines and orography. However, this is the only data assimilation product, besides CAMS, which assimilates satellite observations of aerosol properties and provides height-resolved aerosol distribution such as aerosol mixing ratios, as it is mentioned in the paper. We are aware of the ERA5 data set, which is considered better than its predecessor ERA-Interim. However, ERA5 does not provide aerosol concentrations.

(3) . . ..coordinated in time or/and in space. . . This requires more elaborate and accurate explanation, otherwise looks very unclear.

We rephrased this sentence and further edited the paragraph to make our explanations more clear. The revised paragraph is provided below:

"We combine cloud-screened AERONET radiances and LIDAR backscatter signals to retrieve aerosol properties during the daytime. As AOD data are unavailable during the night, for nighttime retrievals, we use a so-called multi-pixel approach, first introduced by Dubovik et al. (2011) and implemented in GRASP. According to this approach, the retrieval is implemented using a group of observations representing different time and location (e.g., several satellite pixels), to retain the variability of the retrieved parameter. For example, in this study, we invert the closest AERONET measurements obtained the day before and the day after, together with the nighttime LIDAR backscatter data, under some constraints on the temporal variability of the columnar parameters (size distribution, complex refractive index, and sphericity fraction) provided by AERONET measurements. In contrast to other more straightforward retrieval approaches used currently, the multi-pixel technique constrains the retrieval without eliminating the variability within the data. The implemented retrieval approach allows us to retain the variability of columnar properties throughout the night. This approach contrasts with the retrieval approach adopted by Benavent-Oltra et al. (2019), which ignores the variability of columnar properties during the night."

(4) Section 2.2 – the arrangement of the domains needs a better explanation, specifically D02 (west boundary). General circulation here is such that requires likely extension of this domain westward. Specifically, there are patterns engaging circulations over the whole western coast (e.g. https://doi.org/10.1175/JHM-D-16-0048.1) which need to be resolved. Try to comment upon potential problems with this. Also the impact of the lateral outer boundary conditions taken from ECMWF analyses should be discussed better (as the choice for the lateral conditions).

We are aware that some large-scale dust storms also take place across Red Sea a few times a year, for example through Tokar gap. We have already mentioned this in section 2.1 with relevant references. Considering the suggestion, we have added the following lines in section 2.2 to clarify this further.

"Although the western boundary of domain d03 appears close to that of d02, there are 40 grid cells in between, which is ten times higher than generally recommended, and is sufficient to ensure a smooth transition across the boundaries. While a further westward extension of d02 could be desirable to better resolve the synoptic weather phenomena across the Red Sea e.g., through the Tokar gap (Kalenderski and Stenchikov 2016), such phenomena have a minor impact on the diurnal-scale local sea breeze circulation in our site, which is the focus of our study."

The ECMWF operational analysis (restricted data used to build initial and boundary conditions for our simulations) is one of the most reliable and high-resolution (~15km) dataset currently available, so the potential impacts from boundary conditions should not be a problem.

(5) lines 345 and around, fig 3. There is an evident seasonal cycle in the AOD distribution – was it removed before computing correlations?

We agree that there is some seasonality in the AOD data, although not very strong. We also agree that it is more appropriate to remove the seasonal cycle before computing correlations. As suggested, we have recalculated the correlation coefficients after removing the seasonal cycles with monthly means. The new correlations are slightly smaller as we would expect. The new values have been updated in the revised manuscript.

6) Section 3.2. Diurnal cycle of winds should be better subordinated also with info on wind directions (given the paper focus).

Thank you for the comment. We believe that we have discussed the wind directions in detail in section 3.4 (old version). Figures 13-15 (old version) and relevant discussion describe the prevailing wind direction in different seasons and at different altitudes. We have now revised this section with some additional information on breeze formation. We have also revised Figure 9 (old version) description to clarify the relevance of wind directions in dust transport to our site further.

(7) lines 495-497 – analysis of day/night profiles. This para needs edits, as it stands it is very difficult to handle

Thank you for pointing this out. We agree that this paragraph was a bit unclear. As suggested, we have now substantially revised this paragraph to make our points on the cause of elevated dust loading at 1-2km in daytime and 5-7km in nighttime clearer.

(8) Fig 11 – see comment (6) on wind directions

We believe that we have already addressed this point earlier. See the response to comment 6.

(9) lines 694+ the interaction of sea breezes with the Harmattan winds is explained in a very wordy and contradictory manner, the para in a whole needs edits

Thanks for raising an interesting point. We agree it is important to discuss the interaction of harmattan winds with land/sea breezes, along with their effect on dust. Considering your suggestion, we have added following description in the end of section 3.2.3.:

"When the dust-laden harmattan winds arrive at the Red Sea coast, they encounter the land or sea breezes depending upon the time of arrival, as discussed further in section 4.3. When they meet with the opposite sea breeze flow, the air mass rises up, bringing the dust to the upper levels. Such higher intrusion of dust is evident in the KAUST-MPL data (Figure 9, left) in the afternoon, during which the sea breezes are most active. The suspended dust is still visible in the upper levels (~2-3 km) in the night of August 10, because the dust particles have not been deposited yet."

(10) Fig 15 – change please the arrow scale to see the differences in magnitude in the panels. Also you might wish to use a fine resolution for plotting wind arrows.

We understand your suggestion to change the scale of arrows in each figure panel for clarity. However, we would like to use a consistent arrow scale in all the panels to show the difference in winds at different altitudes and seasons. Therefore, we decided to keep the wind scale as it is.

(11) Fig 17 and text. What is plotted is MSLP I guess, not surface pressure. Also consider using contours for SLP, as the color is not effective for identifying circulation patterns.

We considered using contours but contours would reduce the cleanliness of the figure because of the borderlines and the contour numbers. We changed the naming from 'surface pressure' to mean sea level pressure (MSLP) as suggested.

(12) conclusive bullets should be grouped according to the paper flow. Otherwise, they are not convincing, see also general comment.

Thank you for this helpful suggestion. We have now grouped the conclusion in four headings according to paper flow, as suggested, and separated the discussion.

Response to reviewer #2

This paper presents an approach coupling WRF-Chem, vertical profiles of a MPL lidar and photometric measurements (AERONET) to study aerosols on the western coast of the Arabian Peninsula during 2015. The authors also use MODIS, SEVIRI and CALIOP spaceborne observations to help them in their interpretations. The authors aim to better understand the role of coastal breezes on the vertical distribution of dust aerosols and assess the accuracy of the modelling compared to the observations.

This work is of scientific interest in the sense that the role of breezes and their interaction with the general circulation of the atmosphere is not necessarily well evaluated at key locations on the planet, like in the case of the region considered in this article. Dust aerosols are now recognized as having a significant role on the radiative balance of some regions of the globe, but also on economic life (IPCC). This article is therefore interesting, and the results of this research deserve to be published after major revision.

We are grateful to the reviewer for providing encouraging feedback on our manuscript.

This article should be seriously revised and better organized before publication. There is a lot of repetitions throughout the text, which makes reading the article considerably more cumbersome and detracts from highlighting the main ideas. There is a need to group together the elements of discussion spread throughout the various sections. It is also necessary to be clearer about the objectives as this article can be seen as a publication on the validation of WRF-Chem on the one hand and on the other hand it claims an annual study on aerosols above the experimental site. The part on the cross-comparison between instruments and model should be well separated from the scientific interpretations. A "Model validation" section should be done more directly. This study is not conducted over a sufficiently long period of time to be able to speak about climatology. It should therefore be repositioned in a more global context to better highlight its scope. A major event has been observed and is the subject of a "case study", but is this event common in other years? Are the observed dust aerosol contents and their vertical distribution throughout 2015 reportable for other years? The discussion section is confusing and needs to be better organized by a new structure of the article. It would be preferable to separate it from the conclusion, which will then more clearly highlight the major findings of this study.

We agree that our manuscript needs to be better organized. We have extensively revised the paper in different sections to reflect the reviewer's comments. To clarify the presentation, we added a separate section 'Model Validation' by combining section 3.1 (comparison of AOD and aerosol volume concentrations), parts of section 3.3 (diurnal cycle comparison of model winds with observation) and section 3.5 (case study). We have also added a new section for discussion with subheadings according to the flow of the paper.

Regarding the "climatology", we agree with the reviewer's comment. In the revised manuscript, we have avoided using this term. The dust case study, we consider in the paper, is a typical recurring summer time dust event; so it is common in other years. Regarding the possible interannual variability, following the reviewer's suggestion, we have looked at the aerosol profiles for 2015 and 2016 separately. There is some interannual variability, as expected but it is relatively weak. We have now added the following text in the manuscript to clarify this issue:

"We observed some interannual variability while comparing the vertical profiles for 2015 and 2016, but was not too significant (Fig. S9). Therefore, the observed vertical distribution of dust aerosols can be considered 'typical' for our region and possibly for other land-ocean boundaries (e.g., Rasch et al., 2001).

This is understandable because the synoptic winds causing large-scale dust events, and the diurnal-scale breezes that affect the dust distribution, both have strong seasonality over the study region (Kalenderski and Stenchikov, 2016; Parajuli et al., 2019). However, as demonstrated by our results, vertical profiles of aerosols can be affected by regional processes such as breezes, which indicate that the profiles can differ across different regions. Therefore, it is vital to examine the aerosol vertical profiles of a region to understand the regional climate."

Figure S9 is presented below.

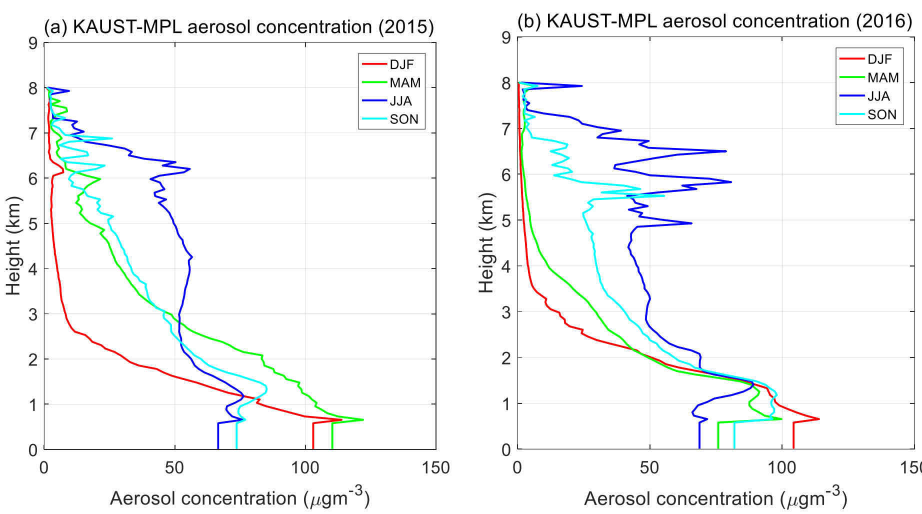

Figure S9. Comparison of KAUST-MPL aerosol vertical profiles for two years, 2015 and 2016.

L63. The vertical distribution of aerosols has been studied for decades using lidar measurements from the ground-based, aircrafts, and satellites (LITE, CALIOP, GLAS) platforms. It is indeed an important parameter for the assessment of the climatic impact of aerosols. Numerous publications exist. For deontological reasons, I prefer to let the authors make their complementary bibliography, without influencing them. They can research what has been done during INDOEX, ACE-2 or AMMA at the international level and elsewhere.

We are aware that our study is far not the first employing lidar observations for dust profile analysis. However, there are no other such studies in the Red Sea coast region. Our research is essential because the presence of breezes over the Red Sea coast affects aerosols' vertical distribution.

We thank the reviewer for providing us examples of previous studies on vertical aerosol profiles using LIDAR data. We have compiled an extensive review of studies using LIDAR from satellites, field experiments, and networks, as suggested. This review is included in the revised manuscript, in the introduction section:

"The vertical distribution of aerosols in the atmosphere has been studied for decades using LIDAR measurements from several ground-based sites, aircraft, and satellite platforms, covering different regions across the globe. Several satellites are equipped with LIDAR to measure the vertical distribution of aerosols. Lidar In-space Technology Experiment (LITE) was the first space lidar launched by NASA in 1994 onboard the Space Shuttle, providing a quick snapshot of aerosols and clouds in the atmosphere on a global scale (Winker et al., 1996). LITE was followed by the Geoscience Laser Altimeter System (GLAS) containing a 532-nm LIDAR, as part of the Ice, Cloud and Land Elevation Satellite (ICESat) mission, which covered the polar regions (Abshire et al., 2005). Cloud-Aerosol Lidar with Orthogonal Polarization (CALIOP) onboard CALIPSO (Cloud-Aerosol Lidar and Infrared Pathfinder Satellite Observations) currently observes aerosol and clouds globally during both the day and night portion of the orbit with a 16-day repeat cycle since 2006 (Winker et al., 2013). Apart from satellites, several field experiments have also been conducted using LIDAR to measure the vertical distribution of aerosols. The Indian Ocean Experiment (INDOEX) field campaign (Collins et al., 2001; Rasch et al., 2001; Welton et al., 2002b) took place in 1999 over the Indian Ocean, Arabian Sea, and the Bay of Bengal, in which an MPL system together with other instruments measured aerosol distribution in the troposphere. Similarly, an MPL system was employed in the Second Aerosol Characterization Experiment (ACE-2) in 1997 over Tenerife, Canary Islands, to understand the vertical distribution of dust/aerosols transported from North Africa and Europe to the Atlantic Ocean (Welton et al., 2000; Ansmann et al., 2002). African Monsoon Multidisciplinary Analysis (AMMA), one of the largest international projects ever carried out in Africa, also measured aerosol vertical distribution using multiple LIDAR systems for a short period in 2006 (Heese and Wiegner, 2008; Lebel et al., 2010). Currently, several other coordinated LIDAR networks are operating in different regions. They include the European Aerosol Research Lidar Network EARLINET (Pappalardo et al., 2014), German Aerosol Lidar Network (Boesenberg et al., 2001), the Latin American Lidar Network LALINET (Guerrero-Rascado et al., 2016), the Asian dust and aerosol lidar observation network AD-Net (Shimizu et al., 2016), and the Commonwealth of Independent States Lidar Network CIS-LiNet (Chaikovsky et al., 2006)."

L92. Clouds necessarily influence the lidar inversion which usually requires a reference, usually molecular in the upper troposphere. Can you clarify your statement?

We agree with the comment. We have clarified the text to highlight the benefit of LIDARs data as compared to the passive satellite sensors, which are generally based on visible bands. We have also added appropriate references in the revised text:

"AERONET stations and passive satellite sensors are further limited because they cannot retrieve aerosol properties during the night. LIDARs help to overcome these limitations because they provide high-frequency measurements, even at night. Furthermore, LIDAR signals can penetrate thin and multilayer clouds, which are usually overlooked by passive satellite sensors (Winker et al., 1996; Winker et al., 2009), thus improving the detection of aerosol layers at different altitudes. Therefore, LIDAR data are essential for understanding the diurnal variability of aerosols and their climatic effect."

Sub-section 2.1. The scheme on the breeze would be better placed in the revised discussion.

Agreed. We have now moved the figure to the revised discussion section.

L157. Use "annual study" rather than "climatology".

We agree that our study is not truly a climatological since we have only two-years of data. Therefore, we have avoided using the term 'climatology' entirely in the revised manuscript. We now use throughout the text the word 'seasonal average', with the averaging period given in bracket.

L163. The CALIOP instrument?

Corrected.

L173. Replace version by data?

Corrected.

L190. Define DOD.

Corrected as suggested.

L210 and following. How do you find the absorption coefficient with a MPL? More needs to be said about the implemental retrieval.

We agree that this statement was not clear. Considering your comment, we have revised the entire paragraph to clarify the implemented retrieval, which is reproduced below:

"The colocation of the KAUST–MPL and AERONET station provides an opportunity to get a more comprehensive microphysical picture when the MPL data are combined with AERONET sun-photometer measurements. We employ GRASP (Generalized Retrieval of Aerosol and Surface Properties, Dubovik et al., 2011, 2014), which is an open-source inversion code that combines different types of remote sensing measurements, such as radiometer and LIDAR observations, to generate fully consistent columnar and vertical aerosol properties (Lopatin et al., 2013). We take aerosol characteristics from the AERONET retrieval including size distribution, absorption, scattering optical depth, and refractive index. These parameters serve as inputs to GRASP, together with MPL data, to generate height-resolved aerosol fields such as aerosol extinction, absorption, and mixing ratios."

L240 and following. Aren't there difficulties in parameterizing turbulence at such scales? Can you justify the choice of the PBL scheme? This is an important element for this type of study.

After reading your comment, we realized that we had wrongly mentioned the PBL scheme that we had used. We actually used YSU PBL scheme Yonsei University YSU (Hong, Noh, and Dudhia, 2006) not MYJ (Janjic, 1994) as mentioned. We have updated this information in the revised manuscript. As suggested, we have added the following justification for the use of PBL scheme in the revised manuscript:

"Several studies compare the performance of PBL schemes in WRF, showing mixed results under different model settings (e.g., Saide et al., 2011; Fountoukis et al., 2018; Fekih and Mohamed, 2019). However, these studies have not directly compared the aerosol vertical profiles. Preliminary results showed that the choice of the PBL parameterization did not have a significant impact on the vertical distribution of aerosols in our case. In our simulations, we use the YSU PBL scheme, which is one of the most commonly used schemes, as suggested in the literature (e.g., Fountoukis et al., 2018; Fekih and Mohamed 2019)."

Sub-grid turbulence is not resolved in our simulations, but is parameterized. We agree that reproducing the turbulence effects is challenging and can be improved in WRF-Chem. However, such exercise is out of scope of this study.

L245. Define MENA.

Done.

L248. Remind the definitions of u and v.

Definitions added.

L300-306. This approach assumes that there is no internal mixing.

Yes, we agree.

L326. Climatology?

We have avoided using this term throughout the manuscript.

L343. Give the equation.

Correlation coefficient and mean bias error are fairly used terms so we chose not to provide the equation for brevity of the manuscript.

L350. The "robust" term is somewhat strong with correlations between 0.6 and 0.7.

We agree. We replaced the term ‘robust’ with ‘reasonable’.

L393-398. Example of duplication.

This is an important suggestion. We have revised and moved these lines to the section 2.1, Study site.

Figure 6a. Define WS. Climatology?

Corrected as suggested.

L403-406. Already mentioned.

We have moved this to section 2.1 and edited to avoid repetition.

L407-417. Combine with what was already mentioned on the sea breeze.

The section has been revised as suggested.

L432-433. No, CALIOP inversions use a lookup table with backscatter, color ratio and depolarization as inputs.

We agree that this statement was not clear. Here, we do not want to provide too much details of CALIOP algorithm; we only want to differentiate CALIOP algorithm in terms of lidar ratio as compared to MPL. We have revised the sentence and the whole paragraph for clarity, as presented below:

“The difference in vertical profiles retrieved from KAUST-MPL and CALIOP data could be related to the differences in the algorithm and resolution between the two datasets. Firstly, while retrieving aerosol extinction profiles, the CALIOP algorithm uses different prescribed extinction-to-backscatter (lidar ratio) for a set of aerosol types from a lookup table (Omar et al., 2009; Winker et al., 2009; Kim et al., 2018). In addition, the CALIOP algorithm has difficulty in identifying the base of aerosol layers accurately. In particular, the level-3 algorithm ignores the ‘clear air’ between the surface and the lowest aerosol layer when averaging to avoid underestimation of extinction in the lower part of the aerosol profile (Winker et al, 2013). In contrast, the MPL algorithm assumes an averaged lidar ratio for the whole column based on the aerosol PSD, refractive index, and sphericity, in such a way that it satisfies both AERONET and MPL co-incident data. Because of the assumption of a constant lidar ratio, MPL retrievals near the surface could be erroneous, especially when multiple aerosol layers are present (Welton et al., 2002a). Secondly, KAUST–MPL is a point measurement that captures the temporal evolution of the dust storms better than CALIOP because it has a higher temporal resolution. For instance, CALIOP can undersample or overlook some dust events that last only for a few hours. On the other hand, CALIOP could sample more spatial details of a dust storm because of its extended coverage along its track compared to KAUST–MPL data. Nonetheless, these two datasets complement one another, and their combined use can be beneficial in understanding the large-scale dust storms."

L440-441. Be careful because the distance between two ground tracks is large.

We understand your point. We only say this in comparison to point measurements such as LIDAR. We have revised this statement (see the response to the previous comment).

Fig. 7. Height is the altitude a.g.l.?

It is above sea level, we added this information in the caption.

Fig. 7c (MPL during nighttime) and related discussion. What we see above 5 km looks like contamination by semi-transparent clouds (or an average with cloudy profiles). This may also be why there is such a large discrepancy with the model.

We have taken your comment on possible cloud contamination in our retrievals seriously. We have added discussion in several places to make the readers aware of this issue. Further, we have done some calculations using depolarization to check such a possibility. We have added relevant discussion mainly in two places: 'data and methods' and another in 'discussion.' The following text is added in the data and methods section to clarify this issue:

"The GRASP algorithm relies on an external cloud masking. Overnight lidar retrievals are performed only when cloud-free AERONET sun-photometric observations are available in the preceding evening and following morning. The AERONET cloud-masking algorithm is considered the golden standard, providing very reliable filtering of thick and broken clouds (Holben et al., 1998). In this regard, only clouds that form specifically at night and are undetectable by sun-photometric observations in the evening and morning could influence our retrieved extinction profiles. At the same time, retrieval of these profiles, to a large extent, relies on detailed columnar aerosol properties retrieved before and after nighttime observations. An attempt to retrieve cloudy profiles under the assumption of cloud-free aerosol columnar properties should result in higher fitting errors, and therefore should be easily detectable."

The following text is added in the discussion:

"To better understand the origin of two elevated dust layers observed (~1-2 and 6-7 km) and investigate the possibility of thin-cloud contamination in our MPL retrievals, we analyzed the volume-depolarization profiles provided by the KAUST-MPL, synchronous to the attenuated backscatter profiles used in the retrievals. The average volume depolarization value in the lower atmosphere (1-2 km) was estimated to be 13-14% on average and 7-8% for the upper part (6-7 km) for the selected period. Such values indicate that high extinction values in this altitude range cannot come exclusively from clouds because pure water clouds generally yield a 1-2% depolarization value and ~30% or even higher in the case of cirrus clouds (e.g., Del Guasta and Valar, 2003). The lower depolarization value in the upper part could be explained by the fact that the aerosol particle sizes are much finer than those in the lower part. At the same time, a lower depolarization value also suggests the possibility of partial influence by thin clouds. The presence of thin clouds can probably cause some overestimation of aerosol concentrations and extinction at these altitudes. However, such an overestimation is expected to increase the fitting errors, which are easily detectable, as mentioned earlier. To ascertain this with full confidence, we plan a further analysis utilizing simultaneous retrieval of sun-photometric observations together with backscatter and volume-depolarization profiles provided by KAUST-MPL in the future."

L458-460. The difficulty in retrieve aerosols close to the surface is not the same for CALIOP and the MPL.

Agreed. We removed the statement here and clarified this in the discussion section added; please refer to our response in the earlier comment.

L468. I do not think it is very good in the spring when the model gives much higher values.

Agreed. We meant to say both summer and spring. We revised the text accordingly.

Sub-section L461. The model does not mark the PBL top well and it gives much higher aerosol extinction coefficients. It would be interesting to see the temporal evolutions of the PBL height deduced from the MPL and the numerical scheme chosen for WRF. A good representation of the PBL is fundamental to take into account the PBL/free troposphere exchanges. Moreover, to compare WRF and the MPL, it would be more interesting to have an OSSE (observing system simulation experiment) as for example in Wang et al. (ACP, 2014).

We have presented the model PBLH in the supplementary information (Figure S5 in the revised supplement), which varies greatly in different seasons. In the MPL profiles, we can assume that the PBL height coincides with the top of an aerosol layers. This height is consistent in all datasets (~7km) with minor discrepancies (Figure 7/8 in the old version). Therefore, we believe that the model calculates the PBL height quite reasonably. Thank you for the suggestion regarding OSSE. We agree that such analysis are meaningful, however, such a detailed analysis is out of scope of this study.

L491-497. I do not understand what is being demonstrated here. Dust aerosol layers are often above the PBL and in coastal areas the PBL is lower.

We agree that this section is confusing as also pointed by other reviewers. We have now revised this section to make our point clearer on the origin of elevated dust loading observed at two heights, one at 1-2 km and another at 6-7 km. We have also modified the text in several other places to connect this concept with the examples. We meant to say that the particular shape of aerosol profile that we observed is similar to the profiles observed in some other studies during ‘dust storms’. We hope this is clear now in the revised text. Please read the last paragraph in the revised text presented in response to the comment on L519 below.

L504-505. Beware of cloud signatures on lidar profiles.

With additional information on possible cloud contamination provided earlier, we believe this is clear now.

L502-503. Aerosols emitted non-locally are most often transported at higher altitudes, above the PBL. This is therefore not an exceptional case.

Agreed. The text is adjusted accordingly.

Sub-section L519. I do not understand what the "clear day"/"dusty day" comparison brings to the understanding of the differences between MPL and model. When there is no dust, it is normal that we do not see anything, it doesn’t prove anything.

We agree that these paragraphs were not clear as also pointed by reviewer #1. We have revised it to convey our intended message, as we are not talking about the difference between MPL and model. Our analysis is to uncover what would be the origin of the elevated dust layer observed in MPL. The revised paragraphs are given below:

“To understand the causes of the elevated dust maxima in the KAUST–MPL profiles at ~1–2 km altitude in the daytime and 5.5–7 km in the nighttime, we separately analyzed the profiles under a clear sky and dusty conditions. We define 'clear days' as the days with a daily mean of AOD at KAUST less than 0.25 and 'dusty days' as the days having daily-mean AOD greater than 0.75, using either MODIS AOD or AERONET AOD to maximize data availability during large-scale dust events.

Figure 12 shows the average extinction profiles for clear and dusty conditions from KAUST–MPL data for 2015/16 obtained using the above criteria. The daytime profile (Fig. 12, left) shows a similarly elevated dust loading at 1-2 km height, as noted earlier in Figures 10/11, but is much more prominent. Since 'dusty days' correspond to very high AOD conditions (AOD>0.75) expected during dust storms, we can infer that the observed elevated dust loading at 1-2 km corresponds to large-scale dust storms. Studies have shown that this shape is characteristic of dust profiles observed during large-scale dust events near land-ocean boundaries (Khan et al., 2015; Senghor et al., 2017). Marenco et al. (2018) also observed a similarly elevated dust loading over the eastern Atlantic at a comparable height in their airplane observations during the 'heavy dust' period.

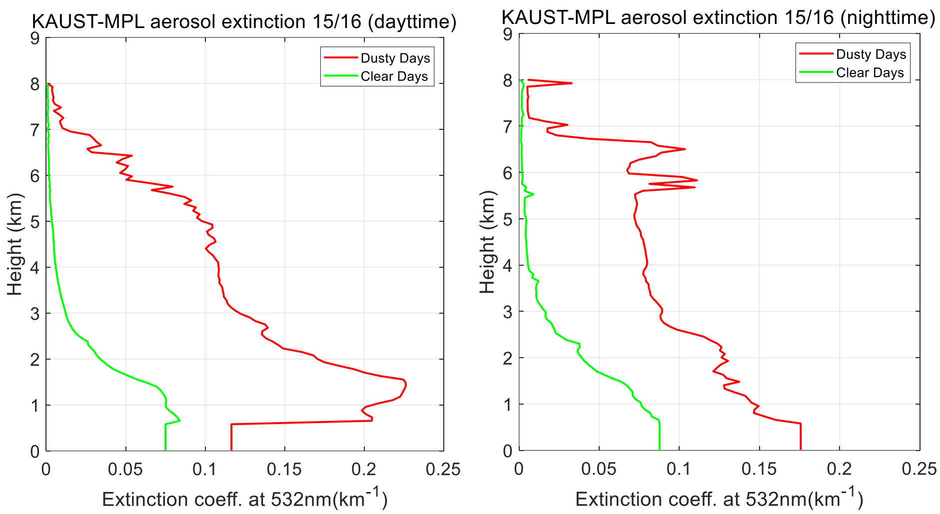

Figure 12. Average vertical profiles of aerosol extinction corresponding to ‘clear days’ and ‘dusty days’ from KAUST–MPL data.

The elevated dust layer during the nighttime at the height of 5.5–7 km observed earlier in summer and fall (Fig. 10/11) is present in the ‘dusty days’ and is absent in ‘clear days’ (Fig. 12, right). The above analysis again tells us that the high dust loadings at 5.5-7 km in the night are also associated with large-scale dust events. However, it becomes vital to understand the source of these large-scale, nighttime dust events. Based on our results, we suggest that this nighttime dust represents transported dust from inland deserts. More vigorous convection in the inland desert regions during the daytime carries aerosols to higher altitudes. Over deserts in summer, convection is most energetic in the afternoon. The planetary boundary layer height (PBLH) can reach well above 5 km (Fig. S5). By the evening, the dust is mixed thoroughly within the PBL by the strong convection (Khan et al., 2015). At night, the PBL weakens and breaks the capping inversion, which allows the dust-laden layer from the PBL to mix into the free troposphere and be transported to long distances. As an example, we noted such high intrusion of dust during the night of August 09 (21:00 and 02:00 UTC) in the LIDAR backscatter data of our case study (Fig. 9). The dust that lies above the PBL is ultimately carried to our site by the accelerated easterly geostrophic winds (Almazroui et al., 2018), and arrives at our site during the night. Therefore, the dust layers at 5-7 km observed in the nighttime likely represent dust of non-local origin transported from inland deserts at higher altitudes."

L521-522. It is normal that the vertical profiles look like each other as they are proportional, and if the cross-section is not very variable, we find the same vertical structures.

Agreed. We have now clarified the purpose of this comparison as below:

"We have presented these plots despite their broad resemblance to extinction profiles presented earlier (Fig. 11) because 'concentrations' are more useful from air quality perspective and MERRA-2 provides mixing ratios of different aerosols rather than extinctions."

L524. As before, the model gives higher values, such as MERRA. The exception is for winter where the agreement is better.

We agree. It could mean that WRF and MERRA have some common physical parametrizations, because of which they show similar features.

L548-550. That is a well-known feature.

We agree that this is well-known feature, but we keep this clarifying statement assuming that it will be helpful for some readers.

Sub-section L557. We return to the diurnal cycles as in section 3.2.

We have revised the heading and organization of the paper substantially and removed this repetition.

Figures 6a and 11b show the same information. Why can't we see the same shift over the winter months?

In Figure 6a, data represent DJF average of two years (2015/16), that means it is the average calculated using 6 months of data. Figure 11b is presented for model evaluation purpose and shows one-month average data for representative months. Because of this difference, variability is expected. The shift in winter is visible in Figure 11b as well, but it is not as strong. Shift appears to vary somewhat from year to year and in different months.

Figure 12. With a logarithmic colour scale the contrasts would stand out better. What are the temporal and vertical resolutions?

As suggested, we have plotted the figure with a logarithmic scale, as presented below.

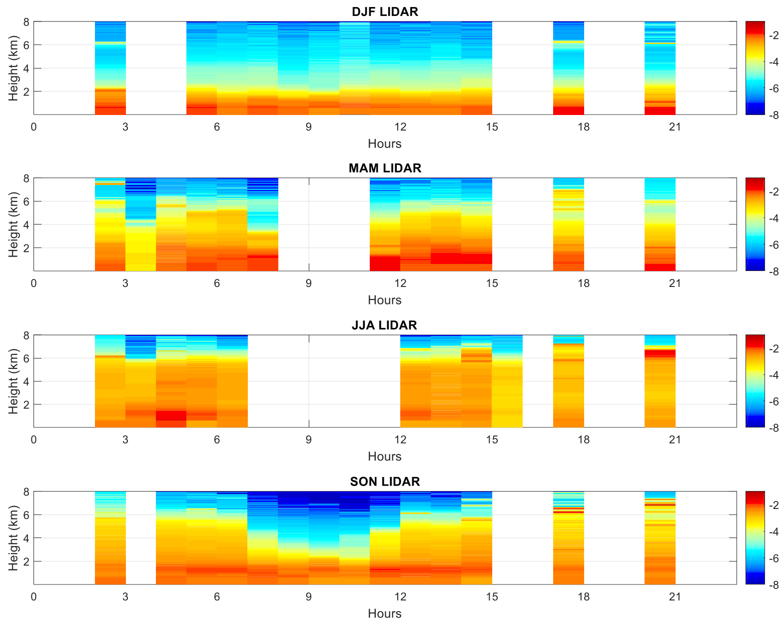

Figure 14. Diurnal profile of the natural logarithm of aerosol extinction coefficient at 532nm (km^{-1}) over the atmospheric column observed by the MPL at KAUST. Times are reported in UTC.

Regarding the temporal resolution, although the original backscatter data is available at a fine 1-minute resolution, because the GRASP algorithm processes only that data which satisfies its quality criteria, data timings are non-uniform. However, data points are close to be hourly. The measurement time of all KAUST–MPL data available for daytime fall between 0500 and 1500 UTC, and for nighttime data fall between 1700 to 0200 UTC, as mentioned in Figure 11 caption (revised manuscript). Vertical resolution is 75m as mentioned in section 2.2.1.

L581. The effect of the breeze has already been discussed; it should be grouped together.

We have revised the text as suggested.

L621-623. So, we don’t replicate what the lidar shows.

Not entirely. The peculiar elevated dust loading was not very obvious in the model, which we have mentioned in the paper.

L630-640. What is described here has already been described for different coastal environments,

such as during INDOEX.

Thank you for pointing this out. We have improved the discussion with a relevant reference (Rasch et al., 2001) as suggested.

L644-651. There were also significant differences in the profiles in Figure 8, and these should be discussed together.

We have compiled relevant discussion in the same place in section 4.2 of the revised manuscript.

L658. The altitude range of the land breeze is not sufficient to explain the low layer dust aerosols.

We agree. Land breezes themselves have a small role in generating that dust; they only mobilize and transport dust from the coastal area. The major portion of the elevated dust layer forms in dust events (haboobs or local dust storms) and is transported by harmattan winds (not the land breezes) to the coast. The height of the harmattan wind is consistent with the height of the elevated dust layer.

L660-666. A typical vertical wind profile would have been interesting.

We have looked at the vertical profile of wind speed. We found that the vertical profile of wind speed is not correlated with the vertical aerosol profiles, so it was not very useful to explain the dust loading at various altitudes. This is not surprising because our study area has a complex topography with bidirectional winds (land and sea breezes). Therefore, we preferred using wind vectors at different altitudes, as shown in Figures 13 and 15 (old version). Typical vertical wind profile plots are presented below:

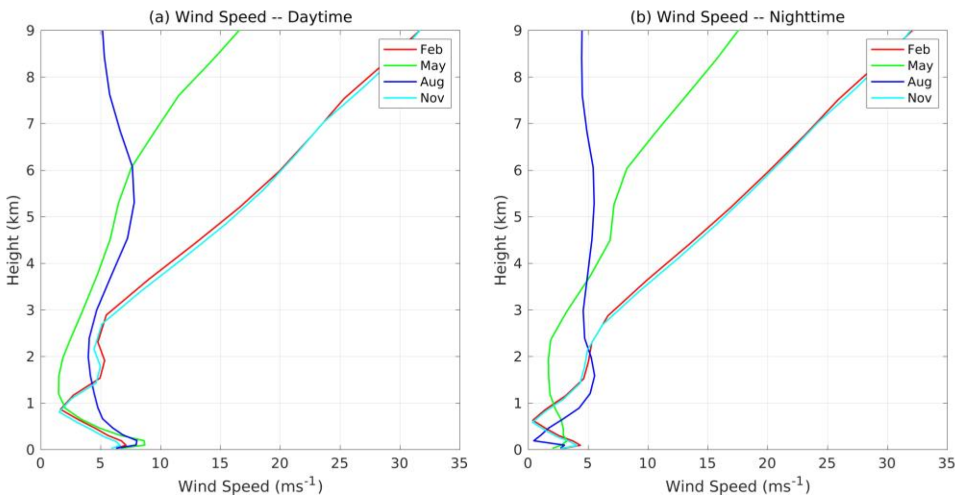

Figure 2. Vertical profile of simulated wind speed at KAUST.

L711-715. I thought that a haboob was rather generated following the collapse of thunderstorms

and the advection of moist air masses.

We believe that this comment refers to line 701-703, not 711-715. We agree. Downdrafts are invariably a part of thunderstorms. Moist air mass is essential, as mentioned. We believe our statement does not contradict your understanding.

L732. These AODs are much lower than the one announced in L684.

That is right; it is the second-largest dust event of the year 2015.

Section 4. This part is too long. The discussion should be separated from the conclusion. It can also be associated with the analysis of each key element of the article. The organization of the conclusion relating the work presented is confusing.

We have now revised the conclusions to make it consistent with the order material is presented in the paper. We also added the discussion section.

<u>Response to reviewer #3</u>

The overall objective of the paper is to "understand the vertical and diurnal profiles of aerosols over the eastern coast of the Red Sea." This overall aim if the paper is divided into four distinctive questions, the vertical profile, the diurnal and seasonal variation, the ability of WRF-chem to model the aerosols and how the prevailing land sea breezes affect the emissions and distribution of the dust over the study region. I believe this is a valuable scientific study that deserves to be published. The authors have employed appropriate data and analysis to answer the questions. Overall the structure of the paper need to be re-worked. The authors should consider grouping ideas in the paper in a more consistent manner. The authors need to ensure that the conclusion that they draw are substantiated in the evidence they present. A major short coming of the paper is the attempt to link the dust to the land –sea breeze system – This link is not made successfully. The discussion ignores the fact the there is a massive escarpment in the domain that rises to approximately 1500 m. Acknowledging and accounting for this in itself will not make the link between circulation and dust but cannot be ignored as the Land sea breeze system in this domain is complex and is partly driven by the topography. The link to the dust and the coastal zone completely ignores the fact that the topography will induce its own local and meso-scale wind systems. It is also unclear from the wind data presented when exactly the winds reach sufficiently high speeds to induce these dust storms. The average wind data never exceeds 8 m.s-1. Overall I would focus the paper on the objectives outlined in the paper without trying to link this to land-sea breeze circulations. Detailed comments follow below.

Thank you very much for your valuable comments. We agree that our paper would benefit from more logical restructuring. The other two reviewers also suggest it. Following the reviewers' comments, we have substantially revised the structure of our paper. We have grouped the results and conclusion in a more consistent, as suggested.

Regarding the link between dust and breezes, we agree that the relationship was not apparent because the results were scattered in different sections. We believe that with a new structure, this link is more evident now in the revised manuscript. We have also moved the summary sketch that we deduced from our results to the discussion section, which combines our findings on dust-breeze connections. Regarding the topographic effect, we extensively discuss them in Section 3.4 (Figure 14), in which the escarpment topography is displayed and discussed, along with its impact on dust concentration. The topography indeed affects the winds, which we have mentioned in the paper, and further clarified in the revised manuscript. We understand the concern about surface winds, which cause dust emission and depend on topography. However, breezes and coastal pain are not the main generators of dust. A lot of dust is transported from Arica and the eastern Arabian deserts. Our paper's focus is on aerosols' vertical profile, so we do not go into too much detail on those wind effects, which can be found in other previous studies (e.g., Davis et al., 2019) as mentioned in our paper.

During dust storms, winds are indeed much stronger, as shown in Figure 17 (case study, old version). The presented wind diurnal cycles show seasonal average wind speeds. Dust emission is caused by wind gusts that occur in a second-time scale, in which the winds reach much higher values. Considering your suggestion, we have added the following paragraph in section 4.1 of the revised manuscript:

"Note that dust emission is generally caused by wind gusts that occur in very short time scales (seconds) (Engelstaedt and Washington, 2007), which are much stronger than the average seasonal wind speed displayed in Figure 2. We can expect these wind gusts to be represented in our simulations because we have used a very small model time-step (8 sec) in our d03 domain. Given our focus on vertical aerosol profiles, further analysis of wind gusts is beyond this study's scope."

Title – I am not sure the title accurately reflects the overall objectives of the paper. The fundamental question posed by the authors is the vertical distribution and the diurnal and seasonal variability of aerosols of the study area. This is as stated by the authors. The land sea breeze is a driver of these two atmospheric aerosol characteristics. The prominence of land sea breezes as expressed in the title is not reflected in the current title of the paper. I suggest the authors re-consider the overall objectives of the paper or modify the title.

Thank you for this suggestion. We agree that our focus is on vertical profile and it should be reflected in the title. We have revised the title accordingly. The new title is presented below:

“Aerosol Vertical Distribution and Interactions with Land/Sea Breezes over the Eastern Coast of the Red Sea from LIDAR Data and High-resolution WRF-Chem Simulations.”

Line 36 – “the LIDAR data: : :: : :remote inland desserts.” – The paper provides no evidence that the dust is transported from remote inland dessert sources. In fact the model domain of the dust emissions don’t even extend to these areas.

The d03 domain covers the desert areas near the observation site, where local dust is likely to be transported. Dust generated in deserts further inland also affects the Red Sea coastal plain. The parent domains d02 and d01 cover the entire MENA region, so dust emission represents the whole region in our simulations. The vertical cross-section (figure 16) from the case study presented in the paper shows dust transported from inland deserts, typical to our observation site.

Figure 1 is could be improved by adding a map of the study region. The current figure 1 could be moved to later in the article where the land-sea breeze is discussed which the authors refer to in line 155.

Figure 1 summarizes the features of breezes and their interaction with dust investigated in this study. The Red Sea and the Sarawat mountains are clearly marked in the illustration. As suggested, we have moved this figure to the discussion section.

Line 172 – The author’s should add details of the KAUST station. It would be very useful to see the actual location on one of the maps. Also what is the altitude of the station and distance from the coast for example as well as the length of the data series?

We have marked KAUST site in several figures (Figures 13, 14, 16, and 17, old version). Altitude, location or distance from the coast is visible in Figure 14 (old version). We have added the lat/lon coordinates of the station in the introduction section as suggested. The length of the data is depicted in the respective figures (Figure 3, 6a, and 11a), in the old version of the manuscript.

Line 216-231 is very difficult to follow. The authors could consider rewording this para-graph to capture the method is a clearer manner. This could be improved by adding more details to the method in this section.

We totally agree. We have revised this section now with some added information about GRASP processing. Please refer to response to reviewer #2 or the revised manuscript section 2.2.2.

Line 227 constraints should be constrains and "do not" should be "does not"

This line has been revised.

Line 232-236 – this paragraph is not entirely connected to the previous paragraph and does not stand alone where it is. The authors mention quality constraints applied to the LIDAR data but don't mention what these were or refer to a publication that documents this process.

The paragraph discusses the resolution of the dataset, which is, we believe, is the relevant information. We have added a reference to the quality constraints applied, as suggested.

Figure 2. The colored section of the figure representing the dust source is too small to be useful to the reader at all. If the dust source function is important (which it is) then the authors should add an additional map to show this clearly.

We agree that the dust sources are not very clear in this Figure. In this figure, we are showing the domains only. The same dust source map is presented in Figure 13 (old paper version), in which the dust sources are clearly visible.

The level of detail in the WRF-Chem model methodology section is not consistent with the detail provided for the other data sets. The authors should consider balancing these sections so that all the study methods are well documented for future studies.

Some additional information is added regarding WRF-Chem methodology as suggested, particularly about PBL scheme. Please refer to the revised manuscript. More details of the WRF-Chem model settings are provided in the online repository as mentioned in the data availability section.

Line 326 – two years of data does not constitute a climatology.

We agree. This was also pointed by reviewer #2. We have now avoid using the term 'climatology' in the revised manuscript.

Line 327 and 329 need to be expanded. It is not clear what this means exactly.

We rephrased this paragraph as suggested.

Line 337-339 – It is not clear why the authors think the mismatch at this stage is due to sampling and measurement frequencies. The most obvious mismatches are the highest peaks of the AOD values seen in the measurements and not in the model AOD. This explanation premature and not convincing given the model temporal resolution or not accurate or both.

We agree with this point. That is why we use the word 'partly' in our explanation. We have explained the cause of these discrepancies further in the new discussion section.

Line 387-391 requires a reference.

We have now added several references as suggested. The revised paragraph reads as follows:

“The coarse mode primarily corresponds to mineral dust (silt) that originates locally and from inland deserts, northeast Africa, and the Tigris-Euphrates source region (Kalenderski and Stenchikov et al., 2016; Parajuli et al., 2019). The composition of the fine mode is much more complex, but usually includes clay particles transported over long distances and anthropogenic aerosols from pollution sources (mainly as sulfate) (Chin et al., 2007; Hu et al., 2016; Prospero et al., 1999). The size distributions of sulfate and sea salt aerosols are presented in the supplementary information (Figs. S3 and S4).”

Line 393-394 should be re-worded.

We have moved this text to the section 2.1, study site, after rephrasing, as suggested.

Line 396-398 – I am not sure that this sentence does justice to the complex transport associated with this process. Land-sea breezes are local scale wind systems that in the case of this study area could become embedded into to meso-scale winds. The link to long-range transport beyond those scales are complex and associated with multiple embedded systems within regional scale transport. The land-sea breeze mechanism is only a small component of that transport process.

We completely agree with the reviewer. Land breezes are only a local-scale circulation subsystem in a meso-scale circulation pattern. The sentence was misleading so we removed it. Thank you for pointing this out.

Line 403-404 –the authors need to be specific about what the impacts might be of dust and include references here. Do these impacts have any bearing on the land-sea breeze system directly or on the results of this study?

Thank you for this careful observation. We agree with your comment and we have revised these lines adding appropriate references. In the first line, we mention general impacts of dust on local climate and in the second line we talk specifically about land-sea breeze. See below:

“Because dust/aerosols are present over the study site for most of the year, they can also interact with the meteorology and thus affect atmospheric winds and temperature at different time scales (Jacobson et al., 2006; Rémy et al., 2015). Land or sea breezes are strongly coupled with dust/aerosols and temperature variability, especially near the surface (Crouvi et al., 2017).”

It would be interesting to see the diurnal temperature pattern of shore of the site. The flat temperature cycle is not ideal for the establishment of a strong land sea breeze system. What creates the temperature gradient shift between daytime and night-time between the land and the sea?

We agree with the reviewer. The station is located close to the Sea, so the station data appear flatter because of the influence of the sea surface temperature. Further inland, the diurnal cycle is much stronger. The breeze circulation is driven by the difference between sea surface temperature and land temperature in the coastal region. For your reference, we have plotted the comparison of the model-simulated diurnal profile of temperature from two adjacent pixels, one on the Sea and another one on land. Clearly, the land profile shows a more robust diurnal cycle, and the temperature contrast in the night drives the land breezes. We have mentioned this earlier in section 2.1. Considering your suggestion, we have added the following text in the revised manuscript and figure S1 in the supplement.

"The time profiles of air temperature (Fig. 2b) are relatively flat, showing a weak diurnal cycle. Winter reveals the most pronounced diurnal cycle. The temperature contrast between day and night is minimal in summer and maximum in winter. The weak diurnal cycle observed in the station-measured temperature is because of the influence of SST, since the station is located very close to the sea. The diurnal cycle of land temperature becomes much stronger as we go further inland in the coastal region (Figure S1), creating a strong temperature gradient between the ocean and the land surface, which ultimately drives the breeze circulation."

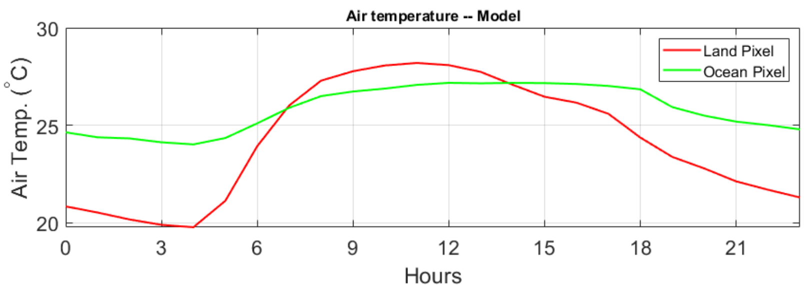

Figure S1. Comparison of diurnal cycle of model-simulated 2-m air temperature between ocean and land pixel near KAUST site for Nov 2015."

Line 421 – 423- in terms of temperature this is not a justified statement. Even in terms of wind speed data the difference between the day and night values id 6 m.s-1 in MAM while in DJF it is at most 4 m.s-1. These differences may be significant in this region but you need to show that. The figure and text earlier points to a weak diurnal temperature cycle in all seasons.

With the added description in response to the earlier comment, we believe that it is justified. Regarding winds, we show average seasonal values. The differences in daily winds are much larger. The difference in wind speed that observed by the reviewer are indeed large. Considering the reviewer's suggestion, we have added the following discussion in section 4.1:

"Accurately representing the surface winds is vital because the dust emission is parameterized as a function of friction wind velocity in WRF-Chem (Marticorena and Bergametti, 1995; LeGrand et al., 2019). Note that dust emissions are generally caused by wind gusts that occur over very short time scales (seconds) (Engelstaedt and Washington, 2007), which are much stronger than the average seasonal wind speed displayed in Figure 2. We can expect these wind gusts to be represented in our simulations because we have used a very small model time-step (8 sec) in our d03 domain. Given our primary focus is on vertical aerosol profiles, further analysis of wind gusts is beyond this study's scope."

Line 426-428 –describing all the aerosols as limited to the height of troposphere is not very useful and not a finding that is noteworthy. The vertical profiles of aerosol data in the absence of a vertical temperature profile I believe is difficult to interpret.

There is no simple relationship between temperature and aerosol vertical profile, so the temperature's vertical profile will only partially help in our interpretation. The aerosol (and potential temperature) are mixed up within the unstable desert boundary layer that could reach 6-7 km in height. The aerosol profile is also affected by long-range transport. Please read our full response on this issue against line 506-511.

Line 455-456 – This needs data or a reference to validate this (or a reference). Also I think you need to refine this discussion as I do not see the same trends as you above 2 km for the two data sets.

We have revised this section as suggested and moved it to the new discussion section added to the revised manuscript. Regarding the reference, this is a general argument based on boundary layer principles, so we do not have any specific reference.

Line 471 – 472 - The model does not show this layer in the daytime either. In fact the layer is observed in the nigh-time and not in the daytime in the MPL data.

We agree. We have revised this paragraph to clarify this issue as below:

"KAUST–MPL data show a distinct aerosol layer located between 5.5 and 7 km, especially in the nighttime, summer, and the fall. The model does not show such dust layers. KAUST–MPL daytime data show a typically elevated maximum of dust extinction in the PBL centered around 1.5 km altitude. The model does not identify such a dust loading profile either. The KAUST-MPL and model profiles agree better in the daytime than in the nighttime, and in winter compared to other seasons. However, there are no significant differences between daytime and nighttime profiles in the model. Note that the shape of the profile is reversed during the nighttime, which the model reproduces weakly. We explore this particularly interesting shape of the extinction profile at ~1–2 km in the daytime in section 3.4. As discussed later, these unique features of the profiles are related to the effect of land/sea breezes and topography."

Line 473-474 – The model daytime and night-time profiles are not very different. I think it is a stretch to infer the model reproduces anything with such a result. The model profile is pretty static for each of the categories graphed. This is over interpretation these data. This should be re-worked.

We agree. We have revised this discussion as suggested, please the revised text in response to the preceding comment.

Line 506-511 – I can't agree with this explanation at all. This requires additional work and temperature profile data to substantiate all the assumptions. The PBL does not break at night and the capping inversion is not broken at night as this is driven in the summer by large scale subsidence which is not dependent on day night changes. The PBL is likely to drop in the evening and possibly a alternative inversion layers form that might trap and concentrate aerosols above. But my explanation is also speculation as it would be easy to see this mechanism from vertical temperature profile data at the very least from the model.

In the paper, we have used this argument as a possible mechanism. Our argument is mainly based on the analysis of LIDAR data. We partially see this mechanism in effect from the model results as well during the case study. We agree that the language that we used was not reflecting the fact that it was our suggestion or speculation. We have now substantially revised this paragraph, as reviewer #2 had also suggested.

Regarding the capping inversion, it can be described in different time scales -- from diurnal to seasonal. Here, our discussion is on diurnal-scale inversion. Inversion layers can possibly trap aerosols in some cities with weak winds, but may not in the desert regions with strong turbulence.

Considering the reviewer's suggestion, we have plotted the vertical profile of temperature during the day and night for the month of August. Remind that he elevated dust layers at 6-7 km height were most prominent in summer (JJA) nights. In the temperature profile, we observed weak temperature inversion within 6-8 km as the reviewer expected, which would possibly be clearer with a higher vertical resolution of the model. We have now revised the explanation to make it clearer, as presented below:

"However, it becomes vital to understand the source of these large-scale, nighttime dust events. Based on our results, we suggest that this nighttime dust represents transported dust from inland deserts. More vigorous convection in the inland desert regions during the daytime carries aerosols to higher altitudes. Over deserts in summer, convection is most energetic in the afternoon. The planetary boundary layer height (PBLH) can reach well above 5 km (Fig. S5). By the evening, the dust is mixed thoroughly within the PBL by the strong convection (Khan et al., 2015). At night, the PBL weakens and breaks the capping inversion (Fig. S6), which allows the dust-laden layer from the PBL to mix into the free troposphere and be transported to long distances. As an example, we noted such high intrusion of dust during the night of August 09 (21:00 and 02:00 UTC) in the LIDAR backscatter data of our case study (Fig. 9). The dust that lies above the PBL is ultimately carried to our site by the accelerated easterly geostrophic winds (Almazroui et al., 2018), and arrives at our site during the night. Therefore, the dust layers at 5-7 km observed in the nighttime likely represent dust of non-local origin transported from inland deserts at higher altitudes."

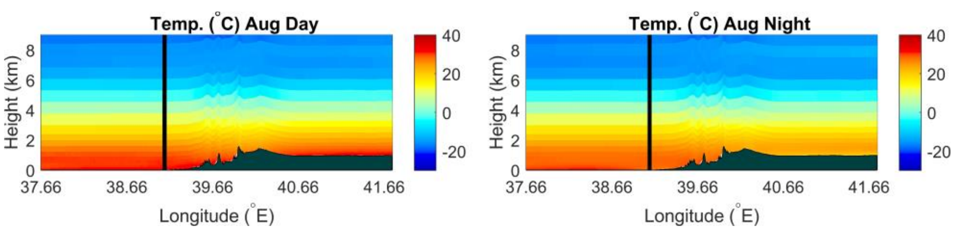

Figure S6. Vertical profile of temperature during the day and night in summer. An inversion layer is visible in the night at ~6-8 km."

Line 541-Line 550 – This has no context. I don't follow where this has come from in the discussion.

Thank you for this suggestion. We agree that the discussion of particle size was not relevant here. We have revised and moved this part to the discussion section in the revised manuscript.

Figure 10 - Does not provide a new information about the vertical profile of the aerosols. I am not sure why this discussion could not be combined with the previous section.

Regarding Figure 10, the comparison is made with additional data (MERRA-2) in terms of Mixing Ratio; MERRA provides mixing ratios of different aerosols included in our model simulations. Further, concentration ($\mu g\ m^{-3}$) is more relevant from an air quality perspective. Considering your suggestion, we have revised Figure 10 caption, mentioning the aerosol types used from the model and MERRA.

Line 568-577 – I am not sure why this was not discussed earlier in the paper in con-junction with figure 6. Also the model and the observations have some real differences in terms of the time of the minimum and maximum values for the different months pre-sented. I think this could be r-worded to more accurately describe what is observed. Again – one year of data is not a climatology!

This is the diurnal profile of aerosols in the whole vertical column, not directly relevant to the surface data presented earlier in Figure 6. Regarding model and observation comparison, this level of agreement is very good. We agree that there are some differences as you noted but still the shift in different season is well simulated by the model. Regarding the climatology, we have already responded earlier.

Figure 13 – I am not sure that the land –sea breeze can be described as covering the entire area of your domain given in Figure 13. Especially if one takes into account that mountainous area lies at about 40 deg E. The wind on the eastern side of the mountainous terrain is almost certainly not associated with land-sea breeze mechanisms anymore but rather on topography induced wind cycles. On the coastal side of the mountains the distance to the coast is about 100 km. Again there has to be a topography component to the wind system in this region which is strengthened by the land sea breeze mechanism.

We completely agree with you on this. Although the whole domain is shown, the breezes are strongest in the coastal region. While addressing your comment, we discovered a small bug in our processing script because of which the land breeze vectors were not displayed correctly. We have updated Figure 13 in the revised manuscript and the high winds look more sensible now, which are confined near the coastal region only. In the schematic diagram (Figure 18, revised manuscript), we have not represented the breeze circulation on the lee side of the mountains.

Line 611-651 – in light of the above I believe this all requires some careful consideration and re-working.

We agree. After revisiting the text, we found some contradictory points in 637-640, which we have corrected based on the reviewer's suggestion.

Line 652-666 – this discussion completely ignores the fact that there is an enormous 1.5 km high escarpment sitting in the middle of the domain. This needs to be ac-counted for in this discussion. The last section of the paper is useful in presenting the occurrence of the high dust events observed in figure 3 that are not captured by the model. This could receive more attention taking into account all the comments above.

We have discussed the possible effect of topography in lines 656/657 and 659 (old version) along with Figure 14 (old version). Considering the reviewer's suggestion, we have added a discussion on how the breezes affect the dust during the case study, section 3.3.2, as presented below:

"When the dust-laden harmattan winds arrive at the Red Sea coast, they encounter the land or sea breezes depending upon the time of arrival, as discussed further in section 4.3. When they meet with the opposite sea breeze flow, the air mass rises up, bringing the dust to the upper levels. Such higher intrusion of dust is evident in the KAUST-MPL data (Figure 9, left) in the afternoon, during which the sea breezes are most active. The suspended dust is still visible in the upper levels (~2-3 km) in the night of August 10, because the dust particles have not been deposited yet."

The discussion and conclusions need to be revised after the changes are made to the paper.

We have separated the discussion and conclusions, as suggested, and considerably modified the text.

Note: Revised manuscript with track changes at the end of this file.

References

Abshire, J. B., Sun, X., Riris, H., Sirota, J. M., McGarry, J. F., Palm, S., Yi, D., and Liiva, P.: Geoscience Laser Altimeter System (GLAS) on the ICESat Mission: On-orbit measurement performance, Geophys. Res. Lett., 32, L21S02, https://doi.org/10.1029/2005GL024028, 2005.

Ansmann, A., Wagner, F., Müller, D., Althausen, D., Herber, A., von Hoyningen-Huene, W., and Wandinger, U., European pollution outbreaks during ACE 2.: Optical particle properties inferred from multiwavelength lidar and star-Sun photometry, J. Geophys. Res., 107(D15), https://doi.org/10.1029/2001JD001109, 2002.

Boesenberg, J., et al.: The German Aerosol Lidar Network: Methodology, Data, Analysis, Report/Max-Planck Institut für Meteorologie, 317, http://hdl.handle.net/21.11116/0000-0003-2DEF-F, 2001.

Chaikovsky, A., Ivanov, A., Balin, Y., Elnikov, A., Tulinov, G., Plusnin, I., Bukin, O. and Chen, B.: Lidar network CIS-LiNet for monitoring aerosol and ozone in CIS regions, In Twelfth Joint International Symposium on Atmospheric and Ocean Optics/Atmospheric Physics, 6160, 616035), International Society for Optics and Photonics, 2006.

Collins, W. D., Rasch, P. J., Eaton, B. E., Khattatov, B. V., Lamarque, J.-F., and Zender, C. S.:, Simulating aerosols using a chemical transport model with assimilation of satellite aerosol retrievals: Methodology for INDOEX, J. Geophys. Res., 106(D7), 7313–7336, https://doi.org/10.1029/2000JD900507, 2001.

Fekih, A. and Mohamed A.: Evaluation of the WRF model on simulating the vertical structure and diurnal cycle of the atmospheric boundary layer over Bordj Badji Mokhtar (southwestern Algeria), Journal of King Saud University - Science, Volume 31(4), 602-611, https://doi.org/10.1016/j.jksus.2017.12.004, 2019.

Guerrero-Rascado, J. L. et al.: Latin American Lidar Network (LALINET) for aerosol research: Diagnosis on network instrumentation, Journal of Atmospheric and Solar-Terrestrial Physics, 138–139, 112-120, https://doi.org/10.1016/j.jastp.2016.01.001, 2016.

Heese, B., and Wiegner, M.: Vertical aerosol profiles from Raman polarization lidar observations during the dry season AMMA field campaign, J. Geophys. Res., 113, D00C11, https://doi.org/10.1029/2007JD009487, 2008.

Kalenderski, S. and G. Stenchikov, G.: High-resolution regional modeling of summertime transport and impact of African dust over the Red Sea and Arabian Peninsula, J. Geophys. Res. Atmos., 121, 6435–6458, https://doi.org/10.1002/2015JD024480, 2016.

Lebel, T., Parker, D.J., Flamant, C., Bourlès, B., Marticorena, B., Mougin, E., Peugeot, C., Diedhiou, A., Haywood, J.M., Ngamini, J.B., Polcher, J., Redelsperger, J.-L. and Thorncroft, C.D.: The AMMA field campaigns: multiscale and multidisciplinary observations in the West African region, Q.J.R. Meteorol. Soc., 136, 8-33, https://doi.org/10.1002/qj.486, 2010.

Omar, A.H., Winker, D.M., Vaughan, M.A., Hu, Y., Trepte, C.R., Ferrare, R.A., Lee, K.P., Hostetler, C.A., Kittaka, C., Rogers, R.R. and Kuehn, R.E.: The CALIPSO Automated Aerosol Classification and Lidar Ratio Selection Algorithm, J. Atmos. Oceanic Technol., 26, 1994–2014, https://doi.org/10.1175/2009JTECHA1231.1, 2009.

Pappalardo, G., Amodeo, A., Apituley, A., Comeron, A., Freudenthaler, V., Linné, H., Ansmann, A., Bösenberg, J., D'Amico, G., Mattis, I. and Mona, L.: EARLINET, Atmos. Meas. Tech., 8, 2389-2409, https://doi.org/10.5194/amt-7-2389-2014, 2014.

Rasch, P. J., Collins, W. D., and Eaton, B. E.: Understanding the Indian Ocean Experiment (INDOEX) aerosol distributions with an aerosol assimilation, Journal of Geophysical Research, 106(D7), 7337–7355, https://doi.org/10.1029/2000JD900508, 2001.

Saide, P. E., Carmichael, G. R., Spak, S. N., Gallardo, L., Osses, A. E., Mena-Carrasco, M. A., and Pagowski, M.: Forecasting urban PM10 and PM2.5 pollution episodes in very stable nocturnal conditions and complex terrain using WRF–Chem CO tracer model, Atmos. Environ., 45, 2769-2780, https://doi.org/10.1016/j.atmosenv.2011.02.001, 2011.

Fountoukis, C., Ayoub, M.A., Ackermann, L., Perez-Astudillo, D., Bachour, D., Gladich, I. and Hoehn, R.D.: Vertical Ozone Concentration Profiles in the Arabian Gulf Region during Summer and Winter: Sensitivity of WRF-Chem to Planetary Boundary Layer Schemes, Aerosol Air Qual. Res., 18, 1183-1197, https://doi.org/10.4209/aaqr.2017.06.0194, 2018.

Shimizu, A., Nishizawa, T., Jin, Y., Kim, S.-W., Wang, Z., Batdorj, D., and Sugimoto, N.: Evolution of a lidar network for tropospheric aerosol detection in East Asia, Opt. Eng. 56(3), 031219, https://doi.org/10.1117/1.OE.56.3.031219, 2016.

Welton, E. J. , Voss, K. J., Quinn, P. K., Flatau, P. J., Markowicz, K., Campbell, J. R., Spinhirne, J. D., Gordon, H. R., and Johnson, J. E.: Measurements of aerosol vertical profiles and optical properties during INDOEX 1999 using micropulse lidars, J. Geophys. Res., 107(D19), 8019, https://doi.org/10.1029/2000JD000038, 2002b.

Welton, E.J., Voss, K.J., Gordon, H.R., Maring, H., Smirnov, A., Holben, B., Schmid, B., Livingston, J.M., Russell, P.B., Durkee, P.A., Formenti, P. and Andreae, M.O.: Ground-based lidar measurements of aerosols during ACE-2: instrument description, results, and comparisons with other ground-based and airborne measurements, Tellus B, 52, 636-651, doi:10.1034/j.1600-0889.2000.00025.x, 2000.

Winker, D. M., Couch, R. H., and McCormick, M. P.: An overview of LITE: NASA's Lidar In-space Technology Experiment, in Proceedings of the IEEE, 84(2), 164-180, https://doi.org/10.1109/5.482227, 1996.

Winker, D.M., Vaughan, M.A., Omar, A., Hu, Y., Powell, K.A., Liu, Z., Hunt, W.H. and Young, S.A.: Overview of the CALIPSO Mission and CALIOP Data Processing Algorithms, J. Atmos. Oceanic Technol., 26, 2310–2323, https://doi.org/10.1175/2009JTECHA1281.1, 2009.

~~Interaction of~~Aerosol Vertical ~~Profiles and Dust Aerosols~~~~their~~Distribution ~~and its~~and Interactions with Land/Sea Breezes over the Eastern Coast of the Red Sea from LIDAR Data and High-resolution WRF-Chem Simulations

Sagar P. Parajuli[1*], Georgiy L. Stenchikov[1], Alexander Ukhov[1], Illia Shevchenko[1], Oleg Dubovik[2], and Anton Lopatin[3]

[1]King Abdullah University of Science and Technology, Thuwal, Saudi Arabia

[2]Univ. Lille, CNRS, UMR 8518 - LOA - Laboratoire d'Optique Atmosphérique, F-59000 Lille, France

[3]GRASP-SAS, Remote Sensing Developments, Université de Lille, Villeneuve D' ASCQ, 59655, France

[*]Corresponding Author, E-mail: psagar@utexas.edu

Abstract

With advances in modeling approaches and the application of satellite and ground-based data in dust-related research, our understanding of the dust cycle has significantly improved in recent decades. However, two aspects of the dust cycle, namely the vertical profiles and diurnal cycles, are not yet adequately understood, mainly due to the sparsity of direct observations. Measurements of backscattering caused by atmospheric aerosols have been ongoing since 2014 at the King Abdullah University of Science and Technology (KAUST) campus using a micro-pulse Lidar~~IDAR~~ (MPL) with a high temporal resolution. KAUST is located on the east coast of the Red Sea~~ (22.3° N, 39.1° E)~~, and currently hosts the only operating LIDAR system in the Arabian Peninsula. We use the data from the~~is~~ ~~LIDAR~~ MPL together with other collocated observations and high-resolution simulations (with 1.33 km grid spacing) from Weather Research and Forecasting model coupled with Chemistry (WRF-Chem)~~ model simulations~~ to study the ~~following aspects of aerosols~~following three aspects of dust~~,~~ ~~with a focus on dust~~ over the Red Sea ~~Arabian~~ coastal plains. ~~Firstly, we investigate the vertical profiles of aerosol extinction and concentration in terms of their seasonal and diurnal variability.~~ ~~Secondly~~Firstly, we ~~evaluate how well the WRF~~ compare ~~Chem model performs~~the model simulated~~ in representing~~ surface winds, aerosol optical depth (AOD), and aerosol size distributions with observations, and ~~the vertical distribution of aerosols~~ evaluate the model performance in representing a typical large-scale dust event over the study site. ~~Firstly~~Secondly, we investigate the vertical profiles of aerosol extinction and concentration in terms of their seasonal and diurnal variability. Thirdly, we explore the interactions between dust aerosols and land/sea breezes, which are the most influential components of the local diurnal circulation in the region.

The WRF-Chem model successfully reproduced the diurnal profile of surface wind speed, AOD, and dust size distributions over the study area compared to observations. The ~~WRF-Chem~~ model ~~successfully~~also captured the onset, demise, and height of a large-scale dust event that occurred in 2015, as compared to the LIDAR data. The vertical profiles of aerosol extinction in different seasons were largely consistent between the ~~LIDAR~~MPL data and~~, MERRA-2 reanalysis, and CALIOP data, as well as in the~~ WRF-Chem simulations along with key observations and reanalyses used in this study. We found a substantial variation in the vertical profile of aerosols in different seasons, and between ~~. We also discovered a marked difference in the~~ daytime and nighttime~~ vertical distribution of aerosols at the study site~~, as revealed by the ~~LIDAR~~ MPL data. The ~~LIDAR~~ MPL data also identified a prominent dust layer at ~5–7 km during the nighttime, which likely represents~~ed~~ the long-range transported dust brought to the site by the easterly flow from remote inland deserts.

~~The vertical profiles of aerosol extinction in different seasons were largely consistent between the LIDAR, MERRA-2 reanalysis, and CALIOP data, as well as in the WRF-Chem simulations.~~ The sea breeze circulation was much deeper (~2 km) than the land breeze circulation (~1 km), but both breeze systems prominently affected the distribution of dust aerosols over the study site. We observed that sea breezes push the dust aerosols upwards along the western slope of the Sarawat Mountains. These sea breezes~~, which~~ eventually collide with the dust-laden northeasterly trade winds coming from nearby inland deserts, thus causing elevated dust maxima at a height of ~1.5 km above sea level over the mountains. Moreover, the sea and land breezes

intensify~~ied~~ dust emissions from the coastal region during the daytime and nighttime, respectively. ~~The WRF-Chem model successfully captured the onset, demise, and height of a large-scale dust event that occurred in 2015, compared to LIDAR data.~~ Our study, although focused on a particular region, has broader environmental implications as it highlights how aerosols and dust emissions from the coastal plains can affect the Red Sea climate and marine habitats.

1. Introduction

Dust aerosols, which mainly originate from natural deserts and disturbed soils such as agricultural areas, have implications for air quality (Prospero, 1999; Parajuli et al., 2019) and the Earth's climate (Sokolik and Toon, 1996; Mahowald et al., 2006; Prakash et al., 2014; Bangalath and Stenchikov, 2015; Kalenderski and Stenchikov, 2016; Di Biagio et al., 2017). The Arabian Peninsula represents a key area within the global dust belt where significant dust emissions occur~~take place~~ in all seasons. However, the spatio-temporal characteristics of dust emissions in the region have not yet been fully described, partly because of the sparsity of observations. Although our understanding of the dust cycle and the related physical processes has substantially improved in recent decades (Shao et al., 2011), in the present context, two aspects of dust aerosol dynamics remain the least explored: the vertical structure and the diurnal cycle. Understanding the vertical structure is important because the vertical distribution of aerosols affects the radiative budget~~effects~~ (Johnson et al., 2008; Osipov et al., 2015) and surface air quality (Chin et al., 2007; Wang et al., 2010; Ukhov et al., 2020a). ~~Similarly~~Moreover, understanding the diurnal cycle of aerosols is important because aerosols scatter and absorb radiation (Sokolik and Toon, 1998; Di Biagio et al., 2017), which ultimately affects the land and sea breezes in coastal areas. L~~On the other hand, l~~and and sea breezes, which are the key diurnal-scale atmospheric processes ~~in~~ over the ~~region~~Red Sea coastal plain, can also affect the distribution and transport of aerosols (Khan et al., 2015) and ~~, as well as~~ their composition (Fernández-Camacho et al., 2010; Derimian et al., 2017).

The vertical distribution of aerosols in the atmosphere has been studied for decades using LIDAR measurements from several ground-based sites, aircraft, and satellite platforms, covering different regions across the globe. Several satellites are equipped with LIDAR to measure the vertical distribution of aerosols. Lidar In-space Technology Experiment (LITE) was the first space lidar launched by NASA in 1994 onboard the Space Shuttle, providing a quick snapshot of aerosols and clouds in the atmosphere on a global scale (Winker et al., 1996). LITE was followed by the Geoscience Laser Altimeter System (GLAS) containing a 532-nm LIDAR, as part of the Ice, Cloud and Land Elevation Satellite (ICESat) mission, which covered the polar regions (Abshire et al., 2005). Cloud-Aerosol Lidar with Orthogonal Polarization (CALIOP) onboard CALIPSO (Cloud-Aerosol Lidar and Infrared Pathfinder Satellite Observations) currently observes aerosol and clouds globally during both the day and night portion of the orbit with a 16-day repeat cycle since 2006 (Winker et al., 2013). Apart from satellites, several field experiments have also been conducted using LIDAR to measure the vertical distribution of aerosols. The Indian Ocean Experiment (INDOEX) field campaign (Collins et al., 2001; Rasch et al., 2001; Welton et al., 2002b) took place in 1999 over the Indian Ocean, Arabian Sea, and the Bay of Bengal, in which an MPL system together with other instruments measured aerosol distribution in the troposphere. Similarly, an MPL system was employed in the Second Aerosol Characterization Experiment (ACE-2) in 1997 over Tenerife, Canary Islands, to understand the vertical distribution of dust/aerosols transported from North Africa and Europe to the Atlantic Ocean (Welton et al., 2000; Ansmann et al., 2002). African Monsoon Multidisciplinary Analysis (AMMA), one of the largest international projects ever carried out in Africa, also measured aerosol vertical distribution using multiple LIDAR systems for a short period in 2006 (Heese and

Wiegner, 2008; Lebel et al., 2010). Currently, several other coordinated LIDAR networks are operating in different regions. They include the European Aerosol Research Lidar Network EARLINET (Pappalardo et al., 2014), German Aerosol Lidar Network (Boesenberg et al., 2001), the Latin American Lidar Network LALINET (Guerrero-Rascado et al., 2016), the Asian dust and aerosol lidar observation network AD-Net (Shimizu et al., 2016), and the Commonwealth of Independent States Lidar Network CIS-LiNet (Chaikovsky et al., 2006).

~~Insert LIDAR review here~~

Formatted: Font color: Red

A micro-pulse LIDAR (MPL) has been operating at King Abdullah University of Science and Technology (KAUST), Thuwal, Saudi Arabia (22.3° N, 39.1° E), since 2014. This LIDAR is collocated with the KAUST AERONET (Aerosol Robotic Network) station. The KAUST MPL site is a part of the Micro-Pulse Lidar Network (MPLNET), maintained by the NASA Goddard Space Flight Center (GSFC) (Welton et al., 2001; Welton et al., 2002a~~1~~). KAUST hosts the only LIDAR site on~~in~~ the ~~Arabian Peninsula~~Red Sea coast, and its colocation with the AERONET station facilitates the retrieval of the vertical profile of aerosols more accurately. Stations that measure a range of parameters of interest for dust-related research (including dust deposition rate, vertical profile, near-surface concentration, and spectral optical depth) are rare across the global dust belt. In addition to the LIDAR and AERONET station, KAUST also has a meteorological station that measures wind speed, air temperature, and incoming short-wave and long-wave radiative fluxes. These collocated data provide an opportunity to get a more complete picture of dust emissions and transport in the region.

The study site ~~Being located in an arid region, large-scale dust events are~~ frequently experienced~~s~~ large-scale dust events~~over the study site~~. ~~However,~~The satellite and ground-based observations such as AERONET have some limitations, because of which they are likely to miss some important details of these dust events. For example, many large-scale dust events are accompanied by cloud cover, which restricts the retrieval of aerosol optical properties in the visible bands (Fernández et al., 2019). Extreme dust events are nonetheless important from a research perspective because they provide an opportunity to understand the associated physical processes. AERONET stations and passive satellite sensors are further limited because they cannot retrieve aerosol properties during the night. LIDARs help to overcome these limitations because they provide high-frequency measurements, even at night. Furthermore, LIDAR signals can penetrate thin and multilayer clouds, which are usually overlooked by passive satellite sensors (Winker et al., 1996; Winker et al., 2009), thus improving the detection of aerosol layers at different altitudes. Therefore, LIDAR data are essential for understanding the diurnal variability of aerosols and their climatic effect~~AERONET stations and passive satellite sensors are further limited because they cannot retrieve aerosol properties during the night. LIDARs help to overcome these limitations because they provide high-frequency measurements even in the night, and their signal can penetrate thin and multilayer clouds (Winker et al., 1996) thus improving the detection of aerosol layers at different altitudescloud cover does not directly affect~~

~~their retrievals. Thereforehus, LIDAR data are essential for understanding the diurnal variability of aerosols and their climatic effect~~.

The location of the Red Sea between the two key dust source regions of North Africa and the Arabian Peninsula provides a unique opportunity to understand the multi-faceted aspects of aerosol-climate interactions that occur in the region. KAUST is located on the eastern coast of the Red Sea, and dust is indeed the dominant aerosol type in this region (Prakash et al., 2014; Kalenderski and Stenchikov, 2016). The sea and land breezes that occur during the day and night, respectively, are the dominant drivers of local air mass circulations (Jiang et al., 2009). Sea breezes facilitate the transport of moisture inland and contribute to the formation of cumulus clouds and mesoscale convection (Davis et al., 2019). The land and sea breezes can themselves also generate dust emissions from the coastal regions (e.g., Crouvi et al., 2017), and also interact with atmospheric dust aerosols in multiple ways.

In this study, we attempt to understand the vertical and diurnal profiles of aerosols over the eastern coast of the Red Sea. We use our multiple collocated datasets collected at KAUST to shed light on the various facets of local-scale dust-climate interactions in the region. Since land and sea breezes are fine-scale features modulated by local topography, high-resolution simulations are essential to resolve these circulations. Therefore, we conduct high-resolution simulations (with 1.33 km grid spacing) using WRF-Chem that interactively accounts for aerosol generation, transport, and deposition to understand the nature of these circulations and their interaction with aerosols. In summary, we aim to answer the following specific research questions:

1. How does ~~WRF-Chem~~the model simulations ~~perform at~~ representing the vertical distribution of aerosols over the study site?
~~1.~~2. How are aerosols distributed in the vertical column over the study site at KAUST?
~~2.~~3. What is the seasonal or diurnal variability in the vertical distribution of aerosols?
~~3.~~~~1.~~~~How does WRF-Chem perform at representing the vertical distribution of aerosols over the study site?~~
4. How do prevailing land and sea breezes affect dust emissions and distribution over the study site?

This paper is organized as follows. We present a description of datasets and methods in section two, where we describe the observational datasets used and the WRF-Chem model settings ~~applied~~. In section three, we present the results. More specifically, we explore the first and second ~~and second~~ research questions listed above in sections 3.2 and 3.3, respectively. Results presented in sections 3.~~3~~2 and 3.4 ~~and 3.5~~ are relevant to the third research question. Section 3.~~5~~4 addresses the fourth question. ~~Finally, w~~We present a general discussion of the results ~~conclusions in section four,~~ along with the limitations of our research ~~and a more~~in section 4. Finally, we present the key conclusions in section 5. ~~general discussion of the results.~~

Formatted: Tab stops: 4.15", Left
Formatted: Font color: Auto
Formatted: Font color: Auto
Formatted: Font color: Auto
Formatted: Font color: Auto
Formatted: Font color: Auto
Formatted: Font color: Auto
Formatted: Font color: Auto
Formatted: Font color: Auto
Formatted: Font color: Auto

~~2.~~ 2. Data and Methods

Formatted: No bullets or numbering

2.1. Study site

The KAUST campus is located in the western Arabian Peninsula, on the east coast of the Red Sea (22.3° N, 39.1° E). This area is affected by local dust storms originating from surrounding inland deserts, by ~~non-local~~distantly-generated dust ~~dust storms arriving from~~ arriving from northeast Africa through the Tokar gap (see, for example, Kalenderski and Stenchikov 2016; Albugami et al., 2019; Kumar et al., 2019), and by dust from as far away as the Tigris-Euphrates regions (Parajuli et al., 2019). Therefore, dust is present in the atmosphere over the study site for ~~most of~~ the entire year.

Although our focus in this study is on dust aerosols, which are the dominant aerosol over~~in~~ the study site (Prakash et al., 2014; Parajuli et al., 2019; Ukhov et al., 2020a), some additional aerosol types also contribute to the aerosol loading at KAUST. Our site is located on the coast; thus, sea salt aerosol, which is of natural origin, inevitably contributes considerably to the atmospheric aerosol loading. Furthermore, the study site has several industrial areas nearby that produce anthropogenic emissions of sulfur dioxide (SO_2),~~,~~ and black and organic carbon (BC and OC) (Ukhov et al., 2020a).

~~Land and sea breezes affect dust aerosol emissions and transport in our study region. When the land and sea breezes are strong, they can cause dust emission from the active dust sources of the coastal regions. The land and sea breezes also transport the emitted dust either towards the ocean or towards the land, depending on the direction of the breeze. Moreover, land breezes can help to transport dust emitted from inland deserts and remote areas during large-scale dust events to the ocean (Prakash et al., 2014).~~

~~Because dust/aerosols are present over the study site for most of the year, they can also interact with the meteorology and thus affect atmospheric winds and temperature at different time scales. Land and sea breezes are strongly coupled with dust/aerosols and temperature variability, especially near the surface.~~

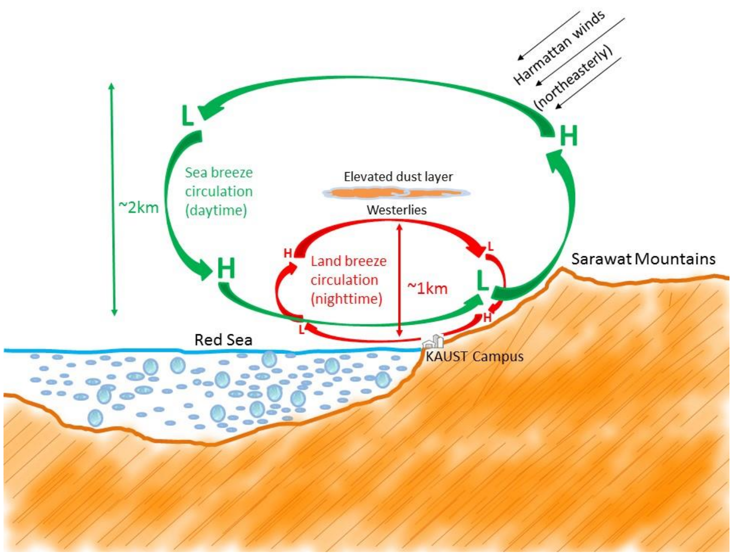

~~Figure 1. Schematic diagram showing sea breeze (daytime, in green) and land breeze (nighttime, in red) circulations and dust distribution over the study site at KAUST.~~

Because the site is located exactly at the land-sea~~ocean~~ boundary, some unique small-scale processes exist that affect the local climate of this region. For instance, land and sea breezes affect the distribution of dust in the atmosphere over the study site. The desert land heats up during the day, which consequently heats the surface air above the land. This warm air mass rises due to convection, creating a local ~~low~~ pressure 'low' at the surface. The cooler and more moist air over the Red Sea then flows towards the low pressure zone, thus forming sea breezes (Simpson, 1994; Miller et al., 2003; Davis et al., 2019). During the night, this flow is reversed to form land breezes, when the land surface temperature cools quicker than the sea surface temperature. Because these breezes are driven by the thermal contrast between the land and the sea, their strengths vary by season. These breezes are further enhanced because of their coupling with slope winds ~~that are~~ generated on the Sarawat Mountains, which run along the western coast of the entire Arabian Peninsula (Davis et al., 2019).

Land and sea breezes affect dust aerosol emissions and transport in our study region. When the land and sea breezes are strong, they can cause dust emission from the coastal regions. Although breezes are not responsible for long-range transport, they can affect the local distribution of dust aerosols over the study site.

Because dust/aerosols are present over the study site for most of the year, they can also interact with the meteorology and thus affect atmospheric winds and temperature at different time scales (Jacobson et al., 2006; Rémy et al., 2015). Land or sea breezes are strongly coupled with dust/aerosols and temperature variability, especially near the surface (Crouvi et al., 2017).

Formatted: Font color: Auto, Pattern: Clear

Formatted: Tab stops: 4.15", Left

Formatted: Font color: Auto, Pattern: Clear

Formatted: Font color: Auto

~~***The salient features of the land and sea breezes over the study region are presented in Fig. 1, which we discuss in detail later.***~~

Formatted: Font: Bold, Italic, Complex Script Font: Bold, Italic

Formatted: Paper, Tab stops: Not at 4.15"

2.2. Observations

We use several datasets~~, described below,~~ to evaluate our model simulations and derive the ~~climatology of the~~average season profiles of aerosol ~~and~~ loading and surface winds ~~for the years~~during 2015-2016, as described below. ~~.~~

2.2.1. Datasets

We collected meteorological data, including wind speed, temperature, and humidity from a tower established at KAUST in 2009 in collaboration with WHOI (Woods Hole Oceanographic Institution) (Farrar et al., 2009; Osipov et al., 2015).

We use cloud-free aerosol extinction profiles retrieved from ~~a~~ CALIOP ~~(Cloud-Aerosol Lidar with Orthogonal Polarization) instrument~~ onboard CALIPSO ~~(Cloud-Aerosol Lidar and Infrared Pathfinder Satellite Observations)~~ for analyzing the vertical structure of aerosols at the study site. CALIPSO is flown in a sun-synchronous polar orbit and is a part of NASA's Afternoon (A-train) constellations (Stephens et al., 2018). ~~CALIOP acquires observations during both the day and night portion of the orbit with a 16-day repeat cycle.~~ We use level-3 day/night aerosol data v3.00, which are monthly aerosol products generated by aggregating level-2 monthly statistics at 2° (lat) × 5° (long) resolution (Winker et al., 2013). The data have 208 vertical levels up to a height of 12 km above sea level.

We also analyze aerosol optical depth (AOD) data from the AERONET station at KAUST (Holben et al., 1998). We use a level 2.0 ~~version~~ data of directly measured AOD values (direct sun algorithm), which are cloud-screened and quality-assured. From AERONET, we also use an aerosol number density and a particle size distribution (PSD) obtained by inversion (Dubovik et al., 2000) to characterize the aerosol particles in the region. We use the AERONET V3, level 2.0 product, which provides volume concentration of aerosols in the atmospheric column in 22 bins between 0.05 and 15 microns in radius (Dubovik et al., 2000; Parajuli et al., 2019; Ukhov et al., 2020a).

We use Moderate Resolution Imaging Spectroradiometer (MODIS) level-2 Deep Blue AOD data (Hsu et al., 2004), which are available daily, for the whole globe, at a resolution of ~ 0.1°× 0.1°. We use the latest version of the MODIS dataset (collection 6) (Hsu et al., 2013) because of its extended coverage and improved Deep Blue aerosol retrieval algorithm, compared to its earlier version (collection 5). We process AOD data of both Terra and Aqua satellites on a daily basis, and use the average of the two data products for our analysis. From MODIS, we also use the true color images for a qualitative analysis of a dust event.

We adopt the Modern-Era Retrospective Analysis for Research and Applications version 2 (MERRA-2) data (Rinecker et al., 2011) for comparing the model simulated AOD and dust concentrations. Aerosol data from the MERRA-2 dataset assimilate several satellite observations, including MODIS AOD (Gelaro et al., 2017). We specifically use tavg1_2d_aer_Nx and inst3_3d_aer_Nv products for getting 2-d AOD/Dust Optical Depth (~~/~~DOD) data and 3-D aerosol concentrations, respectively. MERRA-2 data consist of 72 vertical model levels between ~0.23 to 79.3 km.

We also employ 555nm column AOD from MISR onboard Terra satellite archived under collection MIL3DAE_4, which is a daily product available at 0.5x0.5 degree resolution (Diner, 2009). Because MISR has a wider view with nine viewing angles, MISR identifies thin aerosol layers more accurately and is more sensitive to the shape and size of particles (Kahn et al., 2005).

We also use the RGB composite from SEVIRI (Spinning Enhanced Visible and Infrared Imager) instrument onboard the geostationary Meteosat satellite, which is a composite prepared from specific infrared channels that are sensitive to the presence of dust in the atmosphere (Ackerman, 1997; Schepanski et al., 2007). Dust appears ‘pink’ in these composite images and is thus distinguishable from clouds, which are usually shown in yellow, red, or green.

2.2.2. LIDAR data

Micropulse LIDAR is a fully autonomous active remote-sensing system in which a laser transmitter emits light vertically upward, and an optical sensor receives the backscattered signals. The numbers and the detection time of the backscattered photons provide information about the aerosols and clouds in the atmosphere. We established ~~T~~the LIDAR site~~located~~ on the KAUST campus~~, which is also~~as a part of the MPLNET network~~,~~ in 2014.~~ ~~It operates at a wavelength of 532nm. The data from this LIDAR (hereafter called KAUST–MPL) is the main basis of this paper.

The colocation of the KAUST–MPL and AERONET station provides an opportunity to get a more comprehensive microphysical picture when the MPL data are combined with AERONET sun-photometer measurements. We employ GRASP (Generalized Retrieval of Aerosol and Surface Properties, Dubovik et al., 2011, 2014), which is an open-source inversion code that combines different types of remote sensing measurements, such as radiometer and LIDAR observations, to generate fully consistent columnar and vertical aerosol properties (Lopatin et al., 2013). We take aerosol characteristics from the AERONET retrieval including size distribution, absorption, scattering optical depth, and refractive index. These parameters serve as inputs to GRASP, together with MPL data, to generate height-resolved aerosol fields such as aerosol extinction, absorption, and mixing ratios.~~The colocation of the KAUST–MPL and AERONET station provides a more comprehensive microphysical picture when combined with AERONET sun-photometer measurements. We retrieve height-resolved aerosol properties, including aerosol extinction, absorption, and mixing ratios from the KAUST–MPL. We employ GRASP (Generalized Retrieval of Aerosol and Surface Properties, Dubovik et al., 2011, 2014), which is an open-source inversion code that combines different types of remote sensing measurements, such as radiometer and LIDAR observations, to generate fully consistent columnar and vertical aerosol properties (Lopatin et al., 2013).~~

We ~~use~~combine cloud-screened AERONET radiances and LIDAR backscatter signals~~ combined~~ to retrieve aerosol properties during the daytime. As ~~the~~ AOD data are unavailable during the night, for nighttime retrievals, we use a so-called multi-pixel approach, first introduced by Dubovik et al. (2011) and implemented in GRASP. According to this approach, the retrieval is implemented using a group of observations representing different time and location (e.g., several satellite pixels), ~~in order~~ to retain the variability of the retrieved parameter. For example, in this study, we invert the closest AERONET measurements obtained the day before and the day after, together with the nighttime LIDAR backscatter data, under some constraints on the temporal variability of the columnar parameters (size distribution, complex refractive index, and sphericity fraction) provided by AERONET measurements. In contrast to other ~~simpler~~more straightforward retrieval approaches used currently, the multi-pixel technique constraint~~s~~ the retrieval without eliminating the variability within the data. The implemented retrieval approach allows us to retain the variability of columnar properties throughout the night. This approach ~~is in~~ contrasts with the retrieval approach adopted by Benavent-Oltra et al. (2019), ~~in~~ which ignores the variability of columnar properties during the night ~~is ignored~~.

The GRASP algorithm relies on an external cloud masking. Overnight lidar retrievals are performed only when cloud-free AERONET sun-photometric observations are available in the preceding evening and following morning. The AERONET cloud-masking algorithm is considered the golden standard, providing very reliable filtering of thick and broken clouds (Holben et al., 1998). In this regard, only clouds that form specifically at night and are undetectable by sun-photometric observations in the evening and morning could influence our~~the~~ retrieved extinction profiles. At the same time, retrieval of these profiles, to a large extent, relies on detailed columnar aerosol properties retrieved before and after nighttime observations. An attempt to retrieve cloudy profiles under the assumption of cloud-free aerosol columnar properties should result in higher fitting errors, and therefore should be easily detectable.

~~We use cloud-screened AERONET radiances and LIDAR backscatter signals combined to retrieve aerosol properties during the daytime. As the AOD data are unavailable during the night, for nighttime retrievals, we use a so-called multi-pixel approach, first introduced by Dubovik et al. (2011) and realized in GRASP. According to this approach, retrieval is implemented for a group of observations (e.g., several satellite pixels). coordinated in time or/and in space (e.g., several satellite pixels). Correspondingly, the quality of the retrievals can be improved by using some additional a priori constraints on the time-varying aspect of the retrieved parameters. For example, in this study, we invert the closest AERONET measurements obtained the day before and the day after, together with the nighttime LIDAR backscatter data, under some constraints on the temporal variability of columnar parameters (size distribution, complex refractive index, and sphericity fraction) provided by AERONET measurements. In contrast to other similar but simpler retrieval approaches used currently, multi-pixel concept constraints, but do not eliminate possible variability between parameters. For example, in this study, the implemented retrieval allows us to observe the variability of columnar properties during the night. In contrast, in similar retrieval realized by Benavent-Oltra et al. (2019), any variability of columnar properties through the night was not considered.~~

The retrieved aerosol data has 100 levels in the vertical dimension with a resolution of 75m from 505m to 7700m above sea level. The processed LIDAR extinction data has some data gaps because of the quality constraints applied and cloud filtering (Dubovik et al., 2011). To achieve a complete diurnal picture, we also analyze the raw data of the normalized relative backscatter (NRB) from KAUST-MPL, which gives the total backscatter from both aerosols and clouds at a fine~~,~~ 1-min resolution.

2.~~2~~3. WRF-Chem model set up

We use WRF-Chem (v3.8.1) with some recent updates (Ukhov et al., 2020c) for simulating the emission and transport of dust and other aerosols at high resolution at the study site. The innermost domain (d03), which is marked by a red box in Fig. ~~2~~1, is centered at KAUST and has a fine resolution of 1.33 km, which is required to resolve the essential features of local wind circulation and breezes. The innermost domain is encompassed by a second domain (d02) having a resolution of 4 km that covers the entire Arabian Peninsula. Although the western boundary of domain d03 appears close to that of d02, there are 40 grid cells in between, which is ~~10~~ten times higher than generally recommended, and is sufficient to ensure a smooth transition across the boundaries. While a further westward extension of d02 could be desirable to better resolve the synoptic weather phenomena across the Red Sea e.g., through the Tokar gap (Kalenderski and Stenchikov 2016), such phenomena have a minor impact on the diurnal-scale local sea breeze circulation in our site, which is the focus of our study. To allow full aerosol exchange and cover all major sources of dust in the region, we nest the two inner domains within a larger domain (d01) with a 12 km resolution, which covers the entire Middle East and North Africa (MENA) region shown in Fig. 1. The key physics and chemistry options used in WRF-Chem are presented in Table 1.

~~synoptic weather phenomena across the Red Sea, e.g., through Tokar gap (Kalenderski and Stenchikov 2016), such phenomena have minor impact on the diurnal-scale, local sea breeze circulation in our site, which is the focus of our study. To allow full aerosol exchange and cover all major sources of dust in the region, we nested the two inner domains within a larger domain (d01) with 12 km resolution, which covers the entire Middle East and North Africa (MENA) region shown in Fig. 2. The key physics and chemistry options used in WRF-Chem are presented in Table 1.~~

~~The model top is set at 100 hPa, and the model has 30 vertical levels between ~20 m to 16 km. To better represent winds, we apply 'grid nudging' on the u (zonal velocity) and v (meridional velocity) components of wind above the planetary boundary layer (PBL) in all three domains (Parajuli et al., 2019). We do not use any convective parameterization scheme and resolve deep convection in the innermost domain. We employ two-way nesting, which means that the parent domain provides boundary conditions for the nest, and the nest provides feedback to the parent domain. The model time steps are set to 72, 24, and 8 seconds for the three domains d01, d02, and d03, respectively.~~

Formatted: Tab stops: Not at 4.15"

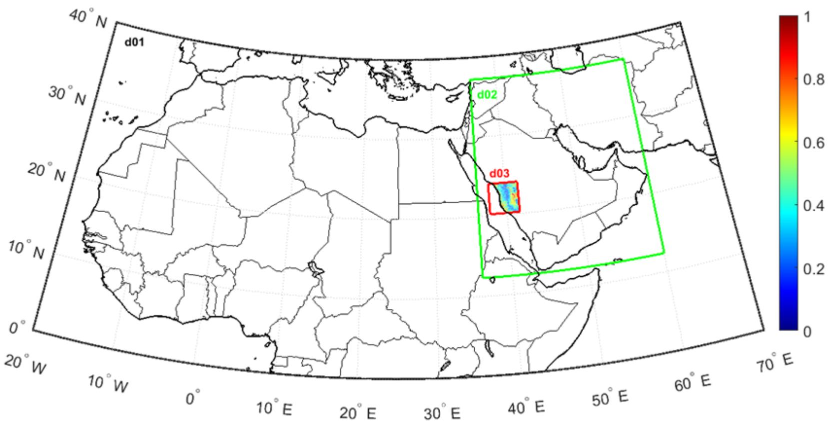

Figure ~~2~~1. The study region over the Red Sea showing the three nests d01 (black), d02 (green), and d03 (red) used in WRF-Chem simulations. The base map within d03 shows the high-resolution dust source function (Parajuli and Zender, 2017) used in this study, in which the values range from zero to one, with the highest value representing the strongest dust source.

Table 1. Details of key physics and chemistry namelist settings used in WRF-Chem.

Description		**Namelist Options**	**References**
Physics	Microphysics	mp_physics = 2	Lin et al. scheme
	Planetary Boundary Layer (PBL) scheme	bl_pbl_physics = ~~2~~1	Yonsei University, YSU (Hong, Noh, and Dudhia, 2006)~~MYJ (Janjic, 1994)~~
	Surface layer physics	sf_sfclay_physics = 2	Monin-Obukhov (Janjic Eta)
	Land Surface Model	sf_surface_physics = 2	Unified Noah land surface model (Chen and Dudhia, 2001)
	Cumulus parameterization	cu_physics = 0 (turned off)	
	Radiative transfer model	ra_lw_physics = 4, ra_sw_physics = 4	Rapid radiative transfer model (RRTMG) (Iacono et al., 2008)
Chemistry	Chemistry option	chem_opt = 301	GOCART coupled with RACM-KPP
	Dust scheme	dust_opt = 3	GOCART with AFWA changes (LeGrand et al., 2019)
	Photolysis scheme	phot_opt = 2	Wild et al., 2000

Formatted: Font: 10 pt, Complex Script Font: 10 pt

Formatted: Font: 10 pt, Complex Script Font: 10 pt

Formatted: Font: 10 pt, Complex Script Font: 10 pt

Formatted: Font: 10 pt, Complex Script Font: 10 pt

Formatted Table

The model top is set at 100 hPa ~~, and the model~~ has 30 vertical levels between ~20 m to 16 km. To ~~better~~ represent winds better, we apply ‘grid nudging’ on the u (zonal velocity) and v (meridional velocity) components of wind above the planetary boundary layer (PBL) in all three domains (Parajuli et al., 2019). We do not use any convective parameterization scheme and resolve deep convection in the innermost domain. We employ two-way nesting, which means that the parent domain provides boundary conditions for the nest, and the nest provides feedback to the parent domain. The model time steps are set to 72, 24, and 8 seconds for the three domains d01, d02, and d03, respectively.

Several studies compare the performance of PBL schemes in WRF, showing mixed results under different model settings (e.g., Saide et al., 2011; Fountoukis et al., 2018; Fekih and Mohamed, 2019). However, these studies have not directly compared the aerosol vertical profiles. Preliminary results showed that the choice of the PBL parameterization did not have a significant impact on the vertical distribution of aerosols in our case. In our simulations, we use the YSU PBL scheme, which is one of the most commonly used schemes, as suggested in the literature (e.g., Fountoukis et al., 2018; Fekih and Mohamed 2019).

We use high-resolution operational analysis data from ECMWF (~15 km) to provide initial and boundary conditions in our model, which are updated every 6 hours. The sea surface temperature (SST) values are also updated in our simulations, using the same ECMWF dataset.

We employ the Global Ozone Chemistry Aerosol Radiation and Transport (GOCART) aerosol scheme in our simulations (Chin et al., 2002). For calculating dust emissions, we use the AFWA dust scheme, which follows the original GOCART dust scheme (Ginoux et al., 2001) modified to account for saltation (Marticorena and Bergametti, 1995; LeGrand et al., 2019). It is important to represent the dust sources at a fine-scale to capture the smaller-scale physical processes accurately. Therefore, we use a recently developed high-resolution sediment supply map (SSM) as the source function (Parajuli and Zender, 2017; Parajuli et al., 2019) in all three model domains. We adopt the tuning process of the dust model described in Parajuli et al. (2019). We tuned the model against CALIOP DOD and the same tuning coefficients obtained from Parajuli et al. (2019) are used in all domains, including the added third domain, which are 0.136, 0.196, 0.120, and 0.110, for DJF, MAM, JJA, and SON, respectively.

We consider dust, sea salt, sulfate, and black and organic carbon (BC and OC) aerosols in our simulations. Biomass burning and biogenic aerosols are not important over the region, and thus we do not include them.

Sea salt emissions in WRF-Chem follow the parameterization developed by Monahan et al.~~,~~ (1986) and Gong (2003). In this parameterization, the rate of sea salt emissions produced via whitecaps and wave disruption is given as a function of particle size and 10-m wind speed.

We take the anthropogenic emissions of OC and BC from the most recent version of EDGAR (Emission Database for Global Atmospheric Research) database v4.3.2 available at 0.1°x0.1° resolution (Crippa et al., 2018). The EDGAR database is a global database that provides gridded emission maps of several greenhouse gases and air pollutants from 1970-2012. We use OC and BC emissions data from 2012.

Sulfur dioxide (SO_2) is of particular concern because it chemically transforms in the atmosphere into secondary sulfate, which is an important and influential aerosol at our study site (Ukhov et al., 2020a, Ukhov et al., 2020b). To achieve a more accurate representation of sulfate aerosols, we use the SO_2 emissions from a time-varying (monthly) inventory developed by NASA for the same year (2015). This SO_2 inventory is developed by combining satellite-based estimates from the ozone monitoring instrument (OMI) with the ground-based inventory developed by the Task Force Hemispheric Transport Air Pollution (HTAP) (Janssens-Maenhout et al., 2015), which provides a more accurate gridded emission dataset with greater spatial and temporal coverage. The data has global coverage with 0.1x0.1 degree resolution (Liu et al., 2018). This dataset does not account for SO_2 emissions produced by ships; therefore, we take ship SO_2 emissions from the EDGAR v4.3.2 dataset. OMI-HTAP emissions in WRF-Chem are satisfactorily reproduced by the observed SO_2 loading in the Middle East region (Ukhov et al., 2020~~a~~b).

We activate both gas and aerosol chemistry in our simulations (gaschem_onoff = 1, aerchem_onoff = 1) and apply the aerosol chemistry options in all three domains.

To determine the contribution of each aerosol species on total AOD, we modify the WRF Chem code, mainly the Fortran ~~files~~ subroutines in *optical_driver.F* and *chem_driver.F* located under the chem folder. For this purpose, we calculate aerosol optical properties twice, first with the mixture containing all aerosols and second after removing a specific aerosol. This calculation is implemented in the subroutine "*optical_averaging*". Thus, we obtain the contribution of specific aerosol species on total AOD by subtracting the AOD obtained without a specific aerosol from the total AOD calculated when all aerosols are accounted for. ~~Note that this method assumes no internal mixing of aerosols.~~

We calculate the total aerosol concentration (TAC) in $\mu g\ m^{-3}$ by summing up the individual concentrations of all aerosol species~~, viz., dust, sea salt, sulfate (SO_4), OC, BC, and other components of PM~~. The equation used to calculate the total aerosol concentration from the standard output variables of WRF Chem is presented below.

TAC ($\mu g\ m^{-3}$) = [(DUST_1+DUST_2+DUST_3+DUST_4+DUST_5) + (SEAS_1+SEAS_2+SEAS_3+SEAS_4) + (OC1+OC2) + (BC1+BC2) + P10 + P25] × 1/ALT + sulf × 1/ALT × 1000 × 96/29.

where, DUST_1…DUST_5 are the dust mass mixing ratios ($\mu g\ kg^{-1}$) in five different size bins; SEAS_1….SEAS_4 are the sea salt mass mixing ratios ($\mu g\ kg^{-1}$) in four different size bins; P10 and P25 are other anthropogenic PM10 and PM2.5 mass mixing ratios ($\mu g\ kg^{-1}$), respectively; OC1 and BC1 are mass mixing ratios ($\mu g\ kg^{-1}$) of hydrophobic organic carbon and black carbon, respectively; OC2 and BC2 are mass mixing ratios ($\mu g\ kg^{-1}$) of hydrophilic organic carbon and black carbon, respectively; sulf is the SO_4 volume mixing ratio (ppmv), ALT is the inverse of air density ($m^3\ kg^{-1}$), and 96/29 is the ratio of the molecular weights ($g\ mol^{-1}$) of sulfate and air.

We conduct the model simulations for the entire year of 2015 on a monthly basis (for computational reasons). For each month, the model simulations start a week before the month begins, and we discard the data from this week as spin-up. We use data for 2015 only for the comparison of the model results with other datasets. However, we use the entire two years of data (2015-16) to derive the ~~climatology~~seasonal profiles. Because we aim to explore the diurnal cycles, we use hourly model output data for analysis. ~~To~~ While comparing point measurements~~e~~ ~~the~~ (LIDAR and ~~other station~~meteorology data) with gridded datasets, we use data ~~corresponding~~ from one~~to a~~ grid cell containing the KAUST site from all gridded datasets.

3. Results

Formatted: No bullets or numbering

3.1. Surface Meteorology

Formatted: Space After: 12 pt

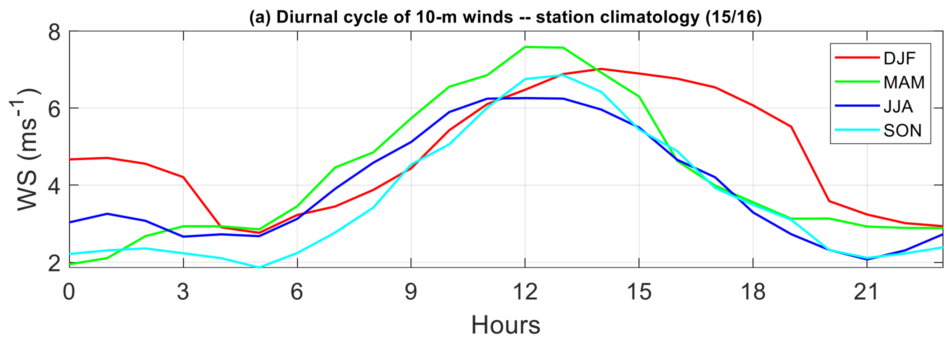

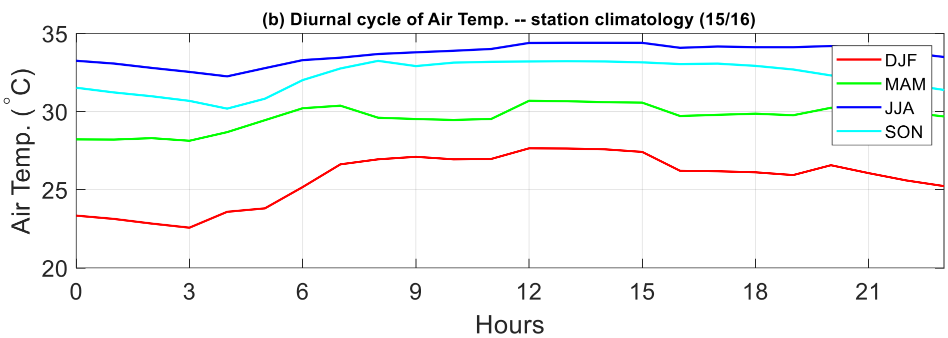

Figure 2~~6~~. (a) Mean diurnal cycle (2015/16) of surface wind speed (WS) and air temperature measured at 10-m height at KAUST station. Times are reported in UTC.

Formatted: Font color: Auto

Formatted: Font color: Auto

Figure ~~6~~2a shows the mean diurnal cycle (2015/16) of station-measured surface wind speed at the study site. The surface winds reach a peak around noon UTC (15:00 local time) for all seasons except winter, consistent with the results of Davis et al. (2019). The aforementioned sea breezes cause these wind peaks in the afternoon. Note that these sea breezes originate at sea and advance landward to reach the coast only later in the afternoon (Estoque et al., 1961), where they are measured at our station. In winter, the wind speed profile shifts to the right, peaking later in the day at around 14:00 UTC. This shift to later in the day occurs because, in winter, it takes more time to reach the required thermal contrast ~~required~~ between the land and the sea ~~for the formation of~~to form sea breezes. Note the existence of a second peak in the wind speed plot during the night, around 01:00 UTC, ~~which~~ representing~~s~~ the land breezes. These land breezes are stronger in winter than in the other seasons.

The time profiles of air temperature (Fig. 2b) are relatively flat, showing a weak diurnal cycle. Winter reveals the most pronounced diurnal cycle. The temperature contrast between day and night is minimal in summer and maximum in winter. The weak diurnal cycle observed in the station-measured temperature is because of the influence of SST, since the station is located very close to the sea. The diurnal cycle of land temperature becomes much stronger as we go further inland in the coastal region (Figure S1), ~~. This~~ creating~~es~~ a strong temperature gradient between the ocean and the land surface, which ultimately drives~~ing~~ the breeze circulation. ~~2 The weak diurnal cycle observed in the station-measured temperature is because of the influence of SST, since the station is located very close to the sea. The diurnal cycle of land temperature becomes much stronger as we go further inland in the coastal region (Figure S1). This creates strong temperature gradient between the ocean and the land surface, which ultimately drives the breeze circulation.~~

Given the strong diurnal cycles of surface winds and temperature, it is evident that the day and night circulation in the study area is remarkably different. Therefore, it becomes important to look at the aerosol vertical profiles separately in the day and night~~ time~~.

3.2. Model ~~validation~~evaluation

Formatted: No bullets or numbering

3.2.1. Surface winds

Formatted: No bullets or numbering

Formatted: Font: Italic, Complex Script Font: Italic

Figures 3~~11~~a and ~~11~~3b show the diurnal cycle of 10m wind speeds compared with the model simulations and station data at KAUST for individual months from different seasons chosen to represent the four seasons. The profiles are in good agreement, although the model slightly overestimates the wind speed magnitudes. Nevertheless, the model captures the seasonal variation of wind speed well. These results indicate that our high-resolution simulations effectively reproduce local features of wind circulations.

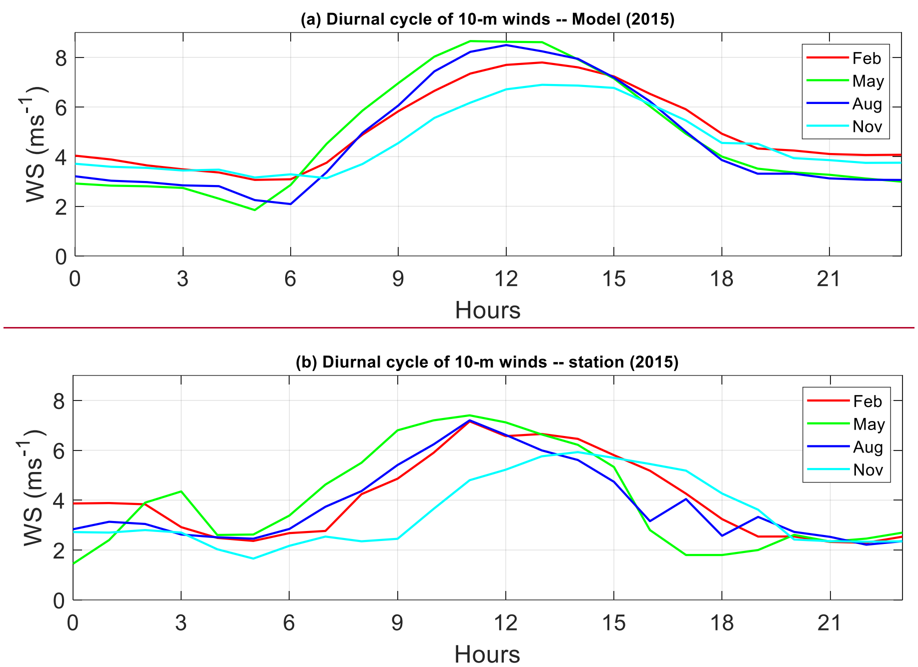

Figure ~~11~~3. (a) Average diurnal cycle (2015) of 10-m winds at KAUST for four different months representing each season from (a) model and (b) station. Times are reported in UTC.

~~**3.**~~

3.~~1~~2.2. Comparison of AOD and aerosol volume concentrations

Figure ~~3~~ 4 shows the model-simulated time series of total columnar AOD at KAUST obtained using daily-average values, compared with several datasets, including AERONET, MODIS, MISR, and MERRA-2. For the model and MERRA-2 data, we only use the daytime data (between 7 AM and 7 PM local time) to make them consistent with AERONET, MODIS, and MISR data. In general, all data are consistent and show similar temporal patterns, except during some large-scale dust events. ~~The model reproduces the AOD time series well in all seasons. There is some mismatch in the AOD profiles among different datasets during some large-scale dust events, which is partly because of the difference in sampling and measurement frequencies among different datasets.~~

Formatted: No bullets or numbering

Formatted: Font: Italic, Complex Script Font: Italic

Formatted: Font: Italic, Complex Script Font: Italic

Formatted: Font: Italic, Complex Script Font: Italic

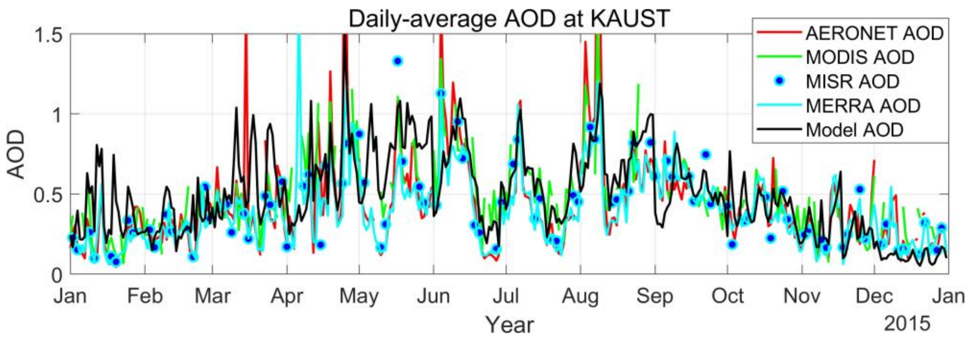

Figure ~~3~~4. Time-series of daily-averaged AOD at KAUST (AERONET, MODIS, MERRA-2, and Model AODs at 550nm and MISR AOD at 555nm).

For a quantitative evaluation of the model results, we calculate the Mean bias error (MBE) of the model AOD against the three sets of observations, viz., AERONET, MODIS, and MISR at KAUST. The MBEs calculated using daily-mean values for 2015 are presented in Table 2. We also calculate the Pearson's correlation coefficient (ρ) of the simulated AOD against the available observations, after removing the seasonal cycle from all observations. The calculated MBE for the model is low against all datasets. The MBE is 13.4 % against the most-reliable AERONET data. The model AOD also shows a good correlation with observations, with a correlation coefficient ~~exceeding 0.6~~close to 0.5 for all datasets. These results demonstrate that the model simulated AOD values are reasonable~~robust~~.

Table 2. Statistics* of simulated AOD compared with different observations at KAUST.

Dataset	AERONET	MODIS	MISR
Pearson's correlation coefficient ρ **	0.53~~61~~	0.~~63~~48	0.52~~71~~
Mean Bias Error (MBE)	0.059	-0.008	0.063
Annual average AOD (Model AOD = 0.49)	0.44	0.47	0.43

*Calculated using daily-average data for 2015. **all correlation coefficients are significant ($p < 0.0001$).

Figure 5~~4~~ shows the contribution of different aerosol species on total AOD at KAUST, as simulated by WRF-Chem. Dust is the major contributor to AOD in all seasons, reaching above 90 % in spring and summer. This result is consistent with earlier reported percentage contributions of dust over the region (Kalenderski et al., 2016). The anthropogenic contribution is highest in winter but contributes less than 15 %. The contribution of sea salt emissions is also small in all seasons (less than 10 %). These results are also qualitatively consistent with the contributions derived from CALIOP data that use histograms of aerosol type in a grid cell containing the KAUST site (Fig. S2~~1~~).

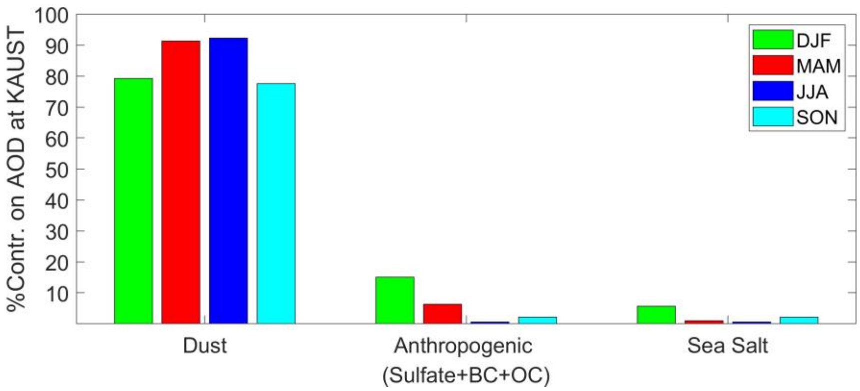

Figure ~~4~~5. Percentage contribution of different aerosol types on total AOD at KAUST as simulated by WRF-Chem.

The size distributions of dust, sea salt, and sulfate are modeled in WRF-Chem using approximations over different size bins. Dust and sea salt are distributed in five and four size bins, respectively, both between 0.1 and 10 μm radius, as detailed in Ukhov et al. (2020a). Sulfate aerosols are distributed in two lognormal modes, the Aitken and Accumulation modes. As discussed earlier, dust is the dominant aerosol type; thus, here we compare the volume size distributions of the modeled dust with the AERONET data. Figure 6 shows the column-integrated volume PSD in the model and AERONET data. The simulated and observed volume PSDs are reasonably well matched in all seasons even though the dust in the model is distributed in five bins only (Parajuli et al., 2019; LeGrand et al., 2019). Although the maximum radius of particles in AERONET data is 15 microns, which is larger than the maximum size in the model (10 microns), the majority of particles in the AERONET data fall within the 10-micron range. Recent measurements from aircraft have shown that dust particles can be much larger (Ryder et al., 2019), up to 40-micron in radius, during large-scale dust events (Marenco et al., 2018). However, the optical contribution of such large particles is relatively small. There are two distinct aerosol modes in AERONET PSD data: one finer mode centered around 0.1 microns, and another coarse mode centered around 2-3 microns. The coarse mode primarily corresponds to mineral dust (silt) that originates locally and from inland deserts, northeast Africa, and the Tigris-Euphrates source region (Kalenderski and Stenchikov et al., 2016; Parajuli et al., 2019). The composition of the fine mode is much more complex, but usually includes clay particles transported over long distances and anthropogenic aerosols from pollution sources (mainly as sulfate) (Chin et al., 2007; Hu et al., 2016; Prospero et al., 1999). The size distributions of sulfate and sea salt aerosols are presented in the supplementary information (Figs. S3 and S4). Note that we use the PSD and AOD data from this AERONET station (KAUST) to retrieve the LIDAR aerosol extinction profiles used in this study.

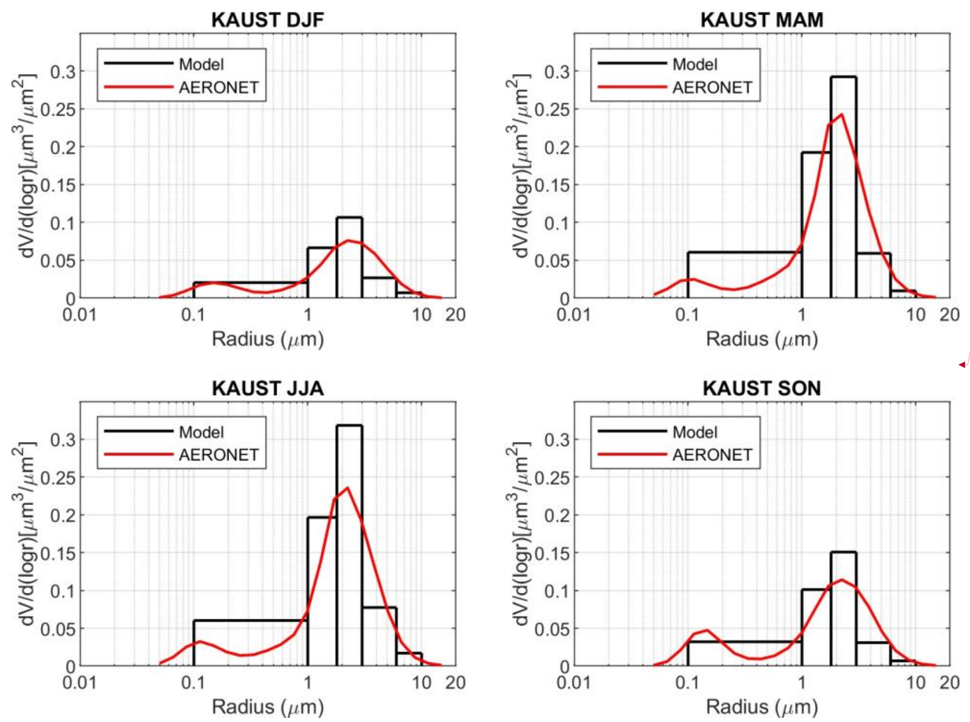

Figure ~~5~~6. Column-integrated volume size distributions and concentrations of only dust from the model, plotted against AERONET aerosol volume concentrations at KAUST.

~~The size distributions of dust, sea salt, and sulfate are modeled in WRF-Chem using approximation over different size bin. Dust and sea salt are distributed in five and four size bins, respectively, both between 0.1 and 10 μm radius, as detailed in Ukhov et al. (2020). Sulfate aerosols are distributed in two lognormal modes, Aitken and Accumulation. As discussed earlier, dust is the dominant aerosol type; thus, here we compare the volume size distributions of the modeled dust with the AERONET data. Figure 5 shows the column-integrated volume PSD in the model and AERONET data. The simulated and observed volume PSDs are reasonably well matched in all seasons even though the dust in the model is distributed in five bins only (Parajuli et al., 2019; LeGrand et al., 2019). Although the maximum radius of particles in AERONET data is 15 microns, which is larger than the maximum size in the model (10 microns), the majority of particles in the AERONET data fall within the 10-micron range. Recent measurements from aircraft have shown that dust particles can be much larger (Ryder et al., 2019), up to 40-micron in radius, during large-scale dust events (Marenco et al., 2018). However, the optical contribution of such large particles is relatively small. There are two distinct aerosol modes in~~

Formatted: Space After: 15 pt, Tab stops: Not at 4.15"

~~AERONET PSD data: one finer mode centered around 0.1 microns, and another coarse mode centered around 2-3 microns. The coarse mode primarily corresponds to mineral dust (silt) that originates mainly from inland deserts, northeast Africa, and the Tigris-Euphrates source region. The composition of the fine mode is much more complex, but usually includes clay particles transported from long distances and anthropogenic aerosols from pollution sources (mainly as sulfate). The size distributions of sulfate and sea salt aerosols are presented in the supplementary information (Figs. S2 and S3). Note that we use the PSD and AOD data from this AERONET station (KAUST) to retrieve the LIDAR aerosol extinction profiles used in this study.~~

3.2.3. Case study of a summer-time dust event

A large-scale dust storm swept over the KAUST site on August 08, 2015, as seen in the MODIS image in Fig. 7~~16~~a. The dust event lasted for two days until August 09. The KAUST AERONET station registered the second-highest AOD of the entire year on August 08, with the AOD daily mean~~ AOD~~ reaching 2.48. The AERONET angstrom exponent (AE 440/675) value showed a sharp reduction on this day, from 0.41 on August 06 to 0.10 on August 08. This reduction indicates the dominance of coarse-mode dust during the event and~~ thus,~~ that the dust event originated from nearby inland deserts. By August 09, the dust storm moved towards the south/southwest and spread to a broader region across the Red Sea and northeast Africa. The MODIS RGB image on August 09 shows a dust plume originating from northeast Africa around Port Sudan, which, after being deflected by the northerly winds, experiences a marked curvature (Fig. ~~16~~7b). The SEVIRI RGB dust composite (Fig. 7c), in which the pink color represents atmospheric dust, also shows strong dust activity around the KAUST site on August 08.

Formatted: Font: Italic, Complex Script Font: Italic

Formatted: Font: Italic, Complex Script Font: Italic

Formatted: Font: Italic, Complex Script Font: Italic

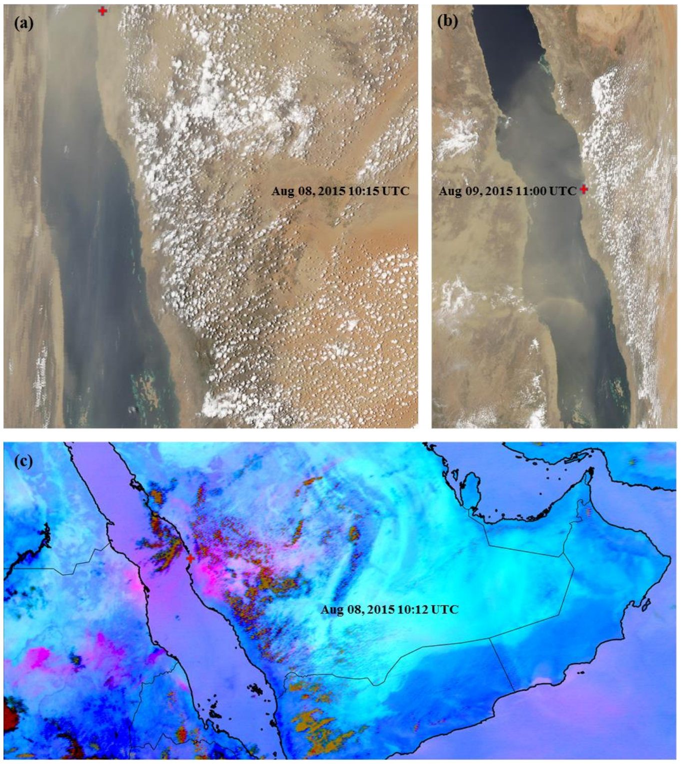

Figure 7~~16~~. MODIS and SEVIRI images during a large-scale dust event. True color images from MODIS on (a) August 08, 2015 10:15 UTC (b) August 09, 2015 11:00 UTC, and (c) Meteosat SEVIRI RGB dust composite for Aug 08, 2015 10:12 UTC. KAUST site is marked by a red (+) mark~~symbol~~.

Formatted: Space After: 15 pt

The synoptic conditions of this dust event are somewhat similar to those of a summer-time dust event reported by Kalenderski and Stenchikov (2016), which was centered over North Sudan. The dust event we describe here is a typical summer-time dust event caused by high winds driven by strong pressure gradients (Alharbi et al., 2013). Although haboob-type dust events commonly occur in the region, analysis of the RGB pink dust composite (Fig. 7c) shows only a few scattered clouds (red and brown patches) over the study site during this period, ruling out the possibility of a haboob dust event. Haboob is a typical dust event that commonly occurs in regions with moist convection, in which dust is generated by strong divergent winds that form around a cold pool of downdrafts (Anisimov et al., 2018).

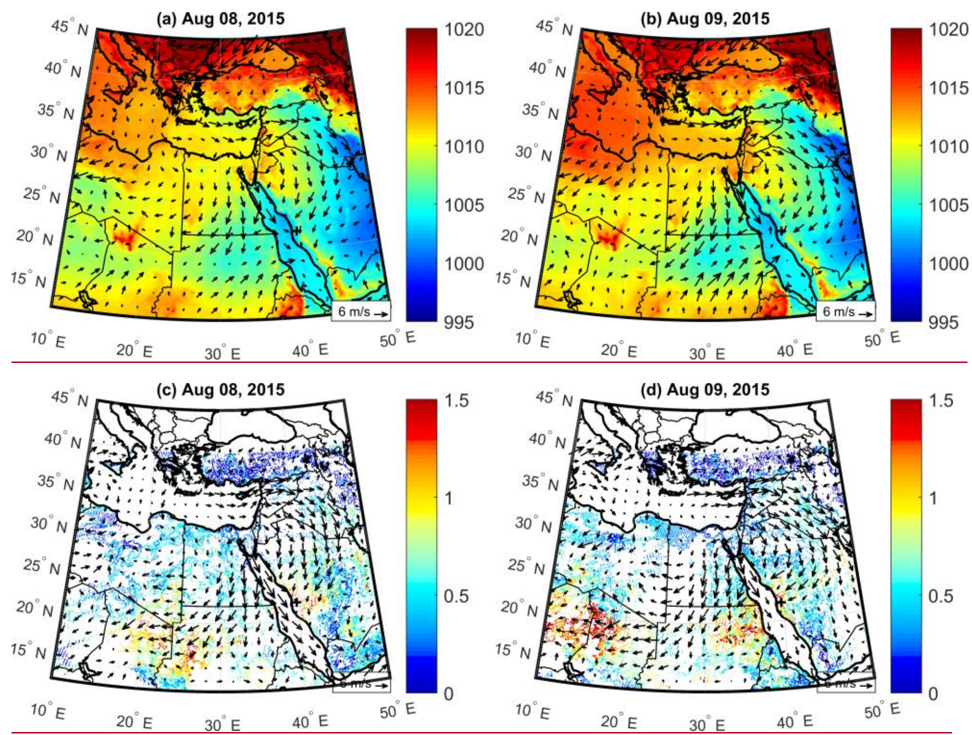

Figure 8~~17~~. Mean sea level pressure (MSLP) and wind vectors from ECMWF operational analysis data during the dust event (a and b), and MODIS deep blue AOD data overlain by model wind vectors (c and d). KAUST site is marked by a + sign.

~~The synoptic conditions of this dust event are somewhat similar to those of a summer-time dust event reported by Kalenderski and Stenchikov (2016), which was centered over North Sudan. The dust event we describe here is a typical summer-time dust event caused by high winds driven by strong pressure gradients (Alharbi et al., 2013). Although haboob-type dust events commonly occur in the region, analysis of the RGB pink dust composite (Fig. 16c) shows only a few scattered clouds over the study site during this period, ruling out the possibility of a haboob dust event. Haboob is a typical dust event that commonly occurs in regions with moisture convection, in which dust is generated by strong divergent winds that form around a cold pool of downdrafts (Anisimov et al., 2018).~~

As seen in Figs. 8~~17~~a, b, a high-pressure system developed in the eastern Mediterranean region and Turkey on August 08, which expanded towards Africa/Middle East and created stronger winds over the region on August 09. On August 08, a low-pressure system developed, which was centered ~~around~~on northeast Africa (Sudan). Winds converging towards this low from the north/northeast adopted a northeasterly flow pattern, which is characteristic of the Harmattan winds prevalent in the region. The winds originating from the eastern Mediterranean were forced to curve by the Hijaz mountains in the western Arabian Peninsula, finally converging with the low-pressure system in northeast Africa and the Red Sea, where the high energy of the flow was finally dissipated. A high-pressure system persisted throughout the dust event over the Ethiopian highlands and south Sudan, as shown in Figs. 8~~16~~a, b. This high-pressure system gave rise to the southerly/southwesterly winds that also converged towards the low-pressure region around northeast Africa and the Red Sea.

MODIS AOD also showed a high aerosol loading around KAUST (+ symbol in Figs. 8~~17~~c, d) on August 08 that spread across a larger area towards northeast Africa on August 09. Figure ~~17~~8 shows that the dust mobilization was evidently caused by the northerly/northeasterly winds moving over the study site. The wind vector patterns are very consistent between ECMWF operational analysis (Figs. 8~~17~~a, b) and model simulations (Figs. 8~~17~~c, d) for most parts of the domain. This observation is not surprising because we use the ECMWF operational analysis data for the boundary conditions and apply ‘grid nudging’ at each model grid using the same ECMWF dataset. The wind patterns in the two figures differ in some areas, however, especially over the Ethiopian highlands. Note that the model winds presented are derived from the coarser 12 km domain to show the wind patterns over a larger region beyond our innermost study domain. In the Ethiopian highlands region, where there is a strong effect from the topography, such a coarse resolution may not be enough to resolve the fine features of the wind circulations. At the study site, however, winds are indeed better resolved in our model because the resolution of the innermost domain is much higher, i.e., 1.33 km.

The model captures the major features of the dust storm reasonably well. Both the model and the AERONET data register this event as the second-largest dust event of 2015. On August 09, the model shows a daily average (daytime only) AOD of 1.18 compared to 1.79 given by the AERONET data (underestimation by ~35 %).

Figure 9~~18~~ compares the vertical profiles of dust ~~as~~ provided by model simulations and the KAUST–MPL data during the dust event. The right column in the figure shows the simulated dust extinction coefficient at 550nm, covering the three days during the dust event. Because of the quality constraints applied in the GRASP algorithm, the processed extinction data from KAUST–MPL are only partially available during this event. Therefore, we present the raw normalized relative backscattering (NRB) from the KAUST–MPL to examine the evolution of this dust event qualitatively, as shown in Fig. 9~~18~~. Note that around noon local time in summer, the KAUST–MPL field of view is covered to avoid the sun glare, which is why there is ~~some~~a gap in the data around this time. In the KAUST–MPL NRB data (Fig. 9~~18~~, left column), the dust plume appears as early as Aug 08 (~05:00 UTC) at a height of 1–1.5 km, indicating the onset of the dust storm. This dust plume becomes strongest by August 09, covering a large part of the atmospheric column with dust. Although the onset of the dust event is slightly earlier in the model compared to KAUST–MPL data, the model also shows high dust activity on August 09, consistent with KAUST–MPL observations. The dust is mainly confined within a height of ~2 km, which is consistent in both datasets. ~~We also observed a higher intrusion of dust into the atmosphere, which is expected because the PBL is well developed in summer.~~

~~Note that t~~The model data ~~also~~ shows a high aerosol extinction at a height of ~6 km on August 09/10, particularly at night (Fig. 9~~18~~), which will be discussed further later~~,~~. ~~which is consistent with the dust layers observed at 6–7 km height in the KAUST–MPL nighttime data (Fig. 8). Although the model data does not identify these dust layers at 6–7 km in the seasonally averaged profiles presented earlier (Fig. 8), the model nonetheless correctly identified these same dust layers in this event (Fig. 18).~~ The demise timing of the dust storm is consistent in both the model and KAUST–MPL data.

When the dust-laden harmattan winds arrive at the Red Sea coast, they encounter the land or sea breezes depending upon the time of arrival, as discussed further in section 4.3. When they meet with the opposite sea breeze flow~~s~~, the air mass rises up, bringing the dust to the upper levels. Such higher intrusion of dust is evident in the KAUST-MPL data (Figure 9, left) in the afternoon, during which the sea breezes are most active. The suspended dust is still visible in the upper levels (~2-3 km) in the night of August 10, because the dust particles have not been deposited yet. ~~We also observed a higher intrusion of dust into the atmosphere, which is expected because the PBL is well developed in summer.~~

~~These results further confirm that the dust layers observed at 6–7 km height correspond to the long-range transported dust during large-scale dust events.~~

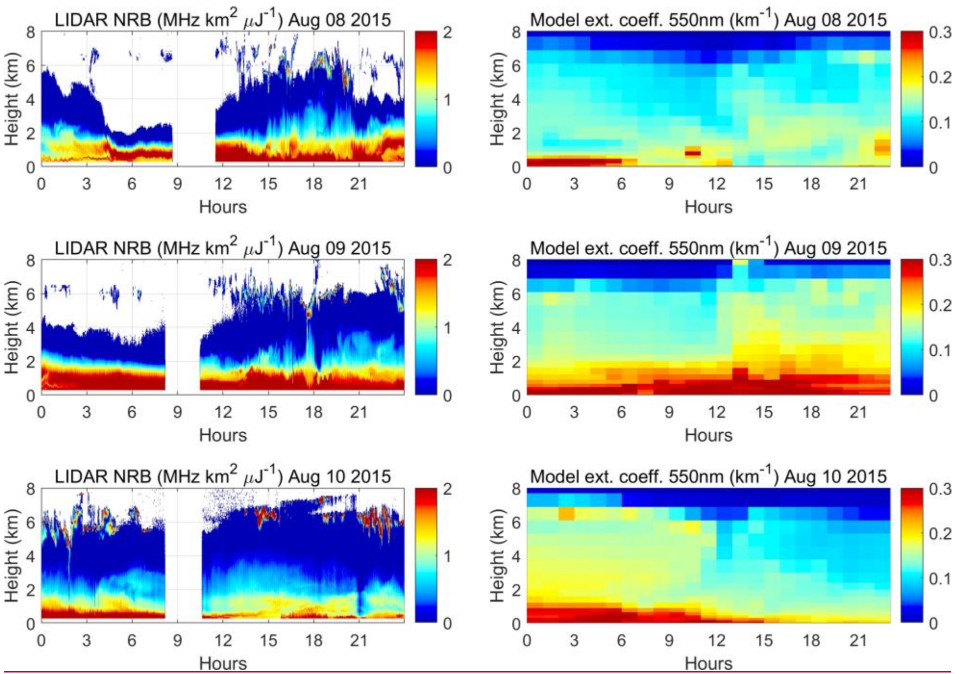

Figure 9~~18~~. Natural logarithm of normalized relative backscatter (NRB) at 532 nm measured at the KAUST–MPLNET station (left column) and the model-simulated dust extinction coefficient at 550 nm (right column) during the dust event of August 08/09. Times are reported in UTC.

~~**3.2. Surface Meteorology**~~

~~Land and sea breezes affect dust aerosol emissions and transport in our study region. When the land and sea breezes are strong, they can cause dust emission from the active dust sources of the coastal regions. The land and sea breezes also transport the emitted dust either towards the ocean or towards the land, depending on the direction of the breeze. Moreover, land breezes can help to transport dust emitted from inland deserts and remote areas during large-scale dust events to the ocean (Prakash et al., 2014).~~

Formatted: Font color: Red

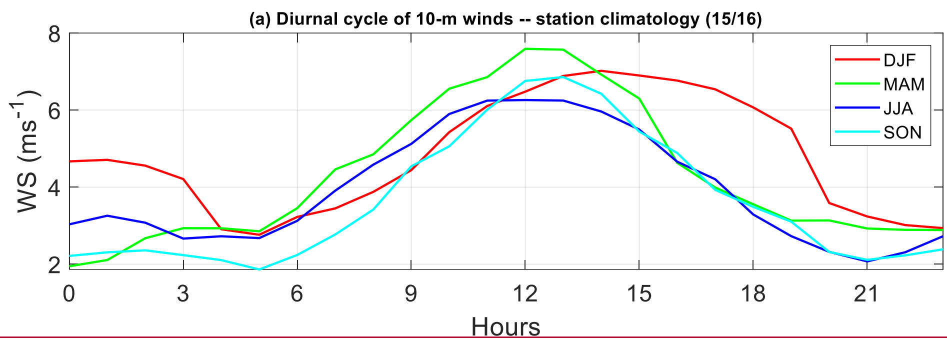

Formatted: Font color: Red

Formatted: Font color: Red

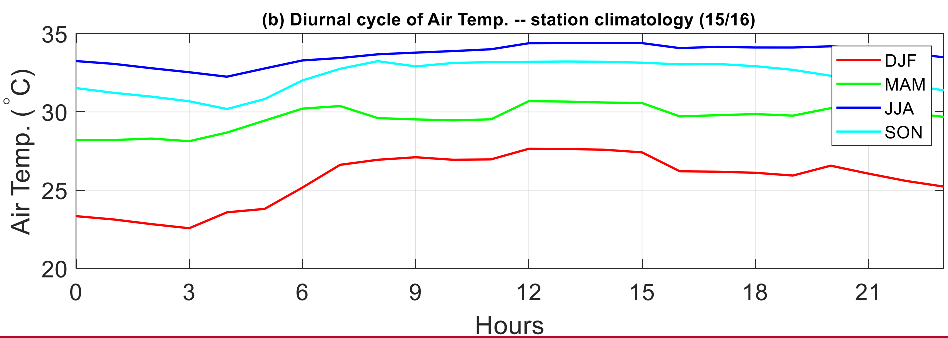

Formatted: Font color: Red

Formatted: Font color: Red

~~Figure 6. (a) Diurnal cycle climatology (2015/16) of surface winds and air temperature measured at KAUST station. Times are reported in UTC.~~

~~Because dust/aerosols are present over the study site for most of the year, they can also interact with the meteorology and thus affect atmospheric winds and temperature at different time scales. Land and sea breezes are strongly coupled with dust/aerosols and temperature variability, especially near the surface.~~

~~Figure 6a shows the diurnal cycle climatology (2015/16) of station-measured surface wind speed at the study site. The surface winds reach a peak around noon UTC (15:00 local time) for all seasons except winter, consistent with the results of Davis et al. (2019). The aforementioned sea breezes cause these wind peaks in the afternoon. Note that these sea breezes originate at sea and advance landward to reach the coast only later in the afternoon (Estoque et al., 1961), where they are measured at our station. In winter, the wind speed profile shifts to the right, peaking later in the day at around 14:00 UTC. This shift to later in the day occurs because, in winter, it takes more time to reach the thermal contrast required between the land and the sea for the formation of sea breezes. Note the existence of a second peak in the wind speed plot during the night, around 01:00 UTC, which represents the land breezes. These land breezes are stronger in winter than in the other seasons.~~

~~The profiles of air temperature (Fig. 6b) are rather flat, showing a weak diurnal cycle. Winter shows the most pronounced diurnal cycle. The temperature contrast between day and night is minimal in summer and maximum in winter.~~

~~Given the strong diurnal cycles of surface winds and temperature, it is evident that the day and night circulation in the study area is remarkably different. Therefore, it becomes important to look at the aerosol vertical profiles separately in day and night time.~~

3.3. Vertical profiles

3.3.1. Comparison of ~~aerosol~~ extinction profiles from~~from~~ KAUST–MPL and~~with~~ CALIOP data

Figure ~~7~~10 shows the comparison of aerosol extinction from KAUST–MPL and CALIOP, both of which show a similar profile. Most aerosols in the atmosphere are confined within the troposphere~~,~~ below 8 km altitude, which is consistent in both datasets. However, the KAUST–MPL underestimates the extinctions near the surface compared to CALIOP data. Moreover, the nighttime dust events observed in the KAUST–MPL data are not present in the CALIOP data.

~~These discrepancies could be related to the differences in algorithm and resolution, between the two datasets. Firstly, while retrieving aerosol extinction profiles, CALIOP algorithm uses an assumed extinction-to-backscatter (lidar ratio) for a set of aerosol types that are defined mostly geographically and on the base of raw lidar signal signatures (Kim et al., 2018). In contrast, the MPL algorithm assumes averaged lidar ratio for the whole column based on aerosol PSD, refractive index and sphericity, in such as way that it will satisfy both AERONET and MPL co-incident data. Secondly, KAUST–MPL is a point measurement that captures the temporal evolution of the dust storms better than CALIOP because it has a higher temporal resolution. For instance, CALIOP can undersample or overlook some dust events that last only for a few hours. On the other hand, CALIOP could sample more spatial details of a dust storm because it has a more extensive spatial coverage than the KAUST–MPL data. Nonetheless, these two datasets complement one another and their combined use can be beneficial in understanding the large-scale dust storms.~~

Formatted: Font color: Text 1, Pattern: Clear
Formatted: Font: Italic, Complex Script Font: Italic
Formatted: Font color: Text 1, Pattern: Clear
Formatted: Font: Italic, Complex Script Font: Italic
Formatted: Font color: Text 1, Pattern: Clear

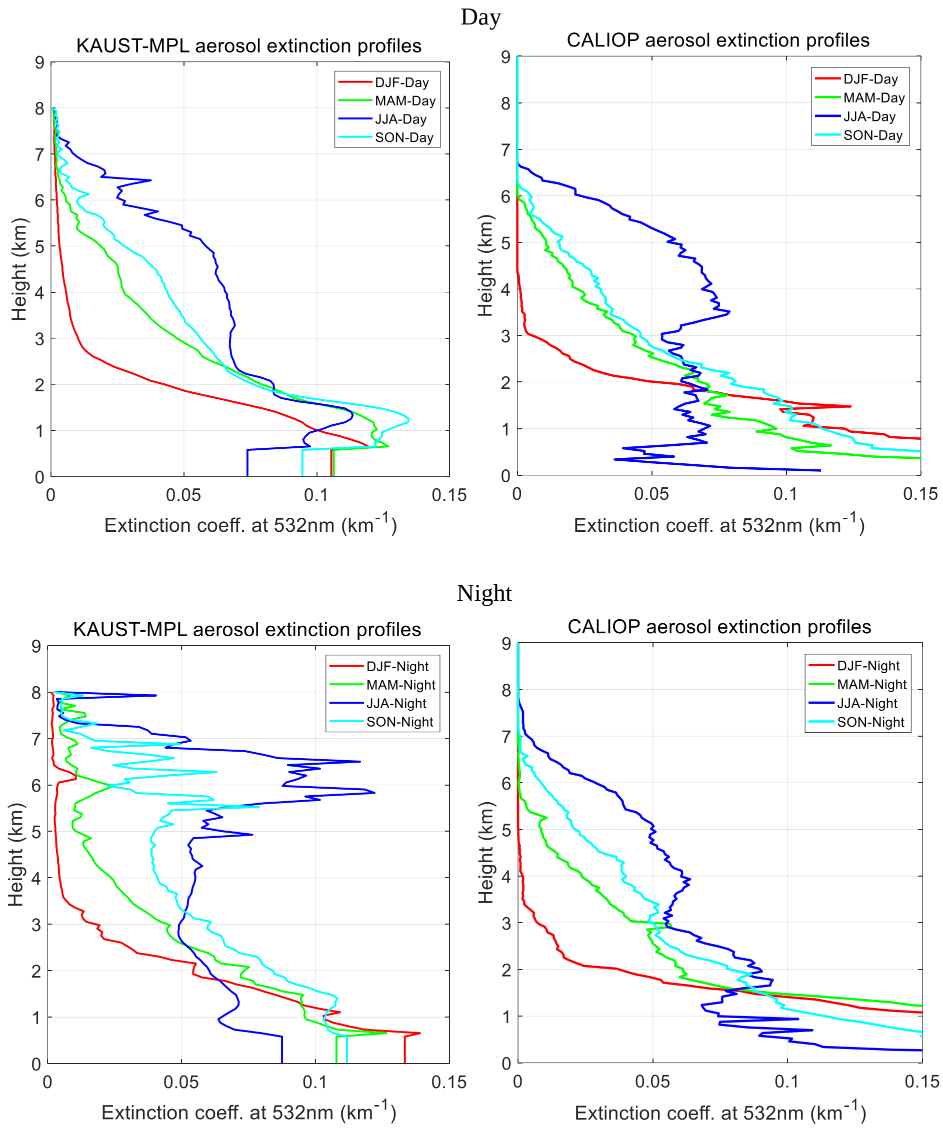

Figure 10~~7~~. Comparison of seasonal ~~climatology~~ average (2015/16) of aerosol extinction from KAUST–MPL (left) and CALIOP (right) shown separately for day (upper two panels) and night (bottom two panels). Heights are above sea level (a.s.l.).

Note that CALIOP extinction profiles represent data averaged over a large grid box (2x5 degree) that contains the KAUST site. As such, CALIOP represents the larger regional-scale vertical structure of aerosols compared to KAUST–MPL, which represents a more local structure. Above ~2 km, except for nights during summer and fall, the profiles of the two datasets are much more similar, indicating the presence of a stable aerosol layer spread throughout the region. This similarity is understandable because local fluctuations closer to ground level do not penetrate much above 2 km in winter. Below ~2 km, there are more significant differences between the profiles. Note that the elevated aerosol loading present in the KAUST–MPL data at about 1-2 km height is not present in the CALIOP data. It is also worth mentioning that the MPL does not provide reliable observations in the lowest 550 m, and CALIOP loses accuracy near the surface.

~~On the other hand, CALIPSO algorithm also has difficulty in identifying the base of aerosol layers accurately and the level-3 algorithm ignores the 'clear air' between the surface and the lowest aerosol layer when averaging in order to avoid underestimation of extinction in the lower part of the aerosol profile (winker et al, 2013). Nearer the surface, both CALIOP and KAUST–MPL have difficulty in retrieving the aerosol extinction for different reasons. For MPL, retrievals near the surface could be erroneous especially when multiple aerosol layers are present because the retrieval algorithms assume a constant LIDAR ratio for all aerosol layers (Welton et al., 2002). On the other hand, CALIPSO algorithm also has difficulty in identifying the base of aerosol layers accurately and the level-3 algorithm ignores the 'clear air' between the surface and the lowest aerosol layer when averaging in order to avoid underestimation of extinction in the lower part of the aerosol profile (winker et al, 2013). This process is known to produce higher magnitude of extinction near the surface as compared to other observations (Koffi et al., 2012; Winker et al, 2013).~~

~~, which is a common problem for all LIDARs (Koffi et al., 2012; Winker et al., 2013; Senghor et al., 2020).~~

3.3.2. Comparison of extinction profiles between KAUST–MPL and model simulations

Figure ~~8~~11 shows the seasonally averaged vertical profiles of aerosol extinction from KAUST–MPL and model simulations, shown separately for day and night. The height of the top of the aerosol layer and the contrast of profiles in different seasons in the KAUST–MPL data and the model output are similar. The vertical profiles compare reasonably well, with similar orders of extinction in the daytime, especially considering the range of discrepancy in the KAUST–MPL and CALIOP data that we discussed above. The magnitude of extinctions in the model and KAUST–MPL are in good agreement in the nighttime as well, except in summer and ~~fall~~spring, in which cases the KAUST–MPL data shows higher extinctions, particularly above the PBL.

KAUST–MPL data show a distinct aerosol layer located between 5.5 and 7 km, especially in the nighttime, summer, and the fall. The model does not show such dust layers. KAUST–MPL daytime data show a typically elevated maximum of dust extinction in the PBL centered around 1.5 km altitude. The model does not identify such a dust loading profile either. The KAUST-MPL and model profiles agree better in the daytime than in the nighttime, and in winter compared to other seasons. However, there are no significant differences between daytime and nighttime profiles in the model. Note that the shape of the profile is reversed during the

Formatted: Highlight

nighttime, which the model ~~weakly~~ reproduces weakly. We explore this particularly interesting shape of the extinction profile at ~1–2 km in the daytime in section 3.4. As discussed later, these unique features of the profiles are related to the effect of land/sea breezes and topography~~KAUST- MPL nighttime data show a distinct aerosol layer located between 5.5 and 7 km~~, especially ~~in~~ nighttime, in ~~summer and the fall. The model does not show such dust layers in the night. KAUST- MPL daytime data shows a typical elevated maxima of dust extinction in the PBL centered around 1.5 km altitude. However, t~~T~~he model does not identify such a dust loading profile either~~. ~~The KAUST-MPL and model profiles agree better in the daytime than in the nighttime, and in winter compared to other seasons. However, there is no much variation between daytime and nighttime profiles in the model. Note that the shape of the profile is reversed during the nighttime, which the model weakly reproduces. We explore this particularly interesting shape of the extinction profile at ~1–2 km in the daytime in section 3.4. As discussed later, these unique features of the profiles are related to the effect of land/sea breezes and topography~~.

Day

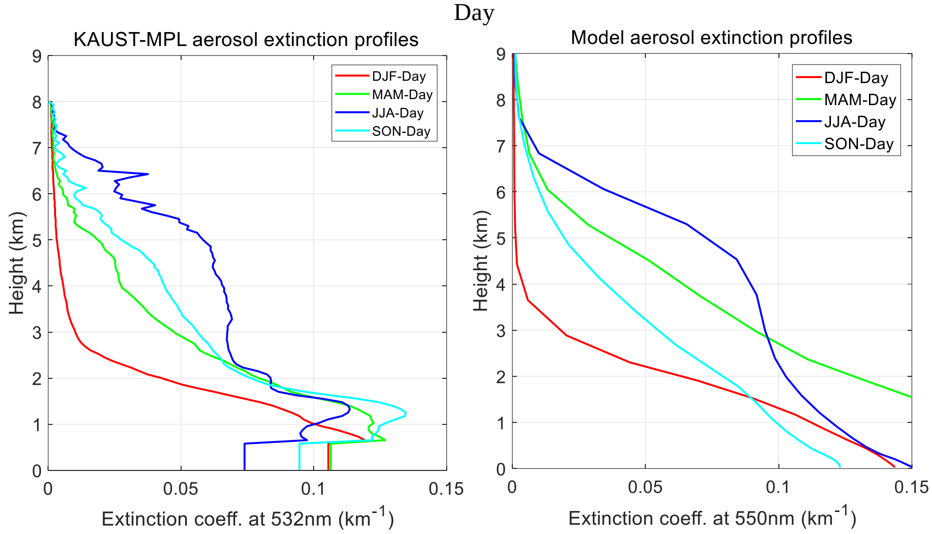

Night

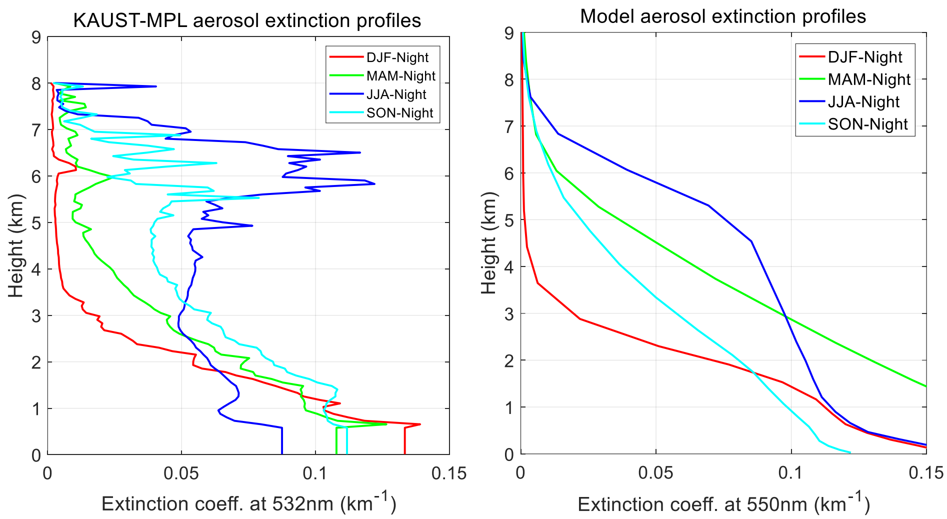

Figure ~~8~~11. KAUST–MPL retrieved (left column) and model-simulated (right column) aerosol extinction profiles for different seasons presented separately for the daytime (upper two panels) and nighttime (bottom two panels). The measurement time of all KAUST–MPL data available for daytime fall between 05:00 and 15:00 UTC, and ~~for~~ nighttime data fall between 17:00 to 02:00 UTC. For the model, the day and nighttime data represent data between these times.

To understand the causes of the elevated dust maxima in the KAUST–MPL profiles at ~1–2 km altitude in the daytime and 5.5–7 km in the nighttime, we separately analyzed the profiles under a clear sky and dusty conditions. We define 'clear days' as the days with a daily mean of AOD at KAUST less than 0.25 and 'dusty days' as the days having daily-mean AOD greater than 0.75, using either MODIS AOD or AERONET AOD to maximize data availability during large-scale dust events.

Figure 12 shows the average extinction profiles for clear and dusty conditions from KAUST–MPL data for 2015/16 obtained using the above criteria. The daytime profile (Fig. 12, left) shows a similarly elevated dust loading at 1-2 km height, as noted earlier in Figures 10/11, but is much more prominent. Since 'dusty days' correspond to very high AOD conditions (AOD>0.75) expected during dust storms, we can infer that the observed elevated dust loading at 1-2 km corresponds to large-scale dust storms. Studies have shown that this shape is characteristic of dust profiles observed during large-scale dust events near land-ocean boundaries (Khan et al., 2015; Senghor et al., 2017). Marenco et al. (2018) also observed a similarly elevated dust loading over the eastern Atlantic at a comparable height in their airplane observations during the 'heavy dust' period. ~~To understand the causes of the elevated dust maxima in the KAUST–MPL profiles at ~1–2 km altitude in the daytime and 5.5–7 km in the nighttime, we separately analyzed the profiles under clear sky and dusty conditions. We define ‘clear days’ as the days with a daily mean of AOD at KAUST less than 0.25 and ‘dusty days’ as the days having daily-~~

~~mean AOD greater than 0.75, using either MODIS AOD or AERONET AOD to maximize data availability during large-scale dust events. Figure 912 shows the average extinction profiles for clear and dusty conditions from KAUST MPL data for 2015/16 obtained using these criteria. The profiles on dusty days differ remarkably from the profiles on clear days, both for the daytime and nighttime. During the daytime (Fig. 912, left), the maximum i10/11s even more prominent than in the profiles shown earlier in Fig. 7. Indeed, studies have shown that this shape is characteristic of dust profiles observed during large-scale dust events that occur near land-ocean boundaries (Khan et al., 2015; Senghor et al., 2017). Marenco et al. (2018) also observed a similarly elevated dust loading over the eastern Atlantic at a comparable height during the 'heavy dust' period of their flight.~~

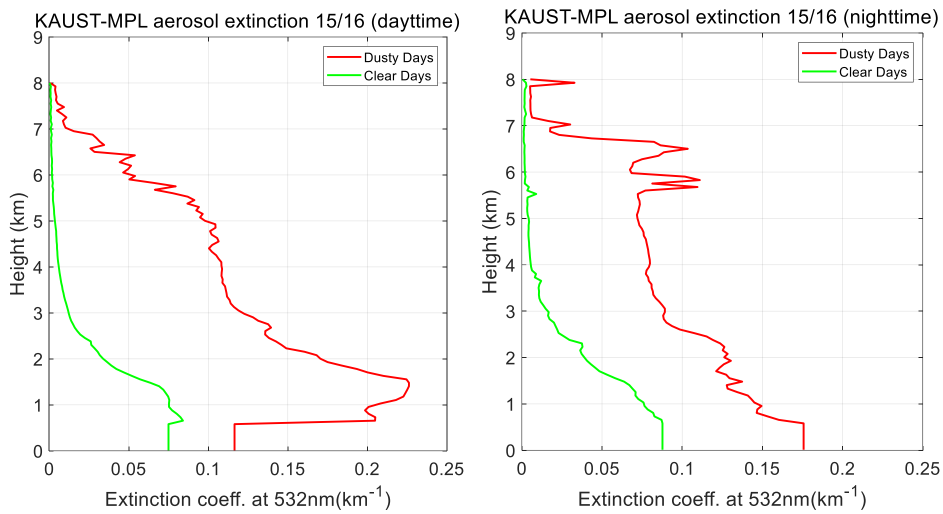

Figure ~~9~~12. Average vertical profiles of aerosol extinction corresponding to 'clear days' and 'dusty days' from KAUST–MPL data.

The elevated dust layer during the nighttime at the height of 5.5–7 km observed earlier in summer and fall (Fig. 10/11) is present in the 'dusty days' and is absent in 'clear days' (Fig. 12, right). The above analysis again tells us that the high dust loadings at 5.5-7 km in the night are also associated with large-scale dust events. However, it becomes vital to understand the source of these large-scale, nighttime dust events. Based on our results, we suggest that this nighttime dust represents transported dust from inland deserts ~~follows~~. More vigorous convection in the inland desert regions during the daytime carries aerosols to higher altitudes. Over deserts in summer, convection is most energetic in the afternoon. The planetary boundary layer height (PBLH) can reach well above 5 km (Fig. S5). By the evening, the dust is mixed thoroughly within the PBL by the strong convection (Khan et al., 2015). At night, the PBL weakens and breaks the capping inversion (Fig. S6), which allows the dust-laden layer from the PBL to mix into the free troposphere and be transported to long distances. As an example, we noted such high intrusion of dust during the night of August 09 (21:00 and 02:00 UTC) in the LIDAR backscatter data of our case study (Fig. 9). The dust that lies above the PBL is ultimately carried to our site by the accelerated easterly geostrophic winds (Almazroui et al., 2018), ~~which~~and arrives at our site during the night. Therefore, the dust layers at 5-7 km observed in the nighttime likely represent dust of non-local origin transported from inland deserts at higher altitudes~~ during large-scale dust events~~.

The dust transport process to our site is evident if we look at the wind vectors at higher altitudes. As Fig. S~~6~~7 shows, the winds are northeasterly below ~6 km, which are the regionally prevalent 'trade winds' commonly called Harmattans. Above ~6 km, the winds are easterly. Thus, these two wind patterns are responsible for ~~the~~ transporting~~ of~~ dust from the inland deserts to the study site. The geostrophic easterly wind transports dust at higher altitudes (6–7 km), and Harmattan transports dust at lower altitudes (1–2 km), which is why KAUST–MPL data shows elevated dust loading at these heights. In the winter, such transport of dust from deserts to our site is impossible because the upper-level winds are westerly (Fig. S8~~7~~).~~10/1112The elevated dust layer during the nighttime at a height of 5.5–7 km observed earlier in summer and fall (Fig. 7) is present in the 'dusty days' and is absent in 'clear days' (Fig. 9, right). Based on our results, we suggest that this nighttime dust represents transported dust from inland deserts follows. We suggest that these dust layers represent dust of non-local origin transported at higher altitudes during large-scale dust events. Next, we explore why such a high dust loading at this altitude in summer is present only in the nighttime and not in the daytime. Stronger convection in the inland desert regions during the daytime carries aerosols to higher altitudes. In the summer in deserts, convection is strongest in the afternoon, and the planetary boundary layer height (PBLH) can reach well above 5 km (Fig. S54). By the evening, the dust is mixed thoroughly within the PBL by this strong convection (Khan et al., 2015). At night, the PBL weakens and breaks the capping inversion, which allows the dust-laden layer from the PBL to mix into the free troposphere. As an example, we noted such high intrusion of dust during the night of August 09 (21:00 and 02:00 UTC) in the LIDAR backscatter data of our case study (Fig. 9). The dust that lies above the PBL is ultimately carried to our site by the accelerated easterly geostrophic winds (Almazroui et al., 2018), which arrive at our site during the night. We suggest that these dust layers likely represent dust of non-local origin transported at higher altitudes during large-scale dust events.~~

~~This process is evident if we look at the wind vectors at higher altitudes. As Fig. S65 shows, the winds are northeasterly below ~6 km, which are the regionally prevalent 'trade winds' commonly called Harmattans. Above ~6 km, the winds are easterly. These two wind patterns are thus responsible for the transport of dust from the inland deserts to the study site. The geostrophic wind transports dust at higher altitudes (6–7 km) and Harmattan transports dust at lower altitudes (1–2 km), which is why KAUST–MPL data shows elevated dust loading at these heights. In the winter, such transport of dust from deserts to our site is not possible because the upper-level winds are westerly (Fig. S7).~~

3.3.3. Comparison of vertical profiles of dust concentrations

Figure 13~~0~~ shows the vertical profile of aerosol concentrations per seasons simulated by the model ~~by seasons as~~ compared with KAUST–MPL data and MERRA-2 reanalysis. We have presented these plots despite their broad resemblance to extinction profiles presented earlier (Fig. 11) because ‘concentrations’ are more useful from air quality perspective and MERRA-2 provides mixing ratios of different aerosols rather than extinctions. ~~The vertical profiles of aerosol concentrations from KAUST–MPL and the model largely resemble the extinction profiles presented earlier in Fig. 7.~~ The variation in concentration profiles in different seasons is reasonably consistent in all three datasets. The elevated dust maxima at a height of ~1.5 km observed in the KAUST–MPL profiles is not present in the model or the MERRA-2 data. Both the model and MERRA-2 tend to overestimate aerosol concentrations compared to KAUST–MPL data in summer and in the lower atmosphere, particularly below 1 km. The model-simulated near-surface concentrations in summer are twice as large as those in the LIDAR data. This overestimation is counter-intuitive because the model AOD agrees well with the AERONET AOD (Fig. 4~~3~~) used to constrain LIDAR aerosol profiles. This discrepancy is related to the size distribution of particles. For AOD to be consistent in the model and LIDAR data, the model must overestimate the concentration of coarse particles in the lower atmosphere. Therefore, we can infer that the model overestimates the concentrations of coarse particles in the lower atmosphere relative to the observed concentrations, which appears to contradict with the results of Ryder et al. (2019).

In winter, the boundary layer is shallower. T~~, and t~~he concentration profile resembles a typical profile that might be expected in a turbulent boundary layer, in which the concentration ~~exponentially~~ rapidly~~increases~~ decreases with height ~~towards the surface~~, as observed in the field (e.g., Selezneva, 1966) and wind tunnel experiments (e.g., Neuman et al., 2009). In summer, the boundary layer is deeper, and the strong turbulent mixing transports dust higher into the atmosphere; consequently, the concentration profile is steeper.

~~During local dust events that originate in the nearby deserts, the atmospheric dust loading is mostly dominated by coarse-mode particles. In contrast, dust events of non-local origin carry long-range transported dust to the site, which typically constitute finer particles. Finer particles can easily reach the upper atmosphere, whereas coarser particles of higher mass fall back to the surface more quickly due to gravitational settling. Thus, coarser particles are usually confined to the lower atmosphere, have shorter atmospheric lifetimes (~1-3 days), and affect hourly/daily scale climate processes such as the diurnal cycle. On the contrary, smaller particles reach higher altitudes and have longer atmospheric lifetimes. The extinction cross-section of an individual large particle is bigger than that of a small particle, but finer particles have stronger radiative effects per unit mass than coarser particles (Khan et al., 2015).~~

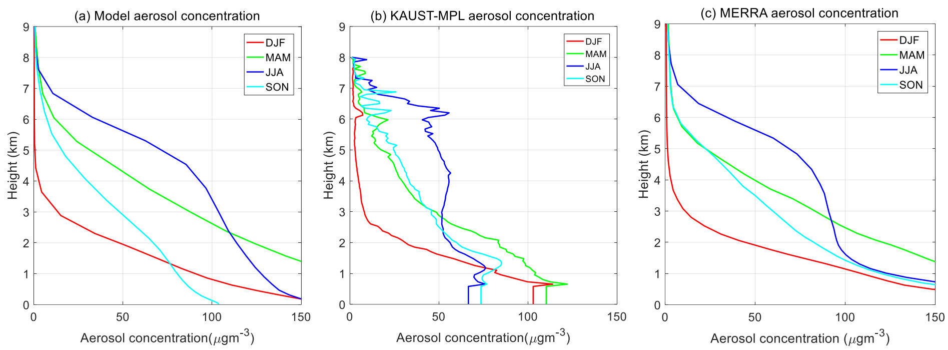

Figure 1~~0~~3. Comparison of the vertical profiles of total aerosol concentrations among (a) the model (b) KAUST–MPL, and (c) MERRA-2 data for different seasons at KAUST. For MERRA-2 and model data, total aerosol concentration is the sum of dust, sea salt, sulfate, OC and BC.

3.4~~3~~. Diurnal cycle of aerosols

~~Figures 11a and 11b show the diurnal cycle of 10m wind speeds compared with the model simulations and station data at KAUST for individual months from different seasons chosen to represent the four seasons. The profiles are in good agreement, although the model slightly overestimates the wind speed magnitudes. Nevertheless, the model captures the seasonal variation of wind speed well. These results indicate that our high-resolution simulations effectively reproduce local features of wind circulations.~~

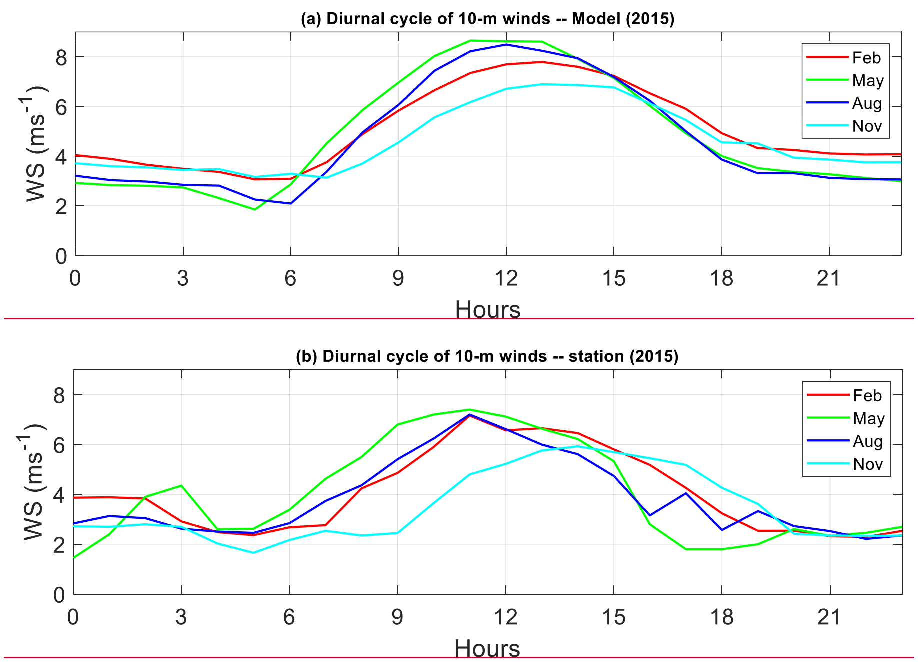

~~Figure 11. (a) Diurnal cycle climatology (2015) of 10-m winds at KAUST for four different months representing each season from (a) model and (b) station. Times are reported in UTC.~~

~~Figure 12 shows the diurnal cycles of aerosol extinction in KAUST_MPL data across the entire atmospheric column. Note that there are some gaps in the KAUST_MPL data because of the quality controls applied. In summer, there is significant dust activity in the morning (~ 06:00 local time), and in spring, dust activity peaks throughout the afternoon. In winter, The KAUST-MPL shows more vigorous dust activity in the nighttime (21:00 to 00:00 local time) near the surface. This increased dust activity at night is due to the effect of land breezes, which are strongest in winter (Fig. 6). We explore the effect of breezes on dust emissions and transport in section 3.4. KAUST_MPL shows high extinctions at a height of 6–7 km in summer, which represent long-range transported dust during large-scale dust events. Such high-intensity dust events are more frequent in summer and fall, as seen in the KAUST_MPL data (Fig. 7).~~

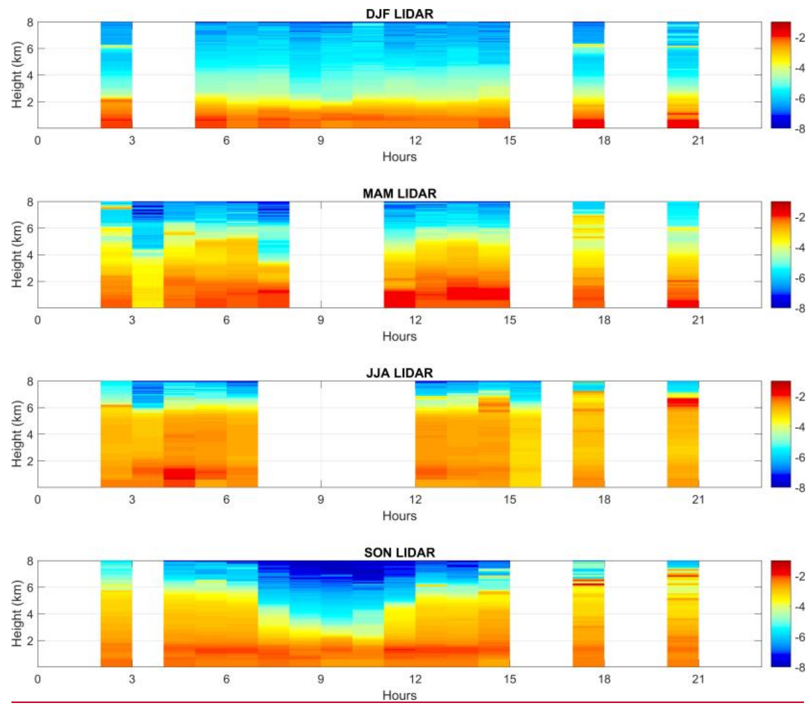
DJF LIDAR
MAM LIDAR
JJA LIDAR
SON LIDAR
Height (km)
Hours

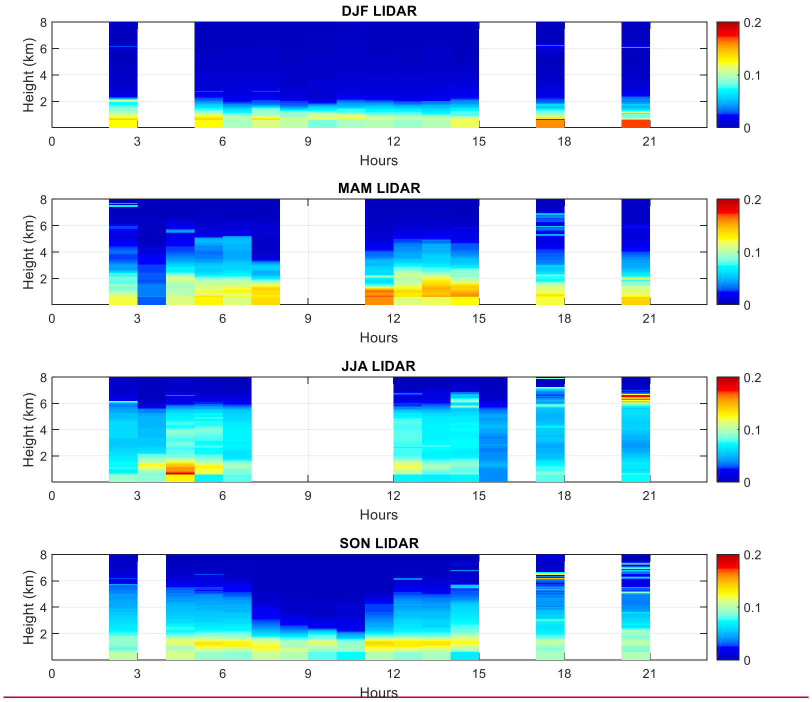

~~Figure 12. Diurnal profile of aerosol extinction coefficient at 532nm (natural logarithm) over the atmospheric column observed by the KAUST–MPL at KAUST. Times are reported in UTC.~~

Figure 14 shows the diurnal cycles of aerosol extinction in KAUST–MPL data across the entire atmospheric column. Dust is generally confined within the lowest ~2 km in winter and reaches ~6 km in summer, following the seasonal and diurnal variations of PBL. Note that there are some gaps in the KAUST–MPL data because of the quality controls applied. In summer, there is significant dust activity in the morning (~ 06:00 local time), and in spring, dust activity peaks throughout the afternoon. In winter, the KAUST–MPL shows more vigorous dust activity in the nighttime (21:00 to 00:00 local time) near the surface. This increased dust activity at night is due to the effect of land breezes, which are strongest in winter (Fig. 2). We explore the effect of breezes on dust emissions and transport in section 3.5. KAUST–MPL shows high extinctions at a height of 6–7 km, particularly in the evening of summer and fall, which represent long-range transported dust during large-scale dust events. Such high-intensity dust events are more frequent in summer and fall, as observed in the KAUST–MPL data (Fig. 10/11).

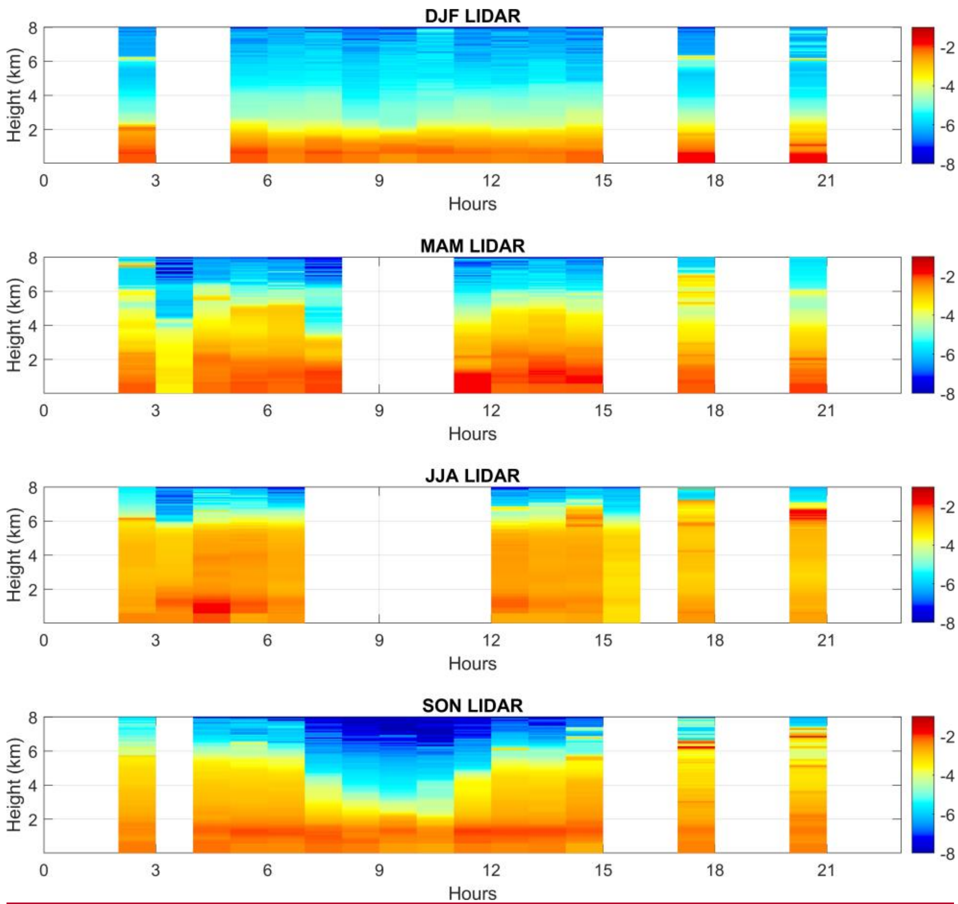

Figure 14. Diurnal profile of the natural logarithm of aerosol extinction coefficient at 532nm (km^{-1}) over the atmospheric column observed by the MPL at KAUST. Times are reported in UTC.

3.5~~4~~. Interaction of dust aerosols with Land/sea breezes

Figure 1~~3~~5 shows the ~~synoptic~~ circulation features of land and sea breezes in the vicinity of the KAUST–MPL site. The base map in the figure shows the high-resolution dust source function used in this study, where red hotspots represent the most dominant dust sources. Significant dust sources are observed on both sides of the Sarawat m~~M~~ountain range, i.e., the coastal sides and the eastern slopes. Sea breezes are strongest in spring and summer. In contrast, land breezes are strongest in winter and fall. In the daytime, sea breezes penetrate further inland, and the

KAUST–MPL site receives northwesterly winds. At night, the KAUST–MPL site experiences northeasterly land breezes, which are strongest in winter.

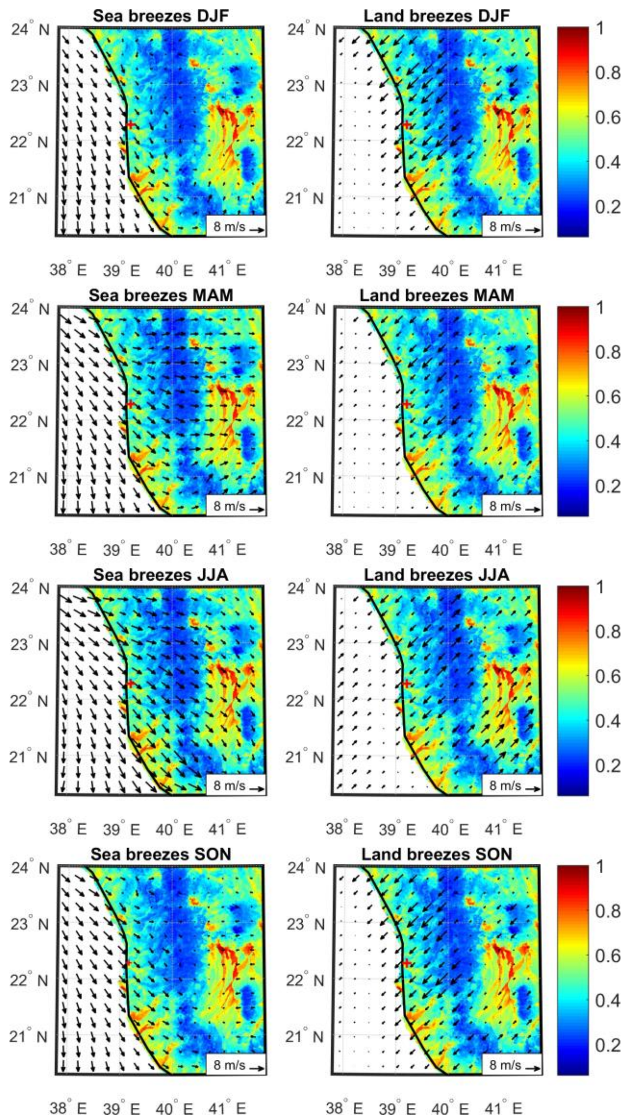
Sea breezes DJF
Land breezes DJF
Sea breezes MAM
Land breezes MAM
Sea breezes JJA
Land breezes JJA
Sea breezes SON
Land breezes SON
24° N
23° N
22° N
21° N
38° E 39° E 40° E 41° E
8 m/s
1
0.8
0.6
0.4
0.2

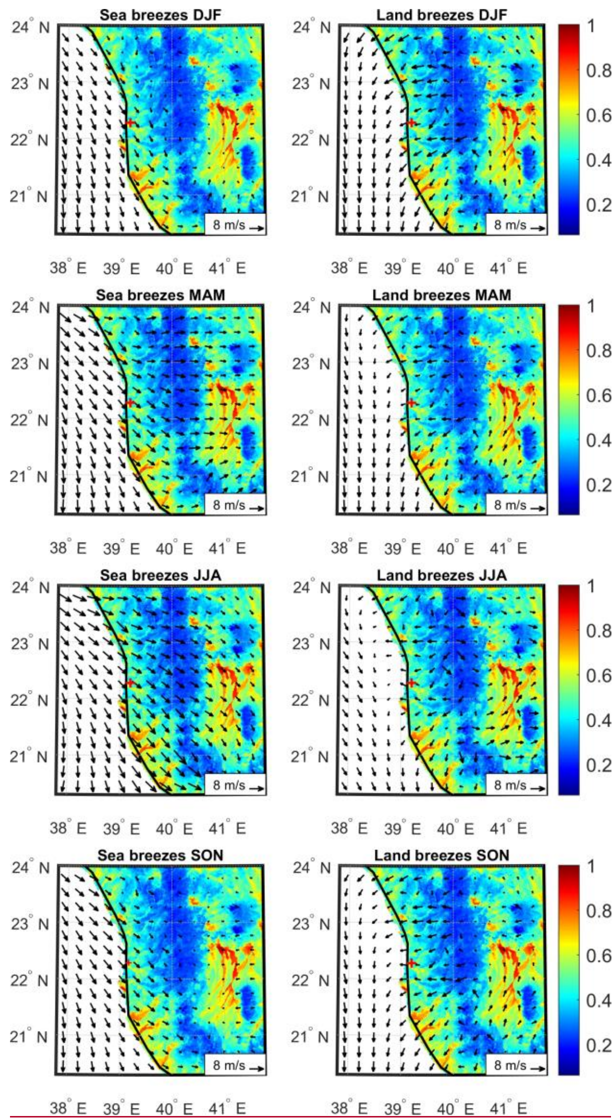

Figure 15~~3~~. Model 10-m wind speed showing the land (right) and sea (left) breezes. The data are averaged during the peaks of land and sea breezes to highlight their patterns, i.e., 01:00 to 03:00 hours UTC for land breezes (night) and 14:00 to 16:00 hours UTC for sea breezes (day). KAUST site is marked by a red (+) mark. The base map shows the high-resolution dust source function (Parajuli and Zender, 2017) used in this study~~, in which.~~ ~~t~~The values range from zero to one with the highest value representing the most significant dust source~~ region~~. ~~Update this figure.~~

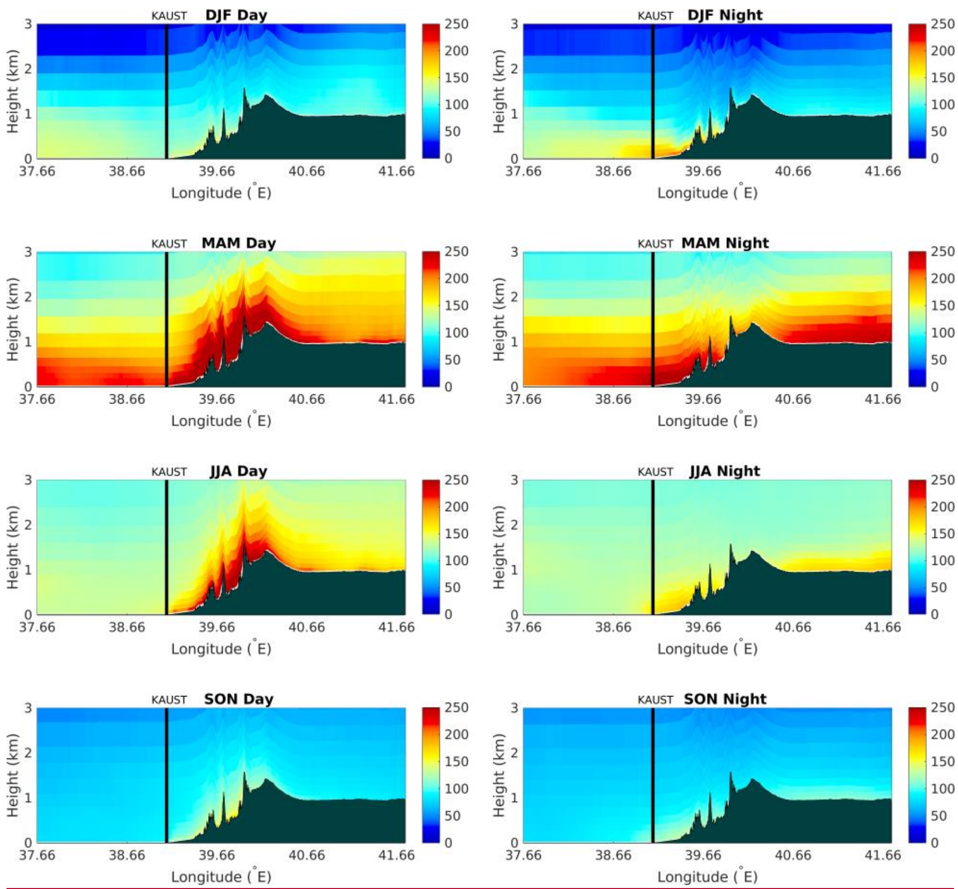

KAUST DJF Day
KAUST DJF Night
KAUST MAM Day
KAUST MAM Night
KAUST JJA Day
KAUST JJA Night
KAUST SON Day
KAUST SON Night
Height (km)
Longitude (°E)
37.66
38.66
39.66
40.66
41.66
0
50
100
150
200
250

1894

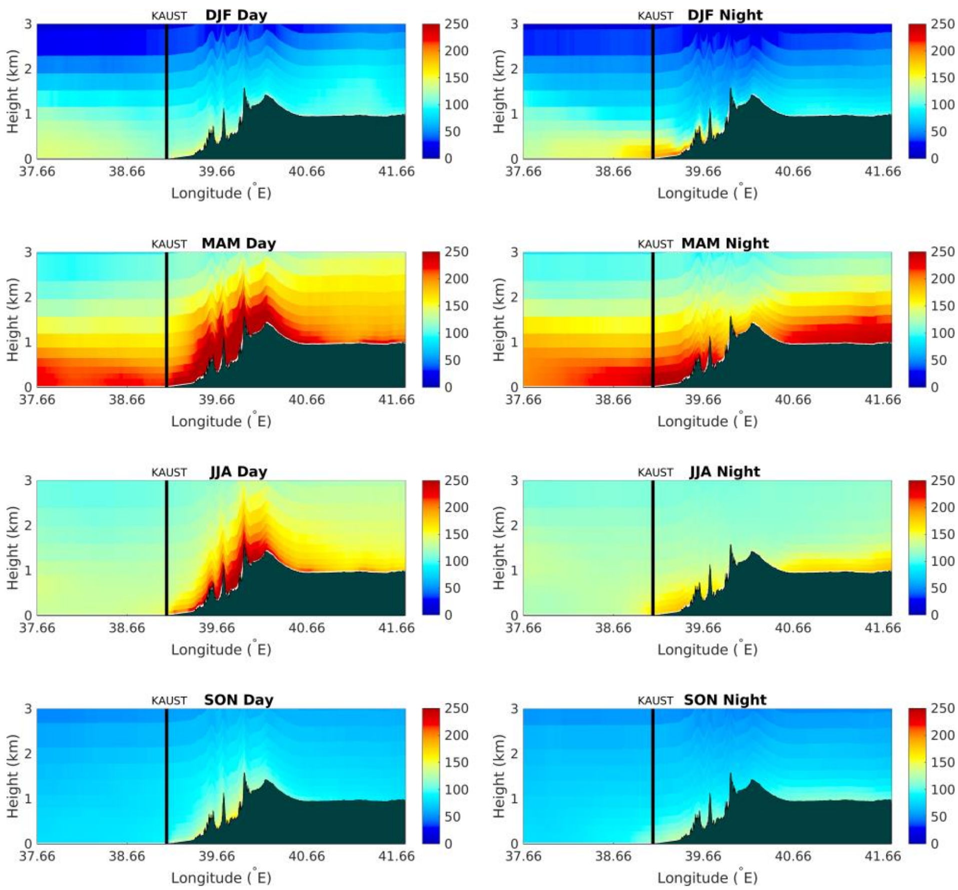

Figure 1~~4~~6. Longitudinal cross-section, perpendicular to the coastline, of aerosol concentrations ($\mu g\ m^{-3}$) over KAUST. Data are averaged seasonally and presented separately for the day (left column) and night (right column). Data averaged during the same period as in Fig. 15~~3~~ to demonstrate the effect of land and sea breezes on dust aerosols. The vertical line in black shows the location of the KAUST site. The land profile along the same section is depicted in black shades, the top of which shows the actual land elevation.

Figure 1~~4~~6 shows the total aerosol concentration ($\mu g\ m^{-3}$) within the innermost model domain (d03) in a longitudinal cross-section perpendicular to the coastline over KAUST. The section also shows the land profile (black shades) where the Sarawat Mountains that run along the eastern coast of the Red Sea and the relatively flat inland deserts that lie on the eastern side of the mountains are visible. The mountains reach a maximum elevation of ~1.5 km above sea level. The effect of land and sea breezes on dust is apparent in Fig. 16~~4~~, as discussed in further detail below.

During winter nights, a thin layer of dust collects over the marine boundary layer and the land near the KAUST site within ~1 km height. This layer ~~of dust~~ is an accumulation of dust that has been mobilized by land breezes from the coastal plains and the western flanks of the mountains. The coastal plains of the Red Sea are rich in fine fluvial sediments deposited by wadis, which are known sources of dust (Anisimov et al., 2017; Parajuli et al., 2019). The western flanks of the mountains also contain fluvial and intermountain deposits along the slope that are suitable for resuspension (Parajuli et al., 2014). This mobilized dust is transported towards the Red Sea, which seems to occur at low altitudes ~500 m (Fig. 16~~4~~). Some dust collects over the Red Sea during the daytime in the winter also, which appears well mixed within the relatively shallow PBL. During the day, the northwesterly sea breezes move landward ~~because of which~~preventing the dust emitted from the coastal region from ~~cannot~~ moveing over the sea. Therefore, this dust observed during the daytime must be the residual dust that accumulated overnight. The dust mobilization from the coastal area by the sea breezes (daytime) is weaker during the winter.

In the spring, there is very high dust loading over the coastal region and the western flanks of the mountains, which is much higher than in winter. This higher dust loading is consistent with stronger sea breezes in spring than in winter (Fig. 15~~3~~). The highest dust loading is observed over the slopes of the mountains at a height of 1–1.5 km. Recall that the LIDAR data shows a high dust loading at ~1–1.5 km height at the KAUST site. Two factors appear to contribute to this high dust loading. First, daytime sea breezes mobilize dust locally from the coastal plains and the western flanks of the mountains. These sea breezes then push the dust inland and upwards along the slope of the mountains, up to 3 km height. At the same time, the northeasterly Harmattan winds also bring dust from the nearby inland deserts towards the mountains. This dust is further uplifted when the dust-laden Harmattan winds encounter the sea breezes coming from the opposite direction. Thus, the interaction of sea breezes with the northeasterly Harmattan winds across the mountains mainly determines the vertical distribution of aerosols over the region. At night, the sea breezes as well as the PBL weaken, and the vertical extent of dust in the atmosphere reduces. ~~However, the atmosphere over the deserts on the eastern side of the mountains also looks remarkably dusty. This is because the land breezes become stronger at night and mobilizes dust from the deserts.~~ The land breezes also appear to transport the dust towards the Red Sea from the western flanks of the mountains at night.

In summer, the patterns of dust mobilization and transport are similar to those in spring but are not quite as pronounced. In fall, the mobilization of dust from the coast and its ocean-ward transport is very weak, and the~~ir~~ patterns are similar to those in winter.

~~The model-simulated vertical distributions of aerosols do not exactly match the KAUST–MPL profiles presented earlier (Fig. 8). Although it is difficult to identify the exact reason for this discrepancy, there are several possible explanations. Although the effect of orography on dust seems to be correctly resolved (Fig. 14), the transport of dust towards the KAUST site may not be fully resolved. Part of this discrepancy could also be because of the coarser model resolution compared to KAUST–MPL data. KAUST–MPL data is a point measurement and the model data represents the profiles at a 1.3x1.3 km grid cell, which, although high-resolution, can still produce a large difference, especially in a land-ocean boundary.~~

Figure 17~~5~~ shows the daytime and nighttime winds at three altitudes for two specific months in summer (August) and winter (February). Note that the winds are shown at different levels for August and February to highlight the features of land and sea breezes better. The depth of sea breezes and land breezes are different, as expected, with the sea breezes being much deeper than the land breezes, primarily because the PBL is higher during the day than at night. The local topography also plays a role. Sea breezes are still strong up to a height of ~1150m; however, the land breezes only reach a height of ~200m. By about 450m, the land breezes subside completely. The land breeze circulation is confined by the height of the mountains, whereas the sea breeze circulation extends to a much higher altitude. The returning flow of the sea breezes takes place at a height of ~2250m in the form of northeasterly trade winds, which are responsible for bringing the dust to our site from the inland deserts. The return flow of the land breezes occurs at a height of ~1500m with a change of direction of nearly 180^{o} of the lower part of the subtropical westerly jets (de Vries et al., 2013) (see supporting information Fig. S6). The variation in the pattern of these winds along the vertical dimension is generally consistent with the profile of modeled dust that we presented earlier (Fig. 16~~4~~).

~~In summary, the timings and patterns of dust emission and transport in the study region are evidently affected by land and sea breezes. These results are summarized in the schematic diagram in Fig. 1. Note that, across the majority of the Arabian Peninsula, the seasonality of dust mobilization is quite different to our study region, where dust emission and transport are maximum during summer (Parajuli et al., 2019).~~

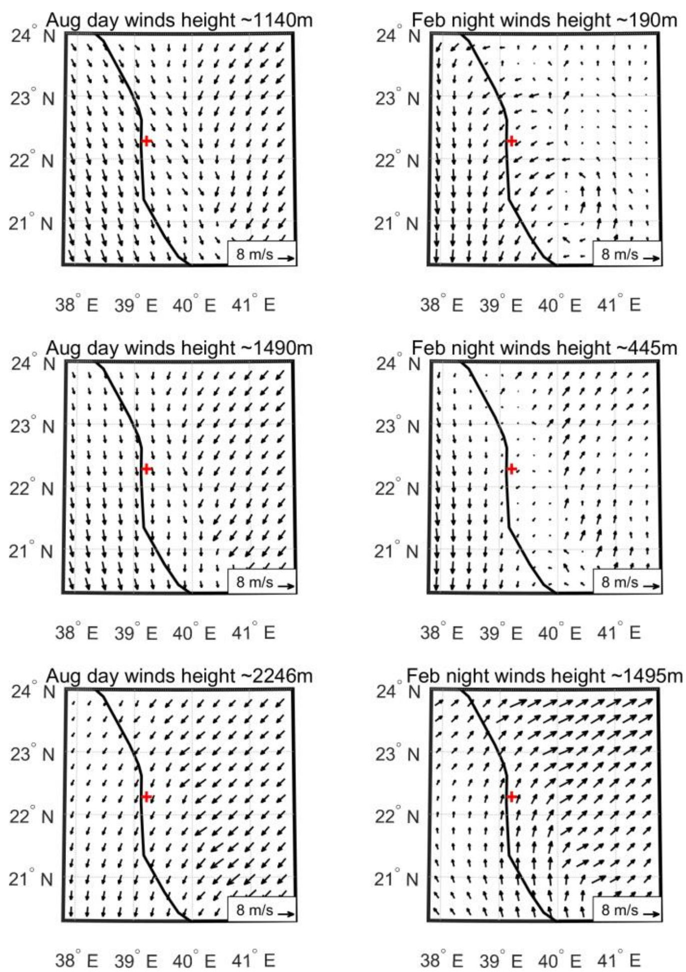

Figure 17~~5~~. Model (WRF) winds at three different elevations for August (left) and February (right) within the study domain. The KAUST site is marked by a red (+) symbol.

In summary, the timings and patterns of dust emission and transport in the study region are evidently affected by land and sea breezes. Note that, across the larger parts of the Arabian Peninsula, the seasonality of dust mobilization is quite different to our study region, where dust emission and transport are maximum during summer (Parajuli et al., 2019).

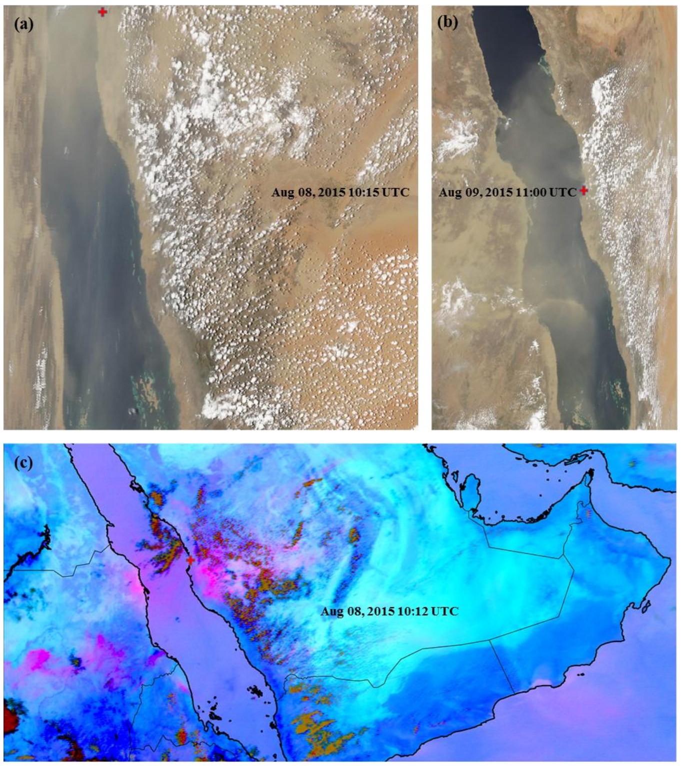

~~Figure 16. MODIS and SEVIRI images during a large-scale dust event. True color images from MODIS on (a) August 08, 2015 10:15 UTC (b) August 09, 2015 11:00 UTC, and (c) Meteosat SEVIRI RGB dust composite for Aug 08, 2015 10:12 UTC. KAUST site is marked by a red (+) symbol.~~

~~3.5. Case study of a summer-time dust event~~

~~A large-scale dust storm swept over the KAUST site on August 08, 2015, as seen in the MODIS image in Fig. 16a. The dust event lasted for two days until August 09. The KAUST AERONET station registered the second-highest AOD of the entire year on August 08 with the daily mean AOD reaching 2.48. The AERONET angstrom exponent (AE 440/675) value showed a sharp reduction on this day, from 0.41 on August 06 to 0.10 on August 08. This reduction indicates the dominance of coarse-mode dust during the event and thus, that the dust event originated from nearby inland deserts. By August 09, the dust storm moved towards the south/southwest and spread to a broader region across the Red Sea and northeast Africa. The MODIS RGB image on August 09 shows a dust plume originating from northeast Africa around Port Sudan, which, after being deflected by the northerly winds, experiences a marked curvature (Fig. 16b).~~

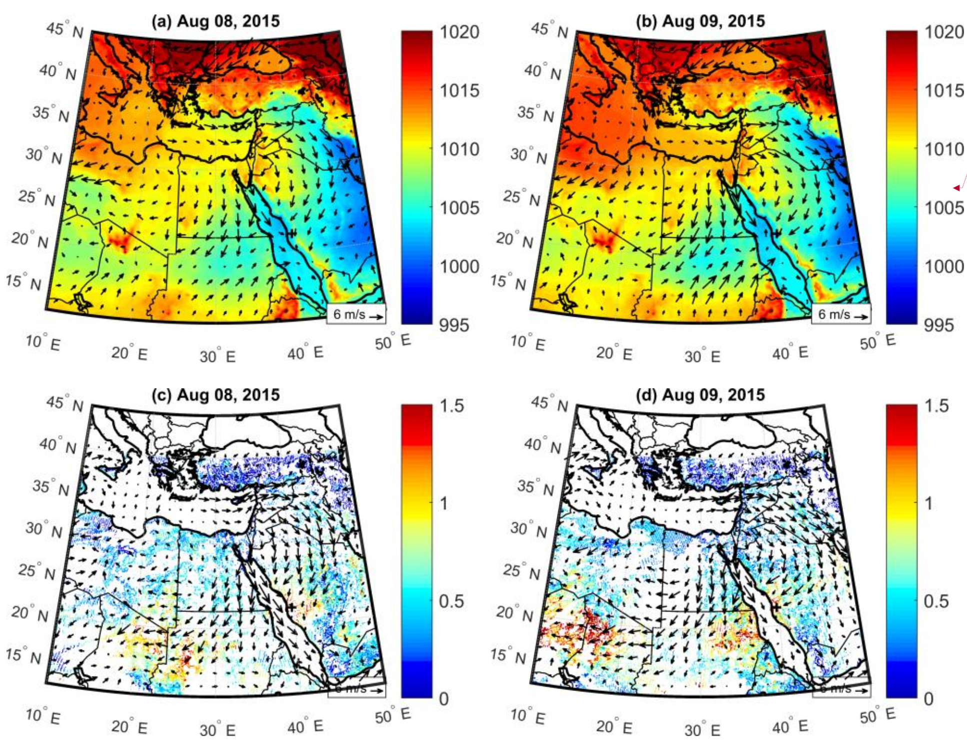

~~**Figure 17. Surface pressure and wind vectors from ECMWF operational analysis data during the dust event (a and b), and MODIS deep blue AOD data overlain by model wind vectors (c and d).**~~

Formatted: Font: Bold, Font color: Text 1, Complex Script Font: Bold, Pattern: Clear

Formatted: Paper, Space After: 0 pt

Formatted: Paper

~~The synoptic conditions of this dust event are somewhat similar to those of a summer-time dust event reported by Kalenderski and Stenchikov (2016), which was centered over North Sudan. The dust event we describe here is a typical summer-time dust event caused by high winds driven by strong pressure gradients (Alharbi et al., 2013). Although haboob-type dust events commonly occur in the region, analysis of the RGB pink dust composite (Fig. 16c) shows only a few scattered clouds over the study site during this period, ruling out the possibility of a haboob dust event. Haboob is a typical dust event that commonly occurs in regions with moisture convection, in which dust is generated by strong divergent winds that form around a cold pool of downdrafts (Anisimov et al., 2018).~~

Formatted: Font: Bold, Complex Script Font: Bold

~~As seen in Figs. 17a, b, a high-pressure system developed in the eastern Mediterranean region and Turkey on August 08, which expanded towards Africa/Middle East and created stronger winds over the region on August 09. On August 08, a low-pressure system developed, which was centered around northeast Africa (Sudan). Winds converging towards this low from the north/northeast adopted a northeasterly flow pattern, which is characteristic of the Harmattan winds prevalent in the region. The winds originating from the eastern Mediterranean were forced to curve by the Hijaz mountains in the western Arabian Peninsula, finally converging with the low-pressure system in northeast Africa and the Red Sea, where the high energy of the flow was finally dissipated. A high-pressure system persisted throughout the dust event over the Ethiopian highlands and south Sudan, as shown in Figs. 16a, b. This high-pressure system gave rise to the southerly/southwesterly winds that also converged towards the low-pressure region around northeast Africa and the Red Sea.~~

Formatted: Font: Bold, Font color: Text 1, Complex Script Font: Bold, Pattern: Clear

~~MODIS AOD also showed a high aerosol loading around KAUST (+ symbol in Figs. 17c, d) on August 08 that spread across a larger area towards northeast Africa on August 09. Figure 17 shows that the dust mobilization was evidently caused by the northerly/northeasterly winds moving over the study site. The wind vector patterns are very consistent between ECMWF operational analysis (Figs. 17a, b) and model simulations (Figs. 17c, d) for most parts of the domain. This observation is not surprising because we use the ECMWF operational analysis data for boundary conditions and apply 'grid nudging' at each model grid using the same ECMWF dataset. The wind patterns in the two figures differ in some areas, however, especially over the Ethiopian highlands. Note that the model winds presented are derived from the coarser 12 km domain to show the wind patterns over a larger region beyond our innermost study domain. In the Ethiopian highlands region, where there is a strong effect from the topography, such a coarse resolution may not be enough to resolve the fine features of the wind circulations. At the study site, however, winds are indeed better resolved in our model because the resolution of the innermost domain is much higher, i.e., 1.33 km.~~

~~The model captures the major features of the dust storm reasonably well. Both the model and the AERONET data register this event as the second-largest dust event of 2015. On August 09, the model shows a daily average (daytime only) AOD of 1.18 compared to 1.79 given by the AERONET data (underestimation by ~35 %).~~

~~Figure 18 compares the vertical profiles of dust as provided by model simulations and the KAUST-MPL data during the dust event. The right column in the figure shows the simulated dust extinction coefficient at 550nm, covering the three days during the dust event. Because of the quality constraints applied, the processed extinction data from KAUST-MPL are only partially available during this event. Therefore, we present the raw normalized relative backscattering (NRB) from the KAUST-MPL to examine the evolution of this dust event qualitatively, as shown in Fig. 18. Note that around noon local time in summer, the KAUST-MPL field of view is covered to avoid the sun glare, which is why there is some gap in the data around this time. In the KAUST-MPL NRB data (Fig. 18, left column), the dust plume appears as early as Aug 08 (~05:00 UTC) at a height of 1-1.5 km, indicating the onset of the dust storm. This dust plume becomes strongest by August 09, covering a large part of the atmospheric column with dust. Although the onset of the dust event is slightly earlier in the model compared to KAUST-MPL data, the model also shows high dust activity on August 09, consistent with KAUST-MPL observations. The dust is mainly confined within a height of ~2 km, which is consistent in both datasets. We also observed a higher intrusion of dust into the atmosphere, which is expected because the PBL is well developed in summer.~~

~~Note that the model data also show a high extinction at a height of ~6 km on August 09/10, particularly at night (Fig. 18), which is consistent with the dust layers observed at 6-7 km height in the KAUST-MPL nighttime data (Fig. 8). Although the model data does not identify these dust layers at 6-7 km in the seasonally averaged profiles presented earlier (Fig. 8), the model nonetheless correctly identified these same dust layers in this event (Fig. 18). The demise timing of the dust storm is consistent in both the model and KAUST-MPL data. These results further confirm that the dust layers observed at 6-7 km height correspond to the long-range transported dust during large-scale dust events.~~

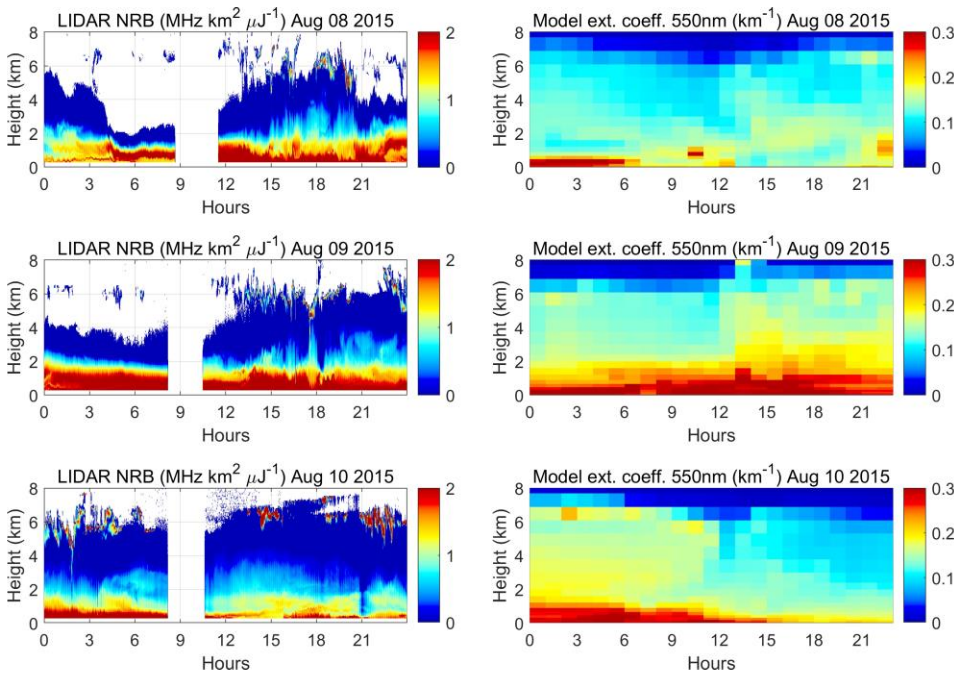

~~**Figure 18. Natural logarithm of normalized relative backscatter (NRB) at 532 nm measured at the KAUST MPLNET station (left column) and the model-simulated dust extinction coefficient at 550 nm (right column) during the dust event of August 08/09. Times are reported in UTC.**~~

~~**4. Discussion and conclusion**~~

4. Discussion

4.1. Model performance

The model simulated the surface wind speed at the KAUST site reasonably well as compared to station data (Fig. 3). Accurately representing the surface winds is vital because the dust emission is parameterized as a function of friction wind velocity in WRF-Chem (Marticorena and Bergametti, 1995; LeGrand et al., 2019). Note that dust emissions ~~is~~are generally caused by wind gusts that occur over~~in~~ very short time scales (seconds) (Engelstaedt and Washington, 2007), which are much stronger than the average seasonal wind speed displayed in Figure 2. We can expect these wind gusts to be represented in our simulations because we have used a very small model time-step (8 sec) in our d03 domain. Given our primary focus is on vertical aerosol profiles, further analysis of wind gusts is beyond this study's scope~~Note that dust emission is generally caused by wind gusts that occur in very short time scales (seconds) (Engelstaedt and~~

Formatted: Paper

Formatted: Font: Bold, Complex Script Font: Bold

~~Washington, 2007), which are much stronger than the average seasonal wind speed displayed in Figure 2. We can expect that these wind gusts are represented in our simulations because we have used a very small model time-step (8 sec) in our d03 domain. Given our focus on aerosol vertical profiles, a further analysis of wind gusts is beyond the scope of this study.~~

The model reproduces the AOD time series well in all seasons as compared with several datasets, including AERONET, MODIS, MISR, and MERRA-2 (Figure 4), with an MBE of 13.4% against AERONET data. There is some mismatch in the AOD profiles among different datasets during some large-scale dust events, ~~which is~~ partly because of the difference in sampling and measurement frequencies~~s among different datasets.~~

The model successfully captured the evolution of a dust event that occurred in 2015 over the study site in terms of its onset and demise, as well as the height of the dust layer (Fig. 9). Our results were consistent with several previous studies, such as in Yuan et al., 2019 and Anisimov et al., 2018. The model generally reproduced the elevated dust layers at ~6 km during the dust event (Fig. 9), which were prominently seen in KAUST-MPL observations (Figs. 10/11). However, the model underestimated the AOD at KAUST by about 35 % during the event compared to AERONET AOD. Simulating these complex, large-scale dust events is extremely challenging, and thus, we do not expect the model to capture them as precisely, since they occur only a few times (~2-3) in a year. We note that the performance of WRF-Chem to simulate these large-scale dust events is case-specific (e.g., Teixeira et al., 2016; Fernández et al., 2019) and should not be generalized. The model performance was indeed sensitive to the type of dust event (e.g., Kim et al., 2017), the details of the dust-emission processes (Klose and Shao, 2012; Klose and Shao, 2013), the dust source function used (Kalenderski and Stenchikov 2016; Parajuli et al., 2019), and the prescribed size distribution of the emitted dust (Kok et al., 2017; Marenco et al. 2018).

4.2. Aerosol vertical profiles

~~In this study, we investigated three main aspects of dust aerosols over the eastern coast of the Red Sea. We used data collected from the only operating LIDAR in the region, located on the KAUST campus, together with other collocated observations and high-resolution WRF-Chem model simulations. To summarize, we first investigated the vertical profile of aerosol extinction and concentrations, as well as their seasonal and diurnal variability over the study site. Secondly, we evaluated how accurately WRF-Chem reproduced the vertical profiles of aerosols over the study site and examined its performance during a large-scale dust event of 2015. Thirdly, we investigated how the prevailing land and sea breezes affected the distribution of dust over the site, which is located exactly at the land-ocean boundary. This study represents a first attempt to understand and describe the interactions between breezes and dust in this largely understudied region. The main findings of this research are summarized as follows.~~

- ~~The simulated AOD obtained from the high-resolution WRF-Chem model setting is reasonably consistent over the study site across all observational datasets, including~~

Formatted: Paper

Formatted: Font: Bold, Complex Script Font: Bold

Formatted: Font color: Custom Color(RGB(28,29,30)), Pattern: Clear (White)

Formatted: List Paragraph, Space After: 15 pt

~~AERONET, MODIS, and MISR. The simulated AOD shows a mean bias error (MBE) of ~13.4 % with the AERONET data.~~

- ~~WRF-Chem simulations show that dust has the highest contribution to total AOD among all aerosol types, contributing up to 92 % in summer. Anthropogenic (sulfate, OC, and BC) and sea salt aerosols contribute up to 15 % and 6 % to the total AOD, respectively, both of which are highest in winter.~~

~~Over the study site, most dust is confined in the troposphere, within a height of 8 km. In winter, dust is confined to lower altitudes than in summer, which is consistent with the lower PBL height in winter than in summer.~~

Formatted: Indent: Before: 0.5", Space After: 15 pt, No bullets or numbering

- ~~There is a marked difference in the daytime and nighttime vertical profile of aerosols in the study site, as shown by the KAUST MPL data. We observed a prominent dust layer at ~5–7 km in the nighttime in the KAUST MPL data, which is supposedly formed by dust lifted up by day-time convection in the central peninsula deserts and transported to the coast by easterly winds.~~

Formatted: Space After: 15 pt

Formatted: Font color: Custom Color(RGB(28,29,30)), Pattern: Clear (White)

~~The climatology of the vertical profile of daytime dust extinction is consistent in the KAUST MPL, MERRA-2, and CALIOP data in all seasons, which is well reproduced by our WRF-Chem simulations. The profiles from the different datasets match better in winter than in summer, which is consistent with the results of Wu et al. (2017).~~

Formatted: Indent: Before: 0.5", Space After: 15 pt, No bullets or numbering

- ~~There is significant diurnal variation in aerosol loading at the study site in all seasons, as shown by the KAUST MPL data. Stronger aerosol activity occurs in the early morning during the summer, in the afternoon during the spring, and in the night during the winter.~~

Formatted: Space After: 15 pt

~~Both sea and land breezes in daytime and nighttime, respectively, create dust emissions from the coastal plains and the western flanks of the Sarawat Mountains. Such dust emissions are most prevalent in spring.~~

Formatted: Indent: Before: 0.5", Space After: 15 pt, No bullets or numbering

~~Sea breezes push the dust mobilized from the coastal plains up along the slope of the Sarawat Mountains, which subsequently encounters the dust-laden northeasterly trade winds coming from inland deserts, causing elevated dust maxima at a height of ~1.5 km above sea level across the mountains.~~

Formatted: Space After: 15 pt

- ~~The nighttime land breezes are strongest in winter; these northeasterly land breezes transport dust aerosols from the coastal plains and the mountain slopes towards the Red Sea. The sea breeze circulation is much deeper (~2 km) than the land breeze circulation (~1 km), as illustrated in Fig. 1.~~

~~Sea breezes push the dust mobilized from the coastal plains up along the slope of the Sarawat Mountains, which subsequently encounters the dust-laden northeasterly trade winds coming from inland deserts, causing elevated dust maxima at a height of ~1.5 km above sea level across the mountains.~~

Formatted: Indent: Before: 0.5", Space After: 15 pt, No bullets or numbering

- ~~WRF-Chem qualitatively captured the evolution of a large-scale summertime dust event in 2015 over the study site. The model simulated the onset, demise, and the height of the dust storms reasonably well.~~

Formatted: Space After: 15 pt

The seasonal ~~climatology of~~ aerosol vertical profiles ~~was~~ were consistent among all datasets that we compared~~,~~ viz. KAUST–MPL, MERRA-2, and CALIOP (Figs. 10/11/13)~~, despite their different vertical and horizontal resolutions~~. These ~~seasonal profiles~~results ~~were~~ are consistent with those reported by Li et al. (2018) over the same region. The WRF-Chem model successfully reproduced the vertical profiles of dust aerosol extinction and concentration in terms of ~~seasonal climatology~~seasonality, when compared with the abovementioned datasets. Nearer the surface, the model showed some disagreement with the observational datasets, as also noted in some previous studies (e.g., Hu et al., 2016; Wu et al., 2017; Flaounas et al., 2017). Note that such disagreement between data collected near the surface exists among the observational datasets as well; this disagreement could arise~~s~~ due to differences in the retrieval algorithms used ~~as well as~~and the ~~differences in~~ ~~the~~ resolution of the datasets, as discussed in detail below.

The difference in vertical profiles retrieved from KAUST-MPL and CALIOP data could be related to the differences in the algorithm and resolution between the two datasets. Firstly, while retrieving aerosol extinction profiles, the CALIOP algorithm uses different prescribed extinction-to-backscatter (lidar ratio) for a set of aerosol types from a lookup table (Omar et al., 2009; Winker et al., 2009; Kim et al., 2018). In addition, the CALIOP algorithm has difficulty in identifying the base of aerosol layers accurately. In particular, the level-3 algorithm ignores the 'clear air' between the surface and the lowest aerosol layer when averaging to avoid underestimation of extinction in the lower part of the aerosol profile (Winker et al, 2013). In contrast, the MPL algorithm assumes an averaged lidar ratio for the whole column based on the aerosol PSD, refractive index, and sphericity, in such ~~as~~ way that it satisfies both AERONET and MPL co-incident data. Because of the assumption of a constant lidar ratio, MPL retrievals near the surface could be erroneous, especially when multiple aerosol layers are present (Welton et al., 2002a). Secondly, KAUST–MPL is a point measurement that captures the temporal evolution of the dust storms better than CALIOP because it has a higher temporal resolution. For instance, CALIOP can undersample or overlook some dust events that last only for a few hours. On the other hand, CALIOP could sample more spatial details of a dust storm because of its extended coverage along its track compared to KAUST–MPL data. Nonetheless, these two datasets complement one another, and their combined use can be beneficial in understanding the large-scale dust storms.

Analysis of the KAUST–MPL data revealed several interesting features of the vertical profile of aerosols over the study site, which ~~had not been~~were not ~~previously~~ documented in ~~other~~ earlier studies. For example, we observed a significant difference between the daytime and nighttime vertical profiles of aerosols. Some of these detailed features were not apparent in the model simulations. The model underestimated the nighttime aerosol extinctions at ~5~~6~~–7 km height in summer and fall compared to the KAUST–MPL data (Figs. 10/11). Although the model data did not identify these dust layers at 6–7 km in the seasonally averaged profiles, the model nonetheless correctly identified these same dust layers during the dust event analyzed in the case study (Fig. 9). This result supports our speculation that the elevated dust layers at ~6-7 km represent transported dust from inland deserts during large-scale dust events.

Formatted: Font: (Default) Times New Roman, 12 pt, Font color: Custom Color(RGB(28,29,30)), Complex Script Font: Times New Roman, 12 pt, Pattern: Clear (White)

Formatted: Font: (Default) Times New Roman, 12 pt, Font color: Custom Color(RGB(28,29,30)), Complex Script Font: Times New Roman, 12 pt, Pattern: Clear (White)

Formatted: Font: (Default) Times New Roman, 12 pt, Font color: Custom Color(RGB(28,29,30)), Complex Script Font: Times New Roman, 12 pt, Pattern: Clear (White)

Formatted: Font: (Default) Times New Roman, 12 pt, Font color: Custom Color(RGB(28,29,30)), Complex Script Font: Times New Roman, 12 pt, Pattern: Clear (White)

Formatted: Font: (Default) Times New Roman, 12 pt, Font color: Custom Color(RGB(28,29,30)), Complex Script Font: Times New Roman, 12 pt, Pattern: Clear (White)

Formatted: Not Highlight

Formatted: Not Highlight

Formatted: Not Highlight

Formatted: Not Highlight

Formatted: Not Highlight

Formatted: Not Highlight

Formatted: Not Highlight

Formatted: Not Highlight

Formatted: Not Highlight

Formatted: Not Highlight

Formatted: Not Highlight

Formatted: Not Highlight

Formatted: Not Highlight

Formatted: Not Highlight

Formatted: Font color: Auto

Formatted: Font color: Auto

~~which is consistent with the dust layers observed at 6–7 km height in the KAUST–MPL nighttime data (Fig. 8). Although the model data does not identify these dust layers at 6–7 km in the seasonally averaged profiles presented earlier (Fig. 8), the model nonetheless correctly identified these same dust layers in this event (Fig. 18).~~~~,~~ It is difficult to identify the exact reason for the above discrepancy between the model and KAUST-MPL data, but there are several possible explanations~~which we attribute~~e~~ed to~~. First, the~~ the~~ model could be deficient in ~~'s inability to~~ representing~~ either~~ the deep convective mixing of dust in the central-peninsula deserts. Second, a~~-~~lthough the effect of orography on dust seems to be correctly resolved (Fig. 16), the long-range transport of dust from the deserts towards the KAUST site may not be fully detected. Third, ~~and/or long-range transport of aerosols to the coastal regions.~~ ~~The model-simulated vertical distributions of aerosols do not exactly match the KAUST–MPL profiles presented earlier (Fig. 8). Although it is difficult to identify the exact reason for this discrepancy, there are several possible explanations. Although the effect of orography on dust seems to be correctly resolved (Fig. 14), the transport of dust towards the KAUST site may not be fully resolved. Part of this~~part of this discrepancy could also be because of the ~~coarser~~insufficient model spatial resolution compared to KAUST–MPL data. KAUST–MPL data is a point measurement ~~and~~while the model data represents the profiles at a 1.3x1.3 km grid cell, which, although high-resolution, can still produce a ~~large~~substantial difference, especially in a land-ocean boundary. Finally, the discrepancy could also be due to the limitation of the GRASP algorithm in handling clouds, because of which the aerosol layers observed at 5-7 km height in the nighttime could be contaminated with clouds, as explained further below.

T~~In order t~~o better understand the origin of two elevated dust layers observed (~1-2 and 6-7 km) and investigate the possibility of thin-cloud contamination in our MPL retrievals, we analyzed the volume-depolariz~~s~~ation profiles provided by the KAUST-MPL, synchronous to the attenuated backscatter profiles used in the retrievals~~z~~. The a~~A~~verage volume depolariz~~s~~ation value in the lower atmosphere (1-2 km) was estimated to be 13-14% on average and 7-8% for the upper part (6-7 km) for the selected ~~–~~period. Such values indicate that high extinction values in this altitude range cannot come exclusively from clouds because pure water clouds generally yield a 1-2% depolariz~~s~~ation value and ~30% or even higher in the case of cirrus clouds (e.g., Del Guasta and Valar, 2003). The lower depolarization value in the upper part could be explained by the fact that the aerosol particle sizes are much finer ~~compared to that~~than those in the lower part. At the same time, a lower depolariz~~s~~ation value also suggests the possibility of partial influence by thin clouds. The presence of thin clouds can probably cause some overestimation of aerosol concentrations and extinction at these altitudes. However, such an overestimation is expected to increase the fitting errors, which are ~~which are~~ easily detectable, as mentioned earlier. To ascertain this with full confidence, we plan a further analysis utiliz~~s~~ing simultaneous retrieval of sun-photometric observations together with backscatter and volume-depolariz~~s~~ation profiles provided by KAUST-MPL in the future.

Although both model results and the KAUST-MPL retrievals have their own limitations, ~~B~~both KAUST–MPL and the model data identified two prominent layers of dust over the study site,

Formatted: Tab stops: Not at 4.15"

Formatted: Font color: Custom Color(RGB(28,29,30)) one at a lower altitude (~1–2 km) and another at a higher altitude (~6–7 km). These two dust layers correspond~~ed~~ to two different dust sources. The lower dust layer corresponded to dust originating from nearby deserts, and the upper dust layer corresponded to dust coming from more remote sources and further inland. The two layers of dust are typical in this region during ~~a large-scale~~ dust events. As explained before, a large-scale disturbance usually brings dust from remote sources at higher altitudes (~6–7 km). When the disturbance comes closer to the site, high surface winds associated with the disturbance also pick up more dust from nearby deserts giving rise to a high dust loading at ~1–2 km height. ~~It is obvious that the upper layer of dust consist of finer particles and the lower layer of coarser particles.~~ Such stratified aerosol layers have been previously observed near land-ocean boundaries, where strong temperature inversion occurs, restricting further mixing of aerosols in the PBL and above (Welton et al., 2002b).

In the lower part (~1-2 km), the atmospheric dust loading is mostly dominated by coarse-mode particles. In contrast, dust in the upper level (~6-7 km) typically constitutes long-range transported finer particles. Finer particles can easily reach the upper atmosphere, whereas coarser particles of higher mass fall back to the surface more quickly due to gravitational settling. Thus, coarser particles are usually confined to the lower atmosphere, have shorter atmospheric lifetimes (~1-3 days), and affect hourly/daily scale climate processes such as the diurnal cycle. On the contrary, smaller particles reach higher altitudes and have longer atmospheric lifetimes. The extinction cross-section of an individual large particle is bigger than that of a small particle, but finer particles have stronger radiative effects per unit mass than coarser particles (Khan et al., 2015).

We observed some interannual variability while comparing the vertical profiles for 2015 and 2016, but ~~it is~~was not ~~too~~ too significant~~large~~ (Fig.~~ure~~ S9~~7~~). Therefore, the observed vertical distribution of dust aerosols can be considered ‘typical’ for our~~the~~ region and possibly for other land-ocean boundaries (e.g., Rasch et al., 2001). This is understandable because the synoptic winds causing large-scale dust events ~~in the region~~, ~~as well as~~and the diurnal-scale breezes that affect the dust distribution, both have strong seasonality over the study region (Kalenderski and Stenchikov, 2016; Parajuli et al., 2019).

~~The aerosol extinction profiles observed in our study site may be broadly representative of typical aerosol profiles near other land-ocean boundaries.~~ However, as demonstrated by our results, vertical profiles of aerosols can be affected by ~~local or~~ regional processes such as breezes, which indicate that the profiles can differ across different regions. Therefore, it is vital to examine the aerosol vertical profiles of a region to understand the regional climate.

4.3. Dust-breeze interactions

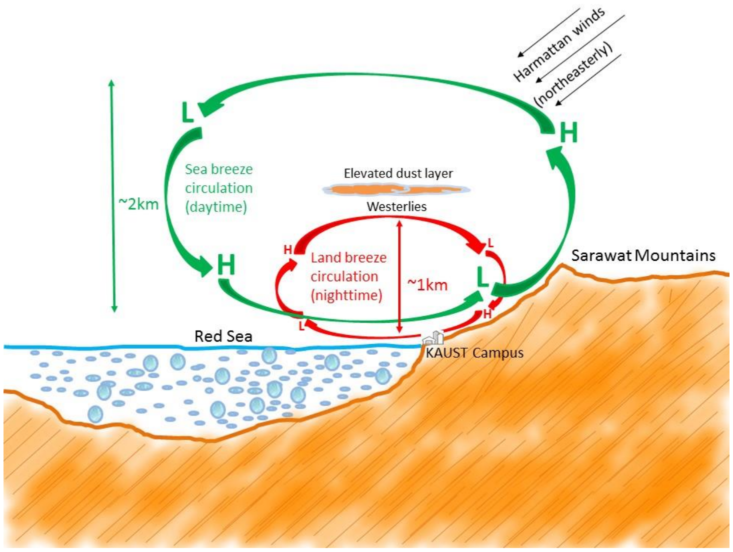

Figure 18. Schematic diagram showing sea breeze (daytime, in green) and land breeze (nighttime, in red) circulations and dust distribution over the study site at KAUST.

KAUST–MPL-retrieved aerosol vertical profiles also provided an opportunity to understand how aerosols interact with land and sea breezes over the eastern coast of the Red Sea. ~~, as summarized in Fig. 1.~~ The salient features of the land and sea breezes over the study region revealed by our study are ~~presented~~summarized in Fig. 18~~, which we discuss in detail later.~~ ~~Such~~These fine-level interactions are often poorly resolved in coarse-scale simulations. Our high-resolution simulations (~1.33x1.33 km) nonetheless correctly resolved these features and showed how breezes affect dust aerosol distribution over the region. Our study is important because the breezes and dust can directly affect the daily life of populations that reside in the coastal area. Furthermore, dust over the region affects the surface temperature of the Red Sea through changes in radiation (Sokolik and Toon, 1998; Osipov et al., 2015, Osipov et al., 2018), which could have an enormous impact on the Red Sea climate and marine habitats. Additionally, changes in dust deposition also affect the availability of nutrients delivered to marine ecosystems (Prakash et al., 2015).

Formatted: Paper

Formatted: Font: Bold, Complex Script Font: Bold

~~The model successfully captured the evolution of a dust event that occurred in 2015 over the study site in terms of its onset and demise, as well as the height of the dust layer. Our results were consistent with several previous studies, such as Yuan et al. (2019) and Anisimov et al. (2018). However, the model underestimated the AOD at KAUST by about 35 % during the event compared to AERONET AOD. Simulating these complex, large-scale dust events is extremely challenging, and thus, we do not expect the model to capture them as precisely, since they occur only a few times (~2-3) in a year. Despite this discrepancy, the average climatological vertical profiles of aerosol concentrations and temporal variations of AODs simulated by the WRF-Chem model were broadly consistent with the observations (Figs. 3, 7, 8, 10). We note that the performance of WRF-Chem to simulate these large-scale dust events is case-specific (e.g., Teixeira et al., 2016; Fernández et al., 2019) and should not be generalized. The model performance was indeed sensitive to the type of dust event (e.g., Kim et al., 2017), the details of the dust-emission processes (Klose and Shao, 2012; Klose and Shao, 2013), the dust source function used (Kalenderski and Stenchikov 2016; Parajuli et al., 2019), and the prescribed size distribution of the emitted dust (Kok et al., 2017; Marenco et al. 2018).~~

4.4. Implications of LIDAR data in atmospheric modeling

Formatted: Paper

Formatted: Font: Bold, Complex Script Font: Bold

Formatted: Font: Bold, Complex Script Font: Bold

MPL data are invaluable for studying the vertical details of aerosols in the atmosphere because they measure backscatter from aerosols and clouds with a high vertical and temporal resolution (Welton et al., 2002b; Winker et al., 2009). Most satellite data only provide aerosol properties over the entire atmospheric column (e.g., Hsu et al., 2004), which are complemented by the MPL data that provides height, depth, and the particle characteristics of the aerosol layers in the atmosphere. Since satellite data usually have a low temporal resolution ~~,~~ and because many large-scale dust events are short-lived, MPL data can reveal additional characteristics of dust storms.

In regional and global climate models, it is a usual practice to constrain the total AOD using some observations (see, for example, ~~e.g.,~~ Zhao et al., 2010; Parajuli et al., 2019). While such constraints are desirable because they help to represent columnar atmospheric properties more precisely, they are not sufficient for certain applications such as air quality modeling, for example (Ukhov et al., 2020a). Unless the model correctly represents the aerosol vertical profiles, the model-estimated surface aerosol concentrations may not be reliable. In this context, KAUST–MPL data can be instrumental in constraining the vertical distribution of aerosols in the models. Such constraints would ideally benefit the operational forecasting of dust storms and air quality (Zhang et al., 2015).

Although derived from actual observations, KAUST–MPL retrievals are also subject to uncertainties, and their accuracy is dependent on assumptions made by the retrieval algorithms. A study that compared the GRASP retrieval scheme employed here against in situ measurements showed that the differences were less than 30 % for the different retrieval schemes (Benavent-Oltra et al., 2019).

5. Conclusion

In this study, we investigated the vertical distribution of~~ three main aspects of~~ ~~dust ~~aerosols over the eastern coast of the Red Sea. We used data collected from the only operating LIDAR in the region, located on the KAUST campus, together with other collocated observations and high-resolution WRF-Chem model simulations, to explore three main aspects of dust aerosols. ~~To summarize, ~~First, ~~Secondly, ~~we evaluated how accurately WRF-Chem reproduces~~d~~ the vertical profiles of aerosols over the study site and examined its performance during a large-scale dust event of 2015. Second, we~~e first~~ investigated the vertical profile of aerosol extinction and concentrations, as well as their seasonal and diurnal variability over the study site. ~~Secondly, we evaluated how accurately WRF-Chem reproduced the vertical profiles of aerosols over the study site and examined its performance during a large-scale dust event of 2015. ~~Thirdly, we investigated how the prevailing land and sea breezes affect~~ed~~ the distribution of dust over the study~~the~~ site, which is located exactly at the land-ocean boundary. This study represents a first attempt to understand and describe the interactions between breezes and dust in this largely understudied region. The main findings of this research are summarized as follows.

Model ~~validation~~evaluation

- The simulated AOD obtained from the high-resolution WRF-Chem model setting is reasonably consistent over the study site across all observational datasets, including AERONET, MODIS, and MISR. The simulated AOD shows a mean bias error (MBE) of ~13.4 % with the AERONET data.
- WRF-Chem qualitatively captured the evolution of a large-scale summertime dust event in 2015 over the study site. The model simulated the onset, demise, and the height of the dust storms reasonably well.
- WRF-Chem simulations show that dust has the highest contribution to total AOD among all aerosol types, contributing up to 92 % in summer. Anthropogenic (sulfate, OC, and BC) and sea salt ~~aerosols ~~contributions to the total AOD could reache up to 15 % and 6 %, ~~ to the total AOD, ~~respectively, especially in winter when ~~both of which are ~~both of them are highest~~ in winter~~.

Vertical profiles of aerosols

- Over the study site, most dust is confined in the troposphere, within a height of 8 km. In winter, dust is confined to lower altitudes than in summer, which is consistent with the lower PBL height in winter than in summer.
- There is a marked difference in the daytime and nighttime vertical profile of aerosols in the study site, as shown by the KAUST–MPL data. We observed a prominent dust layer at ~5–7 km in the nighttime in the KAUST–MPL data. This elevated dust loading is associated with the dust transported from central-peninsula deserts by the easterly winds during the night, which is mobilized and lifted up by the preceding daytime convection.
- The seasonally -averaged vertical profiles of daytime aerosol extinction ~~is~~are consistent in the KAUST–MPL, MERRA-2, and CALIOP data in all seasons, which is well reproduced by our WRF-Chem simulations. The profiles from the different datasets match better in winter than in summer, consistent with the results of Wu et al. (2017).

Diurnal cycles

- There is significant diurnal variation in aerosol loading at the study site in all seasons, as shown by the KAUST–MPL data. Stronger aerosol activity occurs in the early morning during the summer, in the afternoon during the spring, and in the night during the winter.
- Both sea and land breezes cause dust emissions from the coastal plains and the western flanks of the Sarawat Mountains. Such dust emissions are most prevalent in spring.

Interaction of dust and breezes

- Sea breezes push the dust mobilized from the coastal plains up along the slope of the Sarawat Mountains, which subsequently encounters the dust-laden northeasterly trade winds coming from inland deserts, causing elevated dust maxima at a height of ~1.5 km above sea level across the mountains.
- The nighttime land breezes are strongest in winter. These easterly/northeasterly land breezes transport dust aerosols from the coastal plains and the mountain slopes towards the Red Sea.
- The sea breeze circulation is much deeper (~2 km) than the land breeze circulation (~1 km), as illustrated in Fig. 18.

Codes and data availability. The c~~C~~alibrated MPL data used in this study can be obtained from the MPLNET website https://mplnet.gsfc.nasa.gov/. The source code and additional information about the GRASP algorithm can be obtained from the grasp-open web site https://www.grasp-open.com/. MODIS AOD data were downloaded from http://ladsweb.nascom.nasa.gov/data/. MERRA-2 data were obtained from the NASA Goddard Earth Sciences Data and Information Services Center (GES DISC) available at https://disc.sci.gsfc.nasa.gov/daac-bin/FTPSubset2.pl. CALIOP data were retrieved from the website of Atmospheric Science Data Center, NASA Langley Research Center, available at https://eosweb.larc.nasa.gov/project/calipso/cloud-free_aerosol_L3_LIDAR_table. ECMWF Operational Analysis data are restricted data, which were retrieved from http://apps.ecmwf.int/archive-catalogue/?type=4v&class=od&stream=oper&expver=1 with a membership. EDGAR-4.2 is available at http://edgar.jrc.ec.europa.eu/overview.php?v=42. OMI-HTAP data are available at https://avdc.gsfc.nasa.gov/pub/data/project/OMI_HTAP_emis. A copy of the input datasets and details of the WRF-Chem model configuration can be downloaded from the KAUST repository http://hdl.handle.net/10754/662750 or by e-mail request to psagar@utexas.edu.

Acknowledgements. The research reported in this publication was supported by funding from King Abdullah University of Science and Technology (KAUST). We thank the KAUST Supercomputing Laboratory for providing computing resources. We also thank Anatolii Anisimov for providing SEVIRI images and for helpful discussions. We are grateful to Ellsworth Judd Welton of NASA Goddard Space Flight Center for the help in archiving and processing the raw LIDAR data. Thanks are also due to Michael Cusack of KAUST for proofreading the manuscript.

Author contributions. SPP and GLS developed the ~~main~~ central scientific concept of the paper. SPP analyzed the data and wrote the paper with inputs from GLS. IS operated and maintained the KAUST–MPL site. SPP conducted WRF-Chem simulations, and AU contributed on code modifications. OD and AL ran the GRASP code. GLS conceived, designed, and oversaw the study. All authors discussed the results and contributed to the final manuscript.

Competing interests. The authors declare that they have no conflict of interest.

References

Abshire, J. B., Sun, X., Riris, H., Sirota, J. M., McGarry, J. F., Palm, S., Yi, D., and Liiva, P.: Geoscience Laser Altimeter System (GLAS) on the ICESat Mission: On-orbit measurement performance, *Geophys. Res. Lett.*, 32, L21S02, https://doi.org/10.1029/2005GL024028, 2005.

Ackerman, S. A.: Remote Sensing Aerosols Using Satellite Infrared observations, J. Geophys. Res., 102, 17069–17079, https://doi.org/10.1029/96JD03066, 1997.

Albugami S., Palmer S., Cinnamon J., and Meersmans J.: Spatial and Temporal Variations in the Incidence of Dust Storms in Saudi Arabia Revealed from In Situ Observations, Geosciences, 9, 162, https://doi.org/10.3390/geosciences9040162, 2019.

Alharbi, B. H., Maghrabi, A. L., and Tapper, N.: The March 2009 dust event in Saudi Arabia: Precursor and supportive environment, B. Am. Meteorol. Soc., 94, 515-528, https://doi.org/10.1175/BAMS-D-11-00118.1, 2013.

Almazroui, M., Raju, P.V.S., Yusef, A., Hussein, M. A. A., and Omar, M.: Simulation of extreme rainfall event of November 2009 over Jeddah, Saudi Arabia: the explicit role of topography and surface heating, Theor. Appl. Climatol., 132**,** 89–101, https://doi.org/10.1007/s00704-017-2080-2, 2018.

Anisimov, A., Tao, W., Stenchikov, G., Kalenderski, S., Prakash, P. J., Yang, Z.-L., and Shi, M.: Quantifying local-scale dust emission from the Arabian Red Sea coastal plain, Atmos. Chem. Phys., 17, 993–1015, https://doi.org/10.5194/acp-17-993-2017, 2017.

Ansmann, A., Wagner, F., Müller, D., Althausen, D., Herber, A., von Hoyningen-Huene, W., and Wandinger, U., European pollution outbreaks during ACE 2.: Optical particle properties inferred from multiwavelength lidar and star-Sun photometry, J. Geophys. Res., 107(D15), https://doi.org/10.1029/2001JD001109, 2002.

Barnard, J. C., Fast, J. D., Paredes-Miranda, G., Arnott, W. P., and Laskin, A.: Technical Note: Evaluation of the WRF-Chem "Aerosol Chemical to Aerosol Optical Properties" Module using data from the MILAGRO campaign, Atmos. Chem. Phys., 10, 7325–7340, https://doi.org/10.5194/acp-10-7325-2010, 2010.

Bangalath, H. K., and Stenchikov, G.: Role of dust direct radiative effect on the tropical rain belt over Middle East and North Africa: A high-resolution AGCM study, J. Geophys. Res. Atmos., 120, 4564–4584, https://doi.org/10.1002/2015JD023122, 2015.

Benavent-Oltra, J. A., Román, R., Casquero-Vera, J. A., Pérez-Ramírez, D., Lyamani, H., Ortiz-Amezcua, P., Bedoya-Velásquez, A. E., de Arruda Moreira, G., Barreto, Á., Lopatin, A., Fuertes, D., Herrera, M., Torres, B., Dubovik, O., Guerrero-Rascado, J. L., Goloub, P., Olmo-Reyes, F. J., and Alados-Arboledas, L.: Different strategies to retrieve aerosol properties at night-time with the GRASP algorithm, Atmos. Chem. Phys., 19, 14149–14171, https://doi.org/10.5194/acp-19-14149–2019, 2019.

Boesenberg, J., et al.: The German Aerosol Lidar Network: Methodology, Data, Analysis, Report/Max-Planck Institut für Meteorologie, 317, http://hdl.handle.net/21.11116/0000-0003-2DEF-F, 2001.

Chaikovsky, A., Ivanov, A., Balin, Y., Elnikov, A., Tulinov, G., Plusnin, I., Bukin, O. and Chen, B.: Lidar network CIS-LiNet for monitoring aerosol and ozone in CIS regions, In Twelfth Joint International Symposium on Atmospheric and Ocean Optics/Atmospheric Physics, 6160, 616035), International Society for Optics and Photonics, 2006.

Chapman, E. G., Gustafson Jr, W. I., Easter, R. C., Barnard, J. C., Ghan, S. J., Pekour, M. S., and Fast, J. D.: Coupling aerosol-cloud-radiative processes in the WRF-Chem model: Investigating the radiative impact of elevated point sources, Atmos. Chem. Phys., 9, 945–964, https://doi.org/10.5194/acp-9-945-2009, 2009.

Chin, M., Ginoux, P., Kinne, S., Torres, O., Holben, B.N., Duncan, B.N., Martin, R.V., Logan, J.A., Higurashi, A. and Nakajima, T.: Tropospheric aerosol optical thickness from the GOCART

Formatted: Font: Not Italic, Complex Script Font: Not Italic

Formatted: Font: Not Italic, Complex Script Font: Not Italic

model and comparisons with satellite and Sun photometer measurements, J. Atmos. Sci., 59, 461–483, https://doi.org/10.1175/1520-0469(2002)059<0461:TAOTFT>2.0.CO;2, 2002.

Chin, M., Diehl, T., Ginoux, P., and Malm, W.: Intercontinental transport of pollution and dust aerosols: implications for regional air quality, Atmos. Chem. Phys., 7, 5501–5517, https://doi.org/10.5194/acp-7-5501-2007, 2007.

Collins, W. D., Rasch, P. J., Eaton, B. E., Khattatov, B. V., Lamarque, J.-F., and Zender, C. S.: Simulating aerosols using a chemical transport model with assimilation of satellite aerosol retrievals: Methodology for INDOEX, J. Geophys. Res., 106(D7), 7313–7336, https://doi.org/10.1029/2000JD900507, 2001.

~~Collins, W. D., Rasch, P. J., Eaton, B. E., Khattatov, B. V., Lamarque, J.-F., and Zender, C. S. (2001), Simulating aerosols using a chemical transport model with assimilation of satellite aerosol retrievals: Methodology for INDOEX, *J. Geophys. Res.*, 106(D7), 7313–7336, https://doi.org/10.1029/2000JD900507, 2001.~~

Crouvi, O., Dayan, U., Amit, R., and Enzel, Y.: An Israeli haboob: Sea breeze activating local anthropogenic dust sources in the Negev loess, Aeol. Res., 24, 39–52, https://doi.org/10.1016/j.aeolia.2016.12.002, 2017.

Davis, S. R., Farrar, J. T., Weller, R. A., Jiang, H., and Pratt, L. J.: The Land-Sea Breeze of the Red Sea: Observations, Simulations, and Relationships to Regional Moisture Transport, J. Geophys. Res. Atmos., 124, https://doi.org/10.1029/2019JD031007, 2019.

Derimian, Y., Choël, M., Rudich, Y., Deboudt, K., Dubovik, O., Laskin, A., Legrand, M., Damiri, B., Koren, I., Unga, F., Moreau, M., Andreae, M. O., and Karnieli, A.: Effect of sea breeze circulation on aerosol mixing state and radiative properties in a desert setting, Atmos. Chem. Phys., 17, 11331–11353, https://doi.org/10.5194/acp-17-11331-2017, 2017.

de Vries, A. J., Tyrlis, E., Edry, D., Krichak, S. O., Steil, B., and Lelieveld, J.: Extreme precipitation events in the Middle East: Dynamics of the Active Red Sea Trough, J. Geophys. Res. Atmos., 118, 7087– 7108, doi:10.1002/jgrd.50569, 2013.

Di Biagio, C., Formenti, P., Balkanski, Y., Caponi, L., Cazaunau, M., Pangui, E., Journet, E., Nowak, S., Caquineau, S., Andreae, M. O., Kandler, K., Saeed, T., Piketh, S., Seibert, D., Williams, E., and Doussin, J.-F.: Global scale variability of the mineral dust long-wave refractive index: a new dataset of in situ measurements for climate modeling and remote sensing, Atmos. Chem. Phys., 17, 1901-1929, https://doi.org/10.5194/acp-17-1901-2017, 2017.

Diner, D.: MISR Level 3 Component Global Aerosol product covering a day HDF-EOS File - Version 4 [Data set], NASA Langley Atmospheric Science Data Center DAAC, https://doi.org/10.5067/terra/misr/mil3dae_l3.004, 2009.

Dubovik, O., and King, M. D.: A flexible inversion algorithm for retrieval of aerosol optical properties from Sun and sky radiance measurements, J. Geophys. Res., 105, 20673– 20696, https://doi.org/10.1029/2000JD900282, 2000.

Dubovik, O., Herman, M., Holdak, A., Lapyonok, T., Tanré, D., Deuzé, J. L., Ducos, F., Sinyuk, A., and Lopatin, A.: Statistically optimized inversion algorithm for enhanced retrieval of aerosol properties from spectral multi-angle polarimetric satellite observations, Atmos. Meas. Tech., 4, 975–1018, https://doi.org/10.5194/amt-4-975-2011, 2011.

Dubovik, O., Lapyonok, T., Litvinov, P., Herman, M., Fuertes, D., Ducos, F., Lopatin A., Chaikovsky, A., Torres, B., Derimian, Y., Huang, X., Aspetsberger, M., and Federspiel, C.: GRASP: a versatile algorithm for characterizing the atmosphere, SPIE Newsroom, 25, https://doi.org 10.1117/2.1201408.005558, 2014.

Engelstaedter, S., and Washington, R.:, Temporal controls on global dust emissions: The role of surface gustiness, Geophys. Res. Lett., 34, L15805, https://doi.org/10.1029/2007GL029971, 2007.

Estoque, M. A.: A theoretical investigation of the sea breeze, Q.J.R. Meteorol. Soc., 87, 136-146, https://doi.org/10.1002/qj.49708737203, 1961.

Farrar, J., Lentz, S., Churchill, J., Bouchard, P., Smith, J., Kemp, J., Lord, J., Allsup, G., and Hosom, D.: King Abdullah University of Science and Technology (KAUST) mooring deployment cruise and

Formatted: Font: Not Italic, Complex Script Font: Not Italic

Formatted: Font: Not Italic, Complex Script Font: Not Italic

Formatted: Font: Not Italic, Complex Script Font: Not Italic

fieldwork report, Technical report, Woods Hole Oceanographic Institution, WHOI-KAUST-CTR-2009, 2, 2009.

Fast, J.D., Gustafson Jr, W.I., Easter, R.C., Zaveri, R.A., Barnard, J.C., Chapman, E.G., Grell, G.A., and Peckham, S.E.: Evolution of ozone, particulates, and aerosol direct forcing in an urban area using a new fully-coupled meteorology, chemistry, and aerosol model, J. Geophys. Res., 111, https://doi.org/10.1029/2005JD006721, 2006.

Fekih, A. and Mohamed, A.: Evaluation of the WRF model on simulating the vertical structure and diurnal cycle of the atmospheric boundary layer over Bordj Badji Mokhtar (southwestern Algeria), Journal of King Saud University - Science, Volume 31(4), 602-611, https://doi.org/10.1016/j.jksus.2017.12.004, 2019.

Fernández-Camacho, R., Rodríguez, S., de la Rosa, J., Sánchez de la Campa, A. M., Viana, M., Alastuey, A., and Querol, X.: Ultrafine particle formation in the inland sea breeze airflow in Southwest Europe, Atmos. Chem. Phys., 10, 9615–9630, https://doi.org/10.5194/acp-10-9615-2010, 2010.

Fernández, A.J., Sicard, M., Costa, M.J., Guerrero-Rascado, J.L., Gómez-Amo, J.L., Molero, F., Barragán, R., Basart, S., Bortoli, D., Bedoya-Velásquez, A.E. and Utrillas, M.P.: Extreme, wintertime Saharan dust intrusion in the Iberian Peninsula: KAUST–MPL monitoring and evaluation of dust forecast models during the February 2017 event, Atmos. Res., 223–241, https://doi.org/10.1016/j.atmosres.2019.06.007, 2019.

Flaounas, E., Kotroni, V., Lagouvardos, K., Klose, M., Flamant, C., and Giannaros, T. M.: Sensitivity of the WRF-Chem (V3.6.1) model to different dust emission parametrisation: assessment in the broader Mediterranean region, Geosci. Model Dev., 10, 2925–2945, https://doi.org/10.5194/gmd-10-2925-2017, 2017.

Fountoukis, C., Ayoub, M.A., Ackermann, L., Perez-Astudillo, D., Bachour, D., Gladich, I. and Hoehn, R.D.: Vertical Ozone Concentration Profiles in the Arabian Gulf Region during Summer and Winter: Sensitivity of WRF-Chem to Planetary Boundary Layer Schemes, Aerosol Air Qual. Res., 18, 1183-1197, https://doi.org/10.4209/aaqr.2017.06.0194, 2018.

~~Fernández, A.J., Sicard, M., Costa, M.J., Guerrero-Rascado, J.L., Gómez-Amo, J.L., Molero, F., Barragán, R., Basart, S., Bortoli, D., Bedoya-Velásquez, A.E. and Utrillas, M.P.: Extreme, wintertime Saharan dust intrusion in the Iberian Peninsula: KAUST–MPL monitoring and evaluation of dust forecast models during the February 2017 event, Atmos. Res., 223–241, https://doi.org/10.1016/j.atmosres.2019.06.007, 2019.~~

Ginoux, P., Chin, M., Tegen, I., Prospero, J. M., Holben, B., Dubovik, O., and Lin, S.-J.: Sources and distributions of dust aerosols simulated with the GOCART model, J. Geophys. Res., 106, 20255– 20273, doi:10.1029/2000JD000053, 2001.

Guerrero-Rascado, J. L. et al.: Latin American Lidar Network (LALINET) for aerosol research: Diagnosis on network instrumentation, Journal of Atmospheric and Solar-Terrestrial Physics, 138–139, 112-120, https://doi.org/10.1016/j.jastp.2016.01.001, 2016.

Gong, S. L.: A parameterization of sea-salt aerosol source function for sub- and super-micron particles, *Global Biogeochem. Cycles*, 17, 1097, https://doi.org/10.1029/2003GB002079, 2003.

Heese, B., and Wiegner, M.: Vertical aerosol profiles from Raman polarization lidar observations during the dry season AMMA field campaign, J. Geophys. Res., 113, D00C11, https://doi.org/10.1029/2007JD009487, 2008.

Hsu, N. C., Tsay, S. C., King, M. D., and Herman, J. R.: Aerosol properties over bright-reflecting source regions, Geosci. Remote Sens., IEEE Transactions on, *42*(3), 557-569, doi:10.1109/TGRS.2004.824067, 2004.

Formatted: English (United States)

Formatted: Font: Not Italic, Complex Script Font: Not Italic

Formatted: Font: Not Italic, Complex Script Font: Not Italic

Hu, Z., Zhao, C., Huang, J., Leung, L. R., Qian, Y., Yu, H., Huang, L., and Kalashnikova, O. V.: Trans-Pacific transport and evolution of aerosols: evaluation of quasi-global WRF-Chem simulation with multiple observations, Geosci. Model Dev., 9, 1725–1746, https://doi.org/10.5194/gmd-9-1725-2016, 2016.

Hubert, W.E., Hull, A.N., Morford, D.R. and Englebretson, R.E.: Forecasters handbook for the Middle East/Arabian Sea, OCEAN DATA SYSTEMS INC MONTEREY CALIF, 1983.

Jacobson, M. Z. and Kaufman, Y. J.: Wind reduction by aerosol particles, *Geophys. Res. Lett.*, 33, L24814, https://doi.org/10.1029/2006GL027838, 2006.

Janssens-Maenhout, G., Crippa, M., Guizzardi, D., Dentener, F., Muntean, M., Pouliot, G., Keating, T., Zhang, Q., Kurokawa, J., Wankmüller, R., Denier van der Gon, H., Kuenen, J. J. P., Klimont, Z., Frost, G., Darras, S., Koffi, B., and Li, M.: HTAP_v2.2: a mosaic of regional and global emission grid maps for 2008 and 2010 to study hemispheric transport of air pollution, Atmos. Chem. Phys., 15, 11411–11432, https://doi.org/10.5194/acp-15-11411-2015, 2015.

Jiang, H., Farrar, J. T., Beardsley, Chen, R., and Chen, C. (2009), Zonal surface wind jets across the Red Sea due to mountain gap forcing along both sides of the Red Sea, Geophys. Res. Lett., 36, https://doi.org/10.1029/2009GL040008, 2009.

Johnson, B. T., Heese, B., McFarlane, S. A., Chazette, P., Jones, A., and Bellouin, N.: Vertical distribution and radiative effects of mineral dust and biomass burning aerosol over West Africa during DABEX, J. Geophys. Res., 113, https://doi.org/10.1029/2008JD009848, 2008.

Kahn, R. A., Gaitley, B. J., Martonchik, J. V., Diner, D. J., Crean, K. A., and Holben, B.: Multiangle Imaging Spectroradiometer (MISR) global aerosol optical depth validation based on 2 years of coincident Aerosol Robotic Network (AERONET) observations, J. Geophys. Res., 110, https://doi.org/10.1029/2004JD004706, 2005.

Kalenderski, S. and G. Stenchikov, G.: High-resolution regional modeling of summertime transport and impact of African dust over the Red Sea and Arabian Peninsula, J. Geophys. Res. Atmos., 121, 6435–6458, https://doi.org/10.1002/2015JD024480, 2016.

Khan, B., Stenchikov, G., Weinzierl, B., Kalenderski, S., and Osipov, S.: Dust plume formation in the free troposphere and aerosol size distribution during the Saharan Mineral Dust Experiment in North Africa, Tellus B Chem. Phys. Meteorol., 67, https://doi.org/10.3402/tellusb.v67.27170, 2015.

Kim, D., Chin, M., Kemp, E.M., Tao, Z., Peters-KAUST–MPLd, C.D., and Ginoux, P.: Development of high-resolution dynamic dust source function – A case study with a strong dust storm in a regional model, Atm. Environ., 159, 11–25, http://dx.doi.org/ 10.1016/j.atmosenv.2017.03.045, 2017.

Kim, M.-H., Omar, A. H., Tackett, J. L., Vaughan, M. A., Winker, D. M., Trepte, C. R., Hu, Y., Liu, Z., Poole, L. R., Pitts, M. C., Kar, J., and Magill, B. E.: The CALIPSO version 4 automated aerosol classification and lidar ratio selection algorithm, Atmos. Meas. Tech., 11, 6107–6135, https://doi.org/10.5194/amt-11-6107-2018, 2018.

Klose, M. and Shao, Y.: Stochastic parameterization of dust emission and application to convective atmospheric conditions, Atmos. Chem. Phys., 12, 7309-7320, https://doi.org/10.5194/acp-12-7309-2012, 2012.

Klose, M., and Shao, Y.: Large-eddy simulation of turbulent dust emission, Aeol. Res., 8, 49-58, https://doi.org/10.1016/j.aeolia.2012.10.010, 2013.

~~Koffi, B., Schulz, M., Bréon, F.M., Griesfeller, J., Winker, D., Balkanski, Y., Bauer, S., Berntsen, T., Chin, M., Collins, W.D., and Dentener, F.: Application of the CALIOP layer product to evaluate the vertical distribution of aerosols estimated by global models: AeroCom phase I results, J. Geophys. Res., 117, https://doi.org/10.1029/2011JD016858, 2012.~~

Kok, J.F., Ridley, D.A., Zhou, Q., Miller, R.L., Zhao, C., Heald, C.L., Ward, D.S., Albani, S. and Haustein, K.: Smaller desert dust cooling effect estimated from analysis of dust size and abundance, Nature Geosci., 10**,** 274–278, https://doi.org/10.1038/ngeo2912, 2017.

Formatted: Font: Not Italic, Complex Script Font: Not Italic

Kumar, R.K., Attada, R., Dasari, H. P., Vellore, R. K., Abualnaja, Y. O., Asok, K., and Hoteit, I.: On the recent amplification of dust over the Arabian Peninsula during 2002 – 2012, J. Geophys. Res. Atmos., 124, 13220-13229, 2019.

Lebel, T., Parker, D.J., Flamant, C., Bourlès, B., Marticorena, B., Mougin, E., Peugeot, C., Diedhiou, A., Haywood, J.M., Ngamini, J.B., Polcher, J., Redelsperger, J.-L. and Thorncroft, C.D.: The AMMA field campaigns: multiscale and multidisciplinary observations in the West African region, Q.J.R. Meteorol. Soc., 136, 8-33, https://doi.org/10.1002/qj.486, 2010.

Lee, Y. H., Chen, K., and Adams, P. J.: Development of a global model of mineral dust aerosol microphysics, Atmos. Chem. Phys., 9, 2441-2458, https://doi.org/10.5194/acp-9-2441-2009, 2009.

Lee Y. H. and P. J. Adams P. J.: A Fast and Efficient Version of the TwOMoment Aerosol Sectional (TOMAS) Global Aerosol Microphysics Model, Aerosol Sci. ~~ence and~~ Tech.~~nology~~, 46, 678-689, https://doi.org/10.1080/02786826.2011.643259, 2012.

LeGrand, S. L., Polashenski, C., Letcher, T. W., Creighton, G. A., Peckham, S. E., and Cetola, J. D.: The AFWA dust emission scheme for the GOCART aerosol model in WRF-Chem v3.8.1, Geosci. Model Dev., 12, 131-166, https://doi.org/10.5194/gmd-12-131-2019, 2019.

Li, W., El-Askary, H., Qurban, M.A., Proestakis, E., Garay, M.J., Kalashnikova, O.V., Amiridis, V., Gkikas, A., Marinou, E., Piechota, T., and Manikandan, K.P.: An Assessment of Atmospheric and Meteorological Factors Regulating Red Sea Phytoplankton Growth, Remote Sens., 10, 673, http://dx.doi.org/10.3390/rs10050673., 2018.

Lopatin, A., Dubovik, O., Chaikovsky, A., Goloub, P., Lapyonok, T., Tanré, D., and Litvinov, P.: Enhancement of aerosol characterization using synergy of lidar and sun-photometer coincident observations: the GARRLiC algorithm, Atmos. Meas. Tech., 6, 2065–2088, https://doi.org/10.5194/amt-6-2065-2013, 2013.

Mahowald, N.M., Muhs, D.R., Levis, S., Rasch, P.J., Yoshioka, M., Zender, C.S. and Luo, C. (2006), Change in atmospheric mineral aerosols in response to climate: Last glacial period, preindustrial, modern, and doubled carbon dioxide climates, J. Geophys. Res., 111, https://doi.org/10.1029/2005JD006653.

Marenco, F., Ryder, C., Estellés, V., O'Sullivan, D., Brooke, J., Orgill, L., and Gallagher, M.: Unexpected vertical structure of the Saharan Air Layer and giant dust particles during AER-D, Atmos. Chem. Phys., 18, 17655-17668, https://doi.org/10.5194/acp-18-17655-2018, 2018.

Marticorena, B., and Bergametti, G.: Modeling the atmospheric dust cycle: 1. Design of a soil-derived dust emission scheme, J. Geophys. Res., 100(D8), 16415– 16430, https://doi.org/10.1029/95JD00690, 1995.

Miller, S. T. K., Keim, B. D., Talbot, R. W., and Mao, H. (2003), Sea breeze: Structure, forecasting, and impacts, Rev. Geophys., 41, 1011, https://doi.org/10.1029/2003RG000124, 2003.

Monahan E.C., Spiel D.E., and Davidson K.L.: A Model of Marine Aerosol Generation Via Whitecaps and Wave Disruption, in Oceanic Whitecaps, edited by Monahan E.C. and Niocaill G.M., Oceanographic Sciences Library, Springer, Dordrecht, 2, 167–174, https://doi.org/10.1007/978-94-009-4668-2_16, 1986.

Neuman, C.M., Boulton, J.W. and Sanderson, S.: Wind tunnel simulation of environmental controls on fugitive dust emissions from mine tailings, Atmos.~~pheric~~ Environ.~~nment~~, *43*, 520-529, https://doi.org/10.1016/j.atmosenv.2008.10.011, 2009.

Omar, A.H., Winker, D.M., Vaughan, M.A., Hu, Y., Trepte, C.R., Ferrare, R.A., Lee, K.P., Hostetler, C.A., Kittaka, C., Rogers, R.R. and Kuehn, R.E.: The CALIPSO Automated Aerosol Classification and Lidar Ratio Selection Algorithm, J. Atmos. Oceanic Technol., 26, 1994–2014, https://doi.org/10.1175/2009JTECHA1231.1, 2009.

Formatted: Font: Not Italic, Complex Script Font: Not Italic

Osipov, S., Stenchikov, G., Brindley, H., and Banks, J.: Diurnal cycle of the dust instantaneous direct radiative forcing over the Arabian Peninsula, Atmos. Chem. Phys., 15, 9537–9553, https://doi.org/10.5194/acp-15-9537-2015, 2015.

Osipov, S., and Stenchikov, G.: Simulating the regional impact of dust on the Middle East climate and the Red Sea, J. Geophys. R. Oceans, 123, 1032– 1047, https://doi.org/10.1002/2017JC013335, 2018.

Pappalardo, G., Amodeo, A., Apituley, A., Comeron, A., Freudenthaler, V., Linné, H., Ansmann, A., Bösenberg, J., D'Amico, G., Mattis, I. and Mona, L.: EARLINET, Atmos. Meas. Tech., 8, 2389-2409, https://doi.org/10.5194/amt-7-2389-2014, 2014.

Prakash, P. J., G. Stenchikov, S. Kalenderski, S. Osipov, and H. Bangalath (2015), The impact of dust storms on the Arabian Peninsula and the Red Sea (2015), Atmos. Chem. Phys., 15, 199–222, doi:10.5194/acp-15-199-2015, 2015.

Prospero, J. M.: Long-term measurements of the transport of African mineral dust to the southeastern United States: Implications for regional air quality, J. Geophys. Res., 104, 15917–15927, https://doi.org/10.1029/1999JD900072, 1999.

Ramanathan, V., et al.:, Indian Ocean Experiment: An integrated analysis of the climate forcing and effects of the great Indo-Asian haze, Journal of Geophysical Research, 106(D22), 28371– 28398, https://doi.org/10.1029/2001JD900133, 2001.

Rasch, P. J., Collins, W. D., and Eaton, B. E.: Understanding the Indian Ocean Experiment (INDOEX) aerosol distributions with an aerosol assimilation, Journal of Geophysical Research, 106(D7), 7337– 7355, https://doi.org/10.1029/2000JD900508, 2001.

Rémy, S., Benedetti, A., Bozzo, A., Haiden, T., Jones, L., Razinger, M., et al.: Feedbacks of dust and boundary layer meteorology during a dust storm in the eastern Mediterranean, Atmos. Chem. Phys., 15, 12909–12933, https://doi.org/10.5194/acp-15-12909-2015, 2015.

~~Rasch, P. J., Collins, W. D., and Eaton, B. E.: Understanding the Indian Ocean Experiment (INDOEX) aerosol distributions with an aerosol assimilation, Journal of Geophysical Research, 106(D7), 7337– 7355, https://doi.org/10.1029/2000JD900508, 2001.~~

Ryder, C. L., Highwood, E. J., Walser, A., Seibert, P., Philipp, A., and Weinzierl, B.: Coarse and giant particles are ubiquitous in Saharan dust export regions and are radiatively significant over the Sahara, Atmos. Chem. Phys., 19, 15353–15376, https://doi.org/10.5194/acp-19-15353-2019, 2019.

Saide, P.E., Carmichael, G.R., Spak, S.N., Gallardo, L., Osses, A.E., Mena-Carrasco, M.A., and Pagowski, M.: Forecasting urban PM10 and PM2.5 pollution episodes in very stable nocturnal conditions and complex terrain using WRF–Chem CO tracer model, Atmos. Environ., 45, 2769-2780, https://doi.org/10.1016/j.atmosenv.2011.02.001, 2011.

Schepanski, K., Tegen, I., Laurent, B., Heinold, B., and Macke, A.: A new Saharan dust source activation frequency map derived from MSG-SEVIRI IR-channels, Geophys. Res. Lett., 34, https://doi.org/10.1029/2007GL030168, 2007.

Selezneva, E.S.: The main features of condensation nuclei distribution in the free atmosphere over the European territory of the USSR, Tellus, 18, 525-531, doi:10.1111/j.2153-3490.1966.tb00265.x, 1966.

Senghor, H., Machu, É., Hourdin, F., and Gaye, A. T.: Seasonal cycle of desert aerosols in western Africa: analysis of the coastal transition with passive and active sensors, Atmos. Chem. Phys., 17, 8395–8410, https://doi.org/10.5194/acp-17-8395-2017, 2017.

~~Senghor, H., Machu, É., Durán, L., Jenkins, G.S., and Gaye, A.T.: Seasonal Behavior of Aerosol Vertical Concentration in Dakar and Role Played by the Sea-Breeze, Open J. Air Pollut., 9, 11-26, http://dx.doi.org/10.4236/ojap.2020.91002, 2020.~~

Shao, Y., Wyrwoll, K.H., Chappell, A., Huang, J., Lin, Z., McTainsh, G.H., Mikami, M., Tanaka, T.Y., Wang, X., and Yoon, S.: Dust cycle: an emerging core theme in Earth system science, Aeol. Res., 2, 181–204, http://dx.doi.org/10.1016/j.aeolia.2011.02.001, 2011.

Formatted: Font: Not Italic, Complex Script Font: Not Italic

Shimizu, A., Nishizawa, T., Jin, Y., Kim, S.-W., Wang, Z., Batdorj, D., and Sugimoto, N.: Evolution of a lidar network for tropospheric aerosol detection in East Asia, Opt. Eng. 56(3), 031219, https://doi.org/10.1117/1.OE.56.3.031219, 2016.

Simpson, J. E.: Sea breeze and local winds, Cambridge University Press, 1994.
Sokolik, I.N. and Toon, O.B.: Direct radiative forcing by anthropogenic airborne mineral aerosols. Nature, 381, 681–683, http://dx.doi.org/10.1038/381681a0, 1996.
Stephens, G., Winker, D., Pelon, J., Trepte, C., Vane, D., Yuhas, C., L'Ecuyer, T., and Lebsock, M.: CloudSat and CALIPSO within the A-Train: Ten Years of Actively Observing the Earth System, Bull. Amer. Meteor. Soc., 99, 569–581, https://doi.org/10.1175/BAMS-D-16-0324.1, 2018.
Teixeira, J.C., Carvalho, A.C., Tuccella, P., Curci, G., and Rocha, A.: WRF-chem sensitivity to vertical resolution during a saharan dust event, Phys. Chem. Earth Parts A/B/C, 94, 188-195, https://doi.org/10.1016/j.pce.2015.04.002, 2016.
Ukhov, A., Mostamandi, S., da Silva, A., Flemming, J., Alshehri, Y., Shevchenko, I., and Stenchikov, G.: Assessment of natural and anthropogenic aerosol air pollution in the Middle East using MERRA-2, CAMS data assimilation products, and high-resolution WRF-Chem model simulations, Atmos. Chem. Phys., 20, 9281–9310, https://doi.org/10.5194/acp-20-9281-2020, 2020a.~~Ukhov, A., Mostamandi, S., da Silva, A., Flemming, J., Alshehri, Y., Shevchenko, I., and Stenchikov, G.: Assessment of natural and anthropogenic aerosol air pollution in the Middle East using MERRA-2, CAMS data assimilation products,and high-resolution WRF-Chem model simulations, Atmos. Chem. Phys. Discuss., https://doi.org/10.5194/acp-2020-17, in review, 2020a.~~

Ukhov, A., Mostamandi, S., Krotkov, N., Flemming, J., da Silva, A., Li, C., Fioletov. V., McLinden, C., Anisimov, A., Alshehri, Y., and Stenchikov, G.: Study of SO2 pollution in the Middle East using MERRA-2, CAMS data assimilation products, and high-resolution WRF-Chem simulations. J. Geophys. Res. Atmos., 125, e2019JD031993, https://doi.org/10.1029/2019JD031993, 2020b.
Ukhov, A., Ahmadov, R., Grell, G., and Stenchikov, G.: Improving dust simulations in WRF-Chem model v4.1.3 coupled with GOCART aerosol module, Geosci. Model Dev. Discuss., https://doi.org/10.5194/gmd-2020-92, in review, 2020c.
Wang, S.H., Lin, N.H., OuYang, C.F., Wang, J.L., Campbell, J.R., Peng, C.M., Lee, C.T., Sheu, G.R., and Tsay, S.C.: Impact of Asian dust and continental pollutants on cloud chemistry observed in northern Taiwan during the experimental period of ABC/EAREX 2005, J. Geophys. Res., 115, doi:10.1029/2009JD013692, 2010.
Welton, E.J., Voss, K.J., Gordon, H.R., Maring, H., Smirnov, A., Holben, B., Schmid, B., Livingston, J.M., Russell, P.B., Durkee, P.A., Formenti, P. and Andreae, M.O.: Ground-based lidar measurements of aerosols during ACE-2: instrument description, results, and comparisons with other ground-based and airborne measurements, Tellus B, 52, 636-651, https://doi.org/10.1034/j.1600-0889.2000.00025.x, 2000.
Welton, E.J., Campbell, J.R., Spinhirne, J.D., and Scott III, V.S.: Global monitoring of clouds and aerosols using a network of micropulse lidar systems, Proc. SPIE 4153, KAUST–MPL Remote Sensing for Industry and Environment Monitoring, Sendai, Japan, 13 February 2001, https://doi.org/10.1117/12.417040, 2001.

Welton, E.J., Campbell, J.R., Berkoff, T.A., Spinhirne, J.D., Tsay, S.C., Holben, B., Shiobara, M., and Starr, D.O.: The Micro-pulse ~~KAUST–MPL~~lidar Network (~~KAUST–~~MPL-Net), Twenty-first International Laser Radar Conference (ILRC21), Quebec City, Canada, 8-12 July 2002, https://ntrs.nasa.gov/search.jsp?R=20020083050, 2002a.
Welton, E. J. , Voss, K. J., Quinn, P. K., Flatau, P. J., Markowicz, K., Campbell, J. R., Spinhirne, J. D., Gordon, H. R., and Johnson, J. E.: Measurements of aerosol vertical profiles and optical

properties during INDOEX 1999 using micropulse lidars, J. Geophys. Res., 107(D19), 8019, https://doi.org/10.1029/2000JD000038, 2002b.

~~Welton, E.J., Campbell, J.R., Spinhirne, J.D., and Scott III, V.S.: Global monitoring of clouds and aerosols using a network of micropulse KAUST MPL systems, Proc. SPIE 4153, KAUST MPL Remote Sensing for Industry and Environment Monitoring, Sendai, Japan, 13 February 2001, https://doi.org/10.1117/12.417040, 2001.~~

Wild, O., Zhu, X., and Prather, M. J.: Fast-J: accurate simulation of in- and below cloud photolysis in tropospheric chemical models, J. Atmos. Chem., 37, 245–282, https://doi.org/10.1023%2FA%3A1006415919030, 2000.

Winker, D. M., Couch, R. H., and McCormick, M. P.: An overview of LITE: NASA's Lidar In-space Technology Experiment, in Proceedings of the IEEE, 84(2), 164-180, https://doi.org/10.1109/5.482227, 1996.

Winker, D.M., Vaughan, M.A., Omar, A., Hu, Y., Powell, K.A., Liu, Z., Hunt, W.H. and Young, S.A.: Overview of the CALIPSO Mission and CALIOP Data Processing Algorithms, J. Atmos. Oceanic Technol., 26, 2310–2323, https://doi.org/10.1175/2009JTECHA1281.1, 2009.

~~Winker, D. M., Couch, R. H., and McCormick, M. P.: An overview of LITE: NASA's Lidar In-space Technology Experiment, in Proceedings of the IEEE, vol. 84(2), 164-180, https://doi.org/10.1109/5.482227, 1996.~~

Winker, D. M., Tackett, J. L., Getzewich, B. J., Liu, Z., Vaughan, M. A., and Rogers, R. R.: The global 3-D distribution of tropospheric aerosols as characterized by CALIOP, Atmos. Chem. Phys., 13, 3345–3361, https://doi.org/10.5194/acp-13-3345-2013, 2013.

Wu, L., Su, H., Kalashnikova, O. V., Jiang, J. H., Zhao, C., Garay, M. J., Campbell, J. R., and Yu, N.: WRF-Chem simulation of aerosol seasonal variability in the San Joaquin Valley, Atmos. Chem. Phys., 17, 7291–7309, https://doi.org/10.5194/acp-17-7291-2017, 2017.

Yuan, T., Chen, S., Huang, J., Zhang, X., Luo, Y., Ma, X., and Zhang, G.: Sensitivity of simulating a dust storm over Central Asia to different dust schemes using the WRF-Chem model, Atmos. Environ., 207, 16-29, https://doi.org/10.1016/j.atmosenv.2019.03.014, 2019.

Zhao, C., Ruby Leung, L., Easter, R., Hand, J., and Avise, J.: Characterization of speciated aerosol direct radiative forcing over California, J. Geophys. Res. Atmos., 118, 2372–2388, https://doi.org/10.1029/2012JD018364, 2013.

Zhang, Y., Liu, Y., Kucera, P. A., Alharbi, B. H., Pan, L., and Ghulam, A.: Dust modeling over Saudi Arabia using WRF-Chem: March 2009 severe dust case, Atmospheric Environment, 119, 118-130, https://doi.org/10.1016/j.atmosenv.2015.08.032, 2015.

Formatted: Font: Not Italic, Complex Script Font: Not Italic

Formatted: Font: Not Italic, Complex Script Font: Not Italic

Formatted: Font: Not Italic, Complex Script Font: Not Italic

Formatted: Font: (Default) Times New Roman, Complex Script Font: Times New Roman